Simulation of Solid Oxide Fuel Cell-Based Power Generation Processes with CO_2 Capture

by

Wei Zhang

A thesis
presented to the University of Waterloo
in fulfillment of the
thesis requirement for the degree of

Master of Applied Science
in
Chemical Engineering

Waterloo, Ontario, Canada, 2006

I hereby declare that I am the sole author of this thesis. This is a true copy of the thesis, including any required final revisions, as accepted by my examiners.

I understand that my thesis may be made electronically available to the public.

Abstract

The Solid Oxide Fuel Cell (SOFC) is a promising technology for electricity generation. It converts the chemical energy of the fuel gas directly to electricity energy and therefore, very high electrical efficiencies can be achieved. The high operating temperature of the SOFC also provides excellent possibilities for cogeneration applications. In addition to producing power very efficiently, the SOFC has the potential to concentrate CO_2 with a minimum of an overall efficiency loss. Concentration of CO_2 is a desirable feature of a power generation process so that the CO_2 may be subsequently sequestered thus preventing its contribution to global warming. The primary purpose of this research project was to investigate the role of the SOFC technology in power generation processes and explore its potential for CO_2 capture in power plants.

This thesis introduces an AspenPlus™ SOFC stack model based on the natural gas feed tubular internal reforming SOFC technology. It was developed utilizing existing AspenPlus™ functions and unit operation models. This SOFC model is able to provide detailed thermodynamic and parametric analysis of the SOFC operation and can easily be extended to study the entire process consisting of the SOFC stack and balance of plant.

Various SOFC-based power generation cycles were studied in this thesis. Various options for concentrating CO_2 in these power generation systems were also investigated and discussed in detail. All the processes simulations were implemented in AspenPlus™ extending from the developed natural gas feed tubular SOFC stack model. The study shows that the SOFC technology has a promising future not only in generating electricity

in high efficiency but also in facilitating CO_2 concentration, but the cost of the proposed processes still need be reduced so SOFCs can become a technical as well as economic feasible solution for power generation.

Acknowledgements

I would like to thank my supervisors at University of Waterloo, Dr. Eric Croiset, Dr. Peter Douglas and Dr. Michael Fowler who have provided insight and have had a significant input to my thesis.

I would like also to thank CANMET CO_2 Consortium for sponsoring my first year research.

Table of Contents

Table of Contents

List of Tables

List of Figures

1.0 Introduction

Invented in 1839 by Sir. William Grove, fuel cells are one of the oldest electrical conversion technologies known to man. Only recently have they emerged as one of the most promising power-generation technologies for the future. Fuel cells offer many important features that make them favourable as energy conversion devices. The most important one is the combination of relatively high efficiency and very low environment impact (EG&G, 2002).

There are different types of fuel cells that have been realized and are currently in use and development. Among them, Solid Oxide Fuel Cells (SOFCs) have grown in recognition as a viable high temperature fuel cell technology. One of the main attractions of SOFC over other fuel cells is their ability to handle a wide range of hydrocarbon fuels. Their high operating temperature also produces high quality by-product heat for cogeneration or for use in a bottoming cycle that makes them a strong competitor in stationary applications for power generation.

Although a SOFC produces electricity, it only produces dc power and utilizes only processed fuel. Therefore, a SOFC based power generation system requires the integration of many other components beyond the SOFC stack itself. Moreover, to recover the high quality waste heat from the SOFC stack, an efficient integration of co-generation or bottoming system with the fuel cell section is crucial for a SOFC based power generation plant. Since the balance of plant will directly impact the overall system efficiency and may cost more than the SOFC stack itself, it is obvious that the design of a SOFC power

generation system involves more than the optimization of the SOFC unit with respect to efficiency or economics. It also involves balance of plant studies. With SOFC materials and stacks approaching a commercialization stage, there is a need to explore various process designs to obtain optimal efficiency and economics based on specific applications and fuel availability.

AspenPlus™ is a commercially available process simulator for process analysis. It offers a convenient and time saving means for chemical process studies, including system modeling, integration and optimization. It is used in this thesis as a process simulation tool to investigate potential SOFC based power generation cycles including SOFC stack and the balance of plants. To facilitate the study, a natural gas feed tubular SOFC stack model is developed using existing AspenPlus™ functions and unit operation models with minimum requirements for linking of a subroutine. This approach fully utilizes the existing capabilities of this process simulator and provides a convenient way to perform detailed process study of SOFC based power generation cycles.

Several SOFC based power generation systems developed by Siemens-Westinghouse were simulated using the developed SOFC stack model and the results are compared to the reported performances in the literature. The simulations confirm that an atmospheric pressure SOFC based power generation cycle has an efficiency range of 45%-50% and the SOFC and gas turbine hybrid cycle can provide up to 70% of electrical efficiencies %, as presented by Veyo and Lundberg (1999).

Power generation is the largest source of global CO_2 emissions (IEA, 2001). Numerous studies and researchers have been performed or are being performed all over the world in CO_2 capture and separation techniques for power generation plants (Dijkstra and Jansen, 2004). Although commercialized options are available such as amine scrubbing, so far, CO_2 capture for power generation plants is still considered expensive and energy extensive (IEA, 2001). With higher electrical efficiencies, SOFC-based power generation processes consume less fossil fuel per kW produced and therefore can contribute to the reduction of CO_2 emission. Moreover, SOFCs offer great potential for the application of CO_2 separation. It has a unique feature of producing a concentrated CO_2 stream because the oxidation reactions occur in the absence of nitrogen, unlike in typical combustion systems. This feature offers a great opportunity to separate CO_2 from the flue gas of SOFC based power generation plants with much lower efficiency reduction than other conventional power plants.

This thesis investigates several CO_2 capture options based on a conceptual 100 MW atmospheric SOFC and gas turbine hybrid power generation cycle. Performance and economics of these cycles are studied in details. Simulation of each process is performed using the commercial process simulation package, AspenPlus^{TM}. The results demonstrate that with 7-10% efficiency penalty in CO_2 capture and sequestration, the overall system efficiency of the studied atmospheric SOFC based power generation cycles can still reach 60% with 100% CO_2 recovery. A preliminary economic study indicated that the current cost of the SOFC stack need to be further reduced to become competitive in terms of capital cost investment, cost of electricity generation as well as cost of capturing CO_2.

2.0 Literature Review

2.1 Overview of Fuel Cell Technology

2.1.1 History of Fuel Cells

In 1839 Sir William Grove (often referred to as the "Father of the Fuel Cell") discovered that it may be possible to generate electricity by reversing the electrolysis of water. He discovered that by arranging two platinum electrodes with one end of each immersed in a container of sulphuric acid and the other ends separately sealed in containers of oxygen and hydrogen, a constant current would flow between the electrodes. He named this device a "gas battery"– the first fuel cell (Carrette, Friedrich and Stimming, 2001).

It was not until 1889 that two researchers, Charles Langer and Ludwig Mond, coined the term "fuel cell" as they were trying to engineer the first practical fuel cell using air and coal gas. While further attempts were made in the early 1900s to develop fuel cells that could convert coal or carbon into electricity, the advent of the internal combustion engine temporarily delayed further development of the fledgling technology (http://www.sae.org/technology/fuelcells-history.htm).

In 1932, Francis Bacon developed what was perhaps the first successful fuel cell device, with a hydrogen-oxygen cell using alkaline electrolytes and nickel electrodes - inexpensive alternatives to the catalysts used by Mond and Langer. A significant advance in fuel cell technology came from NASA. In the late 1950's, NASA needed a compact way to generate electricity for space missions. Nuclear was too dangerous, batteries were too heavy, and solar power was too cumbersome. The answer was fuel cells. NASA went

on to fund 200 research contracts for FC technology. Fuel cells now have a proven role in the space program, after supplying electricity to several space missions. (http://www.corrosion-doctors.org/FuelCell/History.htm, http://www.sae.org/technology/fuelcells-history.htm).

In the recent decades, the increasing concerns about depleting stocks of natural resources and a growing awareness of the environmental consequences of burning of fossil fuels drive the development of fuel cell technologies for both transport and stationary power generations. Fuel cells now are considered as one of the most promising power generation technology for the future.

2.1.2 Basic Principles of Fuel Cells

A fuel cell is an electrochemical device that converts the chemical energy of a reaction between a fuel (e.g. hydrogen, natural gas, methanol, and gasoline) and an oxidant (air or oxygen) directly into useable electricity. A fuel cell consists of a cathode (negatively charged electrode), an anode (positively charged electrode), an electrolyte and an external load. The anode provides an interface between the fuel and the electrolyte, catalyzes the fuel reaction, and provides a path through which free electrons are conducted to the load via the external circuit. The cathode provides an interface between the oxygen and the electrolyte, catalyzes the oxygen reaction, and provides a path through which free electrons are conducted from the load to the oxygen electrode via the external circuit. The electrolyte acts as the separator between fuel and oxygen to prevent mixing and, therefore, preventing direct combustion. It completes the electrical circuit of transporting ions

between the electrodes (http://www.fuelcellonline.com/basics.htm). As gaseous fuels continuously pass over the anode and the oxygen or air pass over the cathode, the electrochemical reactions take place at the electrodes to generate electricity, by products, primarily water, carbon dioxide and heat. Depending on the input fuel and electrolyte, different chemical reactions will occur.

Using Solid Oxide Fuel Cell (SOFC) technology as an example (refer to Figure 2-1), the cell is constructed with two porous electrodes with an electrolyte in the middle. Air flows along the cathode. When an oxygen molecule contacts the cathode/electrolyte interface, it catalytically acquires four electrons from the cathode and splits into two oxygen ions. The oxygen ions diffuse into the electrolyte material and migrate to the other side of the cell where they encounter the anode. The oxygen ions encounter the fuel at the anode/electrolyte interface and react catalytically, giving off water, carbon dioxide, heat, and most importantly, electrons. The electrons transport through the anode to the external circuit and back to the cathode, providing a source of useful electrical energy in an external circuit.

Note that the electricity generation process continues as long as the fuel and air are supplied to the cell. Unlike batteries, which active elements are consumed by the chemical reaction, fuel cells in principle have much longer service lifetimes and can be continuously recharged with reactants.

.

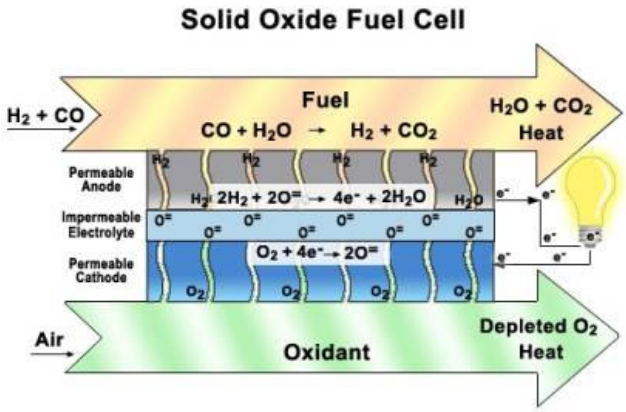

Figure 2-1: Operating Concept of a SOFC (http://www.seca.doe.gov)

2.1.3 Major Types of Fuel Cells

There are a variety of fuel cells that are in different stages of development. The most common classification of fuel cells is by the type of electrolyte used in the cells and includes:

- Polymer Electrolyte Fuel Cell (PEFC)

  The electrolyte in this fuel cell has an ion exchange membrane that is an excellent proton conductor. The limitation of the polymer requiring that it be hydrated with liquid water means that its operating temperature is usually less than 120°C. The PEFC offers an order of magnitude higher power density than any other fuel cell system, with the exception of the advanced aerospace alkaline fuel cell, which has comparable performance. This represents a potential for a significant reduction in stack size and cost over that possible for other systems.

  The PEFC can operate on reformed hydrocarbon fuels with minimum or no CO, with pre-treatment, and on air. The use of a solid polymer electrolyte eliminates the

corrosion and safety concerns associated with liquid electrolyte fuel cells. Its low operating temperature (80°C) provides instant start-up and requires no thermal shielding to protect personnel. High catalyst loading, usually platinum, is required for both the anode and cathode. Carbon monoxide (CO) poisons the catalyst, so the fuel should not contain significant concentrations of CO. Recent advances in performance and design offer the possibility of lower cost than any other fuel cell system (www.kettering.edu).

- Alkaline Fuel Cell (AFC)

  The electrolyte in this fuel cell is concentrated (85 wt%) KOH in fuel cells operating at high temperature, or less concentrated (35-50 wt%) KOH for lower temperature (<120°C) operation (EG&G, 2002). The fuel supply is limited to non-reactive constituents except for hydrogen. Both CO and CO_2 shouldn't be present in the fuel as they form participates in the electrolyte.

  AFCs can achieve power generating efficiencies of up to 70 percent. They were used on the Apollo spacecraft to provide both electricity and drinking water. Until recently they were too costly for commercial applications, but several companies are examining ways to reduce costs and improve operating flexibility. They typically have a cell output from 300 watts to 5 kW (www.kettering.edu).

- Phosphoric Acid Fuel Cell (PAFC)

  The PAFC is the most mature fuel cell technology in terms of system development and commercialization activities, although PEFC technology development as

displaced this technology in many programs do to its lower life cycle cost. The electrolyte in this fuel cell is 100% concentrated phosphoric acid, which operates at 150 to 200°C.

PAFCs generate electricity at more than 40% efficiency -- and nearly 85% of the steam this fuel cell produces can be used for cogeneration. One of the main advantages to this type of fuel cell, besides the nearly 85% cogeneration efficiency, is that it can use impure hydrogen as fuel. PAFCs can tolerate a CO concentration of about 1.5 percent, which broadens the choice of fuels they can use. Existing PAFCs have outputs up to 200 kW, and 1 MW units have been tested (www.fuelcells.org).

- Molten Carbonate Fuel Cell (MCFC)

  The electrolyte in this fuel cell is usually a combination of alkali carbonates. The fuel cell operates at 600-700°C where the alkali carbonates form a highly conductive molten salt, with carbonate ions providing ionic conduction. At the high operating temperature, noble metals are not required for electrodes (EG&G, 2002).

  The high operating temperature of the MCFC offers the possibility that it could operate directly on gaseous hydrocarbon fuels such as natural gas. The natural gas would be reformed to produce hydrogen within the fuel cell itself. The MCFC also produces excess heat at a temperature which is high enough to yield high pressure steam which may be fed to a turbine to generate additional electricity. In combined cycle operation, electrical efficiencies in excess of 60% have been suggested for mature MCFC systems (www.kettering.edu).

- Solid Oxide Fuel Cell (SOFC)

  The electrolyte in this fuel cell is a solid, nonporous metal oxide, usually Y_2O_3-stablilzied ZrO_2. The cell operates at 1000°C where ionic conduction by oxygen ions takes place. The ceramic, solid-phase electrolyte reduces corrosion considerations and eliminates the electrolyte management problems associated with liquid electrolyte fuel cells. At 1000 °C, internal reforming of carbonaceous fuels is possible, and the waste heat from SOFC system would be easily utilized by conventional thermal electricity generating plants to achieve excellent fuel efficiency. SOFC power generating efficiencies could reach 60% and 85% with cogeneration.

Operating temperature is a critical parameter that determines the potential uses of each type of fuel cell. For instance, low temperature fuel cells such as AFC and PEFC have potential applications in transport applications because they do not produce much heat and have a very short start-up period and modulate the electrical output. On the other hand, PAFC, MCFC and SOFC producing high temperature heat are more complex to run and are better fit for stationary applications like power generation or combined heat and power (CHP) (www.europa.eu.int).

Table 2-1 summarizes the major differences of the fuel cell types as well as their advantages and disadvantages.

Table 2-1: Summary of Major Difference of the Fuel Cell Types

(EG&G, 2002; http://europa.eu.int/; Fowler 2000)

	Electrolyte	Operating Temp.	Charge Carrier	Prime Cell Components	Catalyst	Advantages	Disadvantages	Electrical Efficiencies	Area for Further Development
PEFC	Ion Exchange Membranes	80°C	H^+	Carbon-based	Platinum	• Solid electrolyte reduces corrosion, gas crossover and electrolyte management issue. • Low temperature so startup quickly, no heat management issue. • High current densities.	• High platinum loading (cost) • Low tolerance for CO	40%-50%	• Intolerance of the catalyst to CO and SO_2 • Decrease cost, thickness and weight of bipolar plates • Membrane improvement • Improvement in hydrogen utilisation from the reformate flow • Investigation of alloying components and their effect on over voltage. • Utilizing new medium temperature membranes 200-300C.
AFC	Mobilized or Immobilized Potassium Hydroxide	65°C-220°C	OH^-	Carbon-based	Platinum	• Flexibility over a wide range of catalysts. • Active O_2 electrode kinetics	• Can't tolerate CO_2, thus only accept pure H_2 and O_2. • High Cost	55%-65%	• Reduce cost • Improve operating flexibility
PAFC	Immobilized liquid Phosphoric Acid	205°C	H^+	Graphite-based	Platinum	• Co-generation is feasible • Less sensitive to CO (<5%) • CO2 does not react	• High cost • Large weight and size • Low current density • Require external reformer to product H2	37%-42%	• Increase power density • Increase life time of stacks • Develop new stack components with loser cost materials and processes

	Electrolyte	Operating Temp.	Charge Carrier	Prime Cell Components	Catalyst	Advantages	Disadvantages	Electrical Efficiencies	Area for Further Development
MCFC	Immobilized Liquid Molten Carbonate	650°C	$CO3^{=}$	Stainless-based	Nickel	• High temperature – less costly fabrication, inexpensive nickel catalyst, internal reforming possible and allow cogeneration • CO is usable fuel • Operate efficiently with CO_2 containing fuel.	• Corrosive and mobile electrolyte • Low Sulfur tolerance • High temperature promote material problem and mechanical stability	50%-60%	• Anode creep and sintering under compression; • Cathode dissolution (NiO) and reduction of dissolved nickel to a metal particle precipitate in the electrolyte matrix; • Corrosion of steel separator plate on the anode side; • Electrolyte migration in the external manifold; • Pressure optimisation • Selection of reforming type • Use of different fuels (coal mine methane, naphtha.
SOFC	Ceramic	800°C- 1000°C	$O^{=}$	Ceramic	Perovskites	• High temperature – allow internal reforming, which is beneficial to the system efficiency and co-generation • CO is usable fuel • No liquid electrolyte • Low cost materials an catalysts	• High temperature promote material problem and mechanical stability	45-55%	• Manufacturing technology for the ceramic components (especially firing of the thin flat plates; • Internal vs. external reforming • Operation data collection, for a number of critical variables; • Control procedures for stack operation.

2.1.4 Benefits of Fuel Cells

Fuel Cells offer many characteristics that make them promising and attractive as energy conversion devices:

- High fuel efficiency

  Fuel cells directly convert fuel into energy through an electrochemical reaction. Combustion-based energy generation first converts the fuel into heat, and then into mechanical energy, which provides motion or drives a turbine to produce energy.

  Efficiencies of present fuel cell plants are in the range of 40-55% based on the lower heating value (LHV) of the fuel. Hybrid fuel cell/reheat gas turbine cycles that offer efficiencies greater than 70% of LHV have been proposed (EG&G, 2002).

- Low Emissions

  Because fuel cells are efficient, CO_2 emissions are reduced for a given power output. The fuel cell is quiet, emitting only 60 decibels. Emissions of SOx and NOx are 0.003 and 0.0004 pounds/megawatt-hour respectively. These emissions are two or three orders of magnitude lower than conventional cycles.
  (http://www.cheresources.com/fuelcell.shtml)

- Operation Flexibilities and Engineering Simplicities

  Fuel cells are capable of operating on hydrogen, or hydrogen reformed from any of the common fossil fuels available today. They can be located in a variety of areas, both residential and commercial, inside and outside.

Fuel cells operate at a constant temperature, and the heat from the electrochemical reaction is available for cogeneration applications. Moreover, fuel cells operate at nearly constant efficiency, independent of size; small fuel cell plants operate nearly as efficiently as large ones.

Fuel cell stacks do not contain any moving parts. The lack of movement allows for a simpler design, higher reliability, quiet operation and a system that is less likely to fail.

2.1.5 Market Barriers of Fuel Cell Technologies

Although fuel cells could offer numerous benefits, there are still impediments for their widespread use:

- High market entry cost. The cost of the fuel cell plants is still higher (in some cases by one order of magnitude) than comparable conventional technologies;
- Lack of familiarity of the technology by potential users;
- Durability requirements have yet to be demonstrated. Thus fuel cell are a high risk investment as most of these technologies do not guarantee minimum length of operation and demonstration projects have not accumulated a substantial number of operating hours; and,
- Little hydrogen production or distribution infrastructure is currently available

2.2 Introduction of Solid Oxide Fuel Cell (SOFC)

SOFCs are becoming the most desirable fuel cell for generating electricity from hydrocarbon fuels. It is simple, highly efficient, tolerant to impurities, and can at least partially internally reform hydrocarbon fuels. SOFCs have no liquid electrolyte which avoids material corrosion and electrolyte management problem. Due to its high operating temperature, SOFCs have great adaptability with respect to fuel choice, thus reducing operating costs and infrastructure concerns. SOFC plants can also produce high quality by-product heat for cogeneration or for use in a bottoming cycle, therefore high overall fuel use efficiency can be achieved (>80% with co-generation).

2.2.1 SOFC Designs

SOFCs are composed of all-solid-state materials – the anode, cathode and electrolyte are all made from ceramic substances. The solid state character of all SOFC components means that, in principal, there is no restriction on the cell configuration. Instead, it is possible to shape the cell according to criteria such as overcoming design or application issues (EG&G, 2002).

Two possible design configurations for SOFCs have emerged: a planar design (Figure 2-2) and a tubular design (Figure 2-3). In the planar design, the components are assembled in flat stacks, with air and fuel flowing through channels built into the cathode and anode. In the tubular design, components are assembled in the form of a hollow tube, with the cell constructed in layers around a tubular cathode; air flows through the inside of the tube and fuel flows around the exterior.

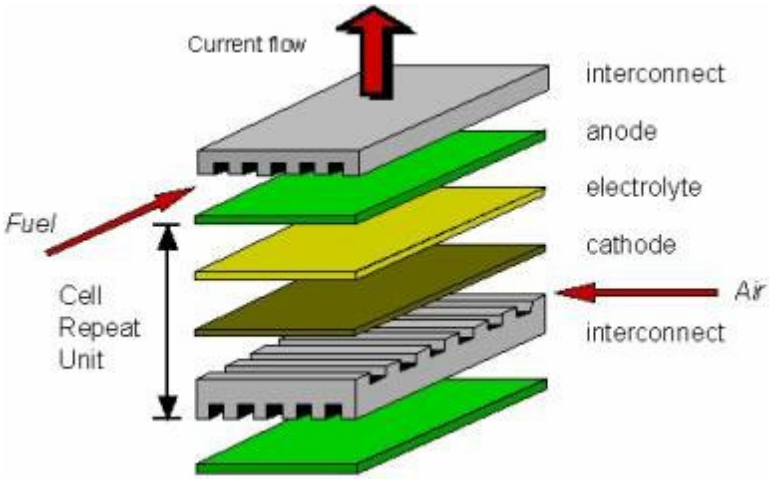

Figure 2-2: Planar SOFC Design (http://www.csa.com/hottopics/fuecel/overview.php)

The planar designs are at an earlier stage of development than the tubular designs. They are simpler to manufacture and consist of flat plates bonded together to form the electrode-electrolyte assemblies. The planar design offers lower ohmic resistance and higher power densities compared to the tubular design, but typically requires high temperature seals and they are not as robust (especially under pressurized conditions). Companies pursuing these concepts in the U.S. are GE, Ceramatec, Inc., Technology Management, Inc., SOFCo, Ztek, Inc. and Versa Power Systems. There are at least seven companies in Japan, eight in Europe, and two in Australia developing this SOFC technology.

Tubular SOFC designs are closer to commercialization and are being produced by Siemens Westinghouse Power Corporation (SWPC), and a few Japanese companies. The tubular SOFC design constructs the stack as a bundle of tubular electrode-electrolyte assemblies. Air is introduced to the inside of each tube and fuel flows around the outside of the tubes to produce electricity. The primary advantage of the tubular design is that it

does not require high temperature seals. Stacks and systems of the tubular design have operated over total of 100,000 hours and have exhibited very little cell degradation (Brouwer, 2002).

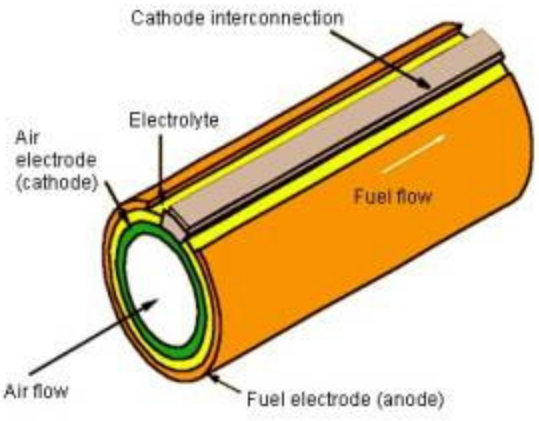

Figure 2-3: Tubular SOFC Design (http://www.csa.com/hottopics/fuecel/overview.php)

Although the operating concept of SOFCs is rather simple, the selection of materials for the individual components presents enormous challenges. Each material must have the electrical and catalytic properties required to perform its function in the cell and there must be enough chemical and structural stability to endure fabrication and operation at high temperatures.

- Anode

  The anode of a SOFC is to provide a surface site where ionization or de-ionization reactions can take place and conduct ions and electrons away from or into the electrode/electrolyte interface. Therefore, its material should be catalytic as well as conductive, porous to hydrogen and the appropriate fuel. It also must function in a

reducing atmosphere and its thermal expansion must compatible with the other cell materials. Ni-YSZ is currently the anode material of choice (EG&G, 2002).

- Cathode

  Similar to the anode, the cathode is a porous structure that must permit rapid mass transport of reactant and product gases. Doped lanthanum manganite is the most commonly used material for the cathode. These perovskites only offers electronic conductivity (no ionic conductivity). It is a desirable feature since the electrons from the open circuit flow back through the cell via the cathode to reduce the oxygen molecules, forcing the oxygen ions through the electrolyte(EG&G, 2002).

- Electrolyte

  The electrolyte conducts ionic charges between the electrodes and thereby completes the cell electric circuit. It also provides a physical barrier to prevent the fuel and oxidant gas from directly mixing. Therefore, the electrolyte must possess a high ionic conductivity and no electrical conductivity. It must be free of porosity to prevent gas from permeating from one side of the electrolyte layer to the other and it should also be as thin as possible to minimize resistive losses in the cell. As with the other materials, it must be chemically, thermally, and structurally stable across a wide temperature range. YSZ is so far the most suitable electrolyte material found (EG&G, 2002).

- Interconnection

  The cell interconnection is exposed to both the cathode and anode, thus, it must be chemically stable in both environments at 1000°C. It must also be impervious to fuel

and oxidant gases and must poses good electronic conductivity. Doped lanthanum chromite is most commonly used for the interconnection material (EG&G, 2002).

2.2.2 SOFC Fundamentals

Hydrogen as well as carbon monoxide (CO) and hydrocarbons such as methane (CH_4) can be used as fuels in SOFC. The fuel stream reacts with oxide ions (O^{2-}) from the electrolyte to produce water or CO_2 and to deposit electrons into the anode. The electrons pass outside the fuel cell, through the load, and back to the cathode where oxygen from air receives the electrons and is converted into oxide ions which are injected into the electrolyte.

The electrochemical reactions in SOFC include:

At anode:

$$H_2 + O^{2-} \rightarrow H_2O + 2e^- \quad \text{(R2-1)}$$

$$CO + O^{2-} \rightarrow CO_2 + 2e^- \quad \text{(R2-2)}$$

$$CH_4 + 4O^{2-} \rightarrow 2H_2O + CO_2 + 8e^- \quad \text{(R2-3)}$$

At cathode:

$$O_2 + 4e^- \rightarrow 2O^{2-} \quad \text{(R2-4)}$$

The overall cell reactions are:

$$H_2 + \frac{1}{2}O_2 \rightarrow H_2O \quad \text{(R2-5)}$$

$$CO + \frac{1}{2}O_2 \rightarrow CO_2 \quad \text{(R2-6)}$$

$$CH_4 + 2O_2 \rightarrow 2H_2O + CO_2 \quad \text{(R2-7)}$$

It is worth noting that, at 1000°C, direct oxidation of the CO and CH_4 contained in the pre-reformed fuel is feasible in the SOFC without a catalyst, but it is less favoured than the water gas shift of CO to H_2 and reforming of CH_4 to H_2. It is common system analysis practice to assume that H_2, the more readily oxidized fuel, is the only fuel electrochemically reacting in the SOFC (EG&G, 2002).

2.2.3 SOFC Performance

To understand SOFC performance ideal conditions and reactions are considered firstly. Once the ideal performance is defined, the actual performance can be determined after deducting the losses.

The ideal performance of the SOFC is defined by its Nernst potential represented as cell voltage. The following Nernst equation (E2-1) provides a relationship between the ideal standard potential (E°) for the SOFC cell reaction (assuming H_2 is the only fuel electrochemically reacting in SOFC) and the ideal equilibrium potential (E) at other temperatures and partial pressure of reactants and products. The ideal standard potential of an H_2/O_2 fuel cell (E°) is 1.18 volts with water product in gaseous state. The ideal potential for a SOFC at 1000°C is 1 volt (EG&G, 2002).

Nernst Equation:

$$E = E^o + \frac{RT}{2F}\ell n\frac{P_{H_2}P_{O_2}^{1/2}}{P_{H_2O}} \qquad \text{(E2-1)}$$

Where P_i represents the partial pressure of reactants and products;

R is the ideal gas constant

F is the Faraday constant

The actual voltage of a SOFC is less than its ideal potential because of irreversible losses including:

- Activation Polarization (losses) – this polarization occurs when the rate of an electrochemical reaction at an electrode surface is controlled by sluggish electrode kinetics. It is a dominant loss at low current density because the electronic barriers have to be overcome prior to current and ion flow.
- Concentration Polarization (losses) - This loss is due to the inability of the surrounding material to maintain the initial concentration of the bulk fluid as a reactant is consumed at the electrode. This loss occurs over the entire range of current density, but become prominent at high currents where it becomes difficult to provide enough reactant flow to the reaction sites.
- Ohmic Polarization (losses): This loss occurs because of resistance to the flow of ions in the electrolyte and resistance of electrons through the electrode materials. It increases as the current increases. Ohmic loss is the dominant loss in SOFCs due the limited conductivity of the ceramic electrolyte.

Due to these voltage losses, the actual voltage that a SOFC can deliver is normally between 0.7 to 0.8 volts at 100-150 mA/cm^2 current density.

Numerous studies have been done in developing large and complex computer models that make use of fundamental physical phenomenon to predict the performance of fuel cells

based on the details of the cell component, stack design and operating conditions. Most codes are proprietary and cumbersome for use in system analysis. One simple approach that is often taken for system studies is to develop empirical or semi-empirical correlations from thermodynamic modeling that depict cell performance based on various cell operating conditions, such as temperature, pressure and gas constituents.

For tubular SOFC, the following correlations are commonly used (Campanari, 2001; EG&G, 2002):

- Operating Pressure

$$\Delta V_p(mv) = 76 \times \ell og \frac{P}{P_{ref}} \quad \text{(E2-2)}$$

Where P is the operating pressure (1-10 bar) and P_{ref} is the reference operating pressure.

- Operating Temperature and Current Density

$$\Delta V_T(mV) = 0.008 \times (T - T_{ref})(^oC) \times I_c(mA/cm^2) \quad \text{(E2-3)}$$

Where T is the operating temperature (950-1050°C), I_c is the current density in mA/cm^2 and T_{ref} is the reference operating temperature.

- Fuel Composition

$$\Delta V_{anode}(mV) = 172 \times \ell og \frac{P_{H_2} / P_{H_2O}}{(P_{H_2} / P_{H_2O})_{ref}} \quad \text{(E2-4)}$$

Where P_{H_2} / P_{H_2O} is the ratio of H_2 and steam partial pressure in the system and (P_{H_2} / P_{H_2O})$_{ref}$ is ratio of H_2 and steam partial pressure in the system under reference condition.

- Oxidant Composition

$$\Delta V_{Cathod}(mv) = 92 \times \ell og \frac{(P_{O_2})}{(P_{O_2})_{ref}} \quad \text{(E2-5)}$$

Where P_{O_2} and $(P_{O_2})_{ref}$ are the average oxygen partial pressure at the cathode for the actual case and the reference case, respectively.

The actual voltage of a SOFC can then be estimated based on the above correlations as:

$$V_C(mv) = V_{ref} + \Delta V_p + \Delta V_T + \Delta V_{Cathod} + \Delta V_{anode} \quad \text{(E2-6)}$$

Section 3 of this thesis introduces a new approach in SOFC model development using the commercial simulation software - AspenPlus™. This approach fully utilizes the existing capabilities of the process simulator and provides a convenient way to perform detailed thermodynamic and parametric analysis of SOFC based power generation cycles. It is developed using the correlations mentioned above.

2.2.4 The Future of SOFCs

Due to their high-energy conversion efficiency (up to 40-60%), low toxic emission, and flexibility in fuel choice (e.g. natural gas, diesel, gasoline, liquid petroleum gas, biomass, hydrogen), SOFCs are being developed for the whole range of possible applications: stationary, transportation (or mobile), military, and portable. They are expected to play a significant role in residential combined heat and power (CHP) applications (1 to 10 kW) and commercial CHP applications (up to 250 kW), or power plant stationary applications. To a limited extent SOFCs are likely to find applications in both trucks and automobiles

as auxiliary power generators. In addition, SOFCs are of high interest to the military because they can be established on-site in remote locations, are quiet, non-polluting and could significantly reduce deployment costs, and can make use of existing military logistical fuels (Colson-Inam, 2003; De Guire, 2003).

The main challenges that SOFC has to overcome to reach full commercialization within the next decade or so are cost, reliability, and performance (especially with respect to fast thermal cycling). Although great progress has been made in the last 10 years, it is very important to have further materials and technical improvements in design toward lower manufacturing, system costs and develop electrolyte materials that can operate at lower temperatures with high ionic conductivities. In addition, as with other fuel cell systems, the development of a proper parallel fuel delivery support structure (fuel infrastructure and distribution channels) is critical (Colson-Inam, 2003).

In the fall of 1999, a Solid State Energy Conversion Alliance (SECA) program was launched by the US Department of Energy (DOE). This program was created to accelerate the development of SOFCs and get them to the market as quickly as possible while making them an affordable option for energy generation. The goal of this program is to deliver SOFCs that provide 3-10kW at a cost of $400 or less per kilowatt by 2010, nearly a factor of 10 less than the cost of today's SOFC designs (about $4500/kW). The key players in this program include Siemens Westinghouse, Delphi Automotive and General Electric Power Systems. According to SECA, the long term goal is to produce 100MW

scale hybrid SOFC systems by 2020, where efficiencies are increased by using waste heat to drive turbines and generate additional electricity (www.fossil.energy.gov).

There is little doubt that SOFC technology will be implemented. According to SECA, SOFC should be ready to move from 'research and development' to pre-commercialization stages in 2005 and then mass-commercialized around 2010 for stationary applications. Commercial mobile applications are not foreseen until 2015-2020. Global market value of SOFC is forecasted to reach $347 millions by 2008 with an average annual growth rate of 22% per year within the North American market. Analysts expect that the overall market for fuel cell technology could reach $95 billion by the year 2010 (De Guire, 2003; Colson-Inam, 2003).

2.3 SOFC Based Power Generation Systems

As other types of fuel cells, a SOFC produces only DC power and requires processed fuel. It also produces high quality heat due to its high operating temperature. Beyond the SOFC stack itself, a typical SOFC power system includes: a reformer to start the hydrogen production process, a fuel conditioner to cleanup the pollutants that could otherwise poison the fuel cell elements, a power conditioner to convert direct current from the fuel cell to the appropriate voltage range and current type depending on the application., and a cogeneration or bottoming cycle to utilize the rejected heat to achieve high system efficiency. The system also requires the most common balance of plant equipments such as heat exchangers, air blower and fuel compressors, controls systems, and safety systems.

2.3.1 Fuel Processing

Fuel processing converts a commercially available fuel to a fuel gas suitable for the fuel cell anode reaction. Typical fuel processing steps include:

- Desulphurization, where a catalyst is used to remove sulphur contaminants in the fuel. Sulphur compounds are noxious, and they can also bind catalysts used in later stages of fuel reformation poisoning the catalyst.
- Reformation, where the fuel is mixed with steam and then passed over a catalyst to break it down into hydrogen, as well as carbon dioxide and carbon monoxide,
- Shift conversion, where the carbon monoxide reacts with steam over a catalyst to produce more hydrogen and carbon dioxide.

Low temperature fuel cells (e.g. PEFC, PAFC.) use noble-metal catalyst electrodes, which must be fed with a high purity hydrogen fuel. This requires all the steps above in order to provide the necessary pre-processing for hydrocarbon fuels, and the CO levels fed to the fuel cell stack must be very low. It is a complex and expensive fuel processing system and the energy consumed in performing this processing also limits the overall system efficiency. On the other hand, high operating temperature SOFCs can accommodate internal reforming by means of a CO-tolerant nickel catalyst, so they can operate on natural gas with minimum pre-processing of the fuel. This will not only reduce the capital cost of the SOFC system, but also can be beneficial to system efficiency because there is an effective transfer of heat from the exothermic cell reaction to satisfy the endothermic reforming reaction.

Hydrogen sulfide, hydrogen chloride and ammonia are impurities typically found in coal gas. Some of these substances maybe harmful to the performance of SOFCs (EG&G, 2002). Therefore a SOFC system will require fuel cleanup equipment such as desulfurizer depending on the raw fuel components.

2.3.2 Rejected Heat Utilization

At 1000°C operating temperature, SOFCs produce a tremendous amount of waste heat while generating electricity. In order to obtain the highest possible system efficiency, the heat must be recovered by producing hot water, steam, or additional electricity. In a large SOFC power system (>100MW), production of electricity via a steam turbine bottoming cycle maybe advantageous. In pressurized fuel cell systems, it may also be advantageous to utilize a gas turbine before the steam generation (EG&G, 2002).

2.3.3 Power Conditioners

A power conditioner for a fuel cell power plant used to supply AC rated equipment includes DC to AC inversion and current, voltage and frequency control. Transient response control equipment may also be included. The efficiency of the power conversion is typically on the order of 94 to 98% (EG&G, 2002).

2.3.4 Status of SOFC Power Systems Development

The design of a SOFC power generation system involves more than the optimization of the SOFC unit with respect to efficiency or economics. It also involves balance of plant study and system integration and optimization. As SOFC materials and stacks approach a

commercialization stage, more and more SOFC based power systems are proposed, developed and demonstrated. Below are some highlights of these systems:

Tubular SOFC

(Haines, etc 2002; www.powergeneration.**siemens**.com/en/fuelcells/demonstrations,)

- In December 1997, an 100 kW atmospheric SOFC power generation system supplied by Siemens Power Generation began operation in the Netherlands under a program with a consortium of Dutch and Danish utilities (EDB/ELSAM), where it operated for 16,667 hours at a peak power of ~140 kW with 109 kW fed into the local grid and 64 kW of hot water into the local district heating system and operated consistently at an electrical efficiency of 46%. In March 2001, the system was moved from the Netherlands to a site in Essen, Germany, where it was operated by the German utility RWE for an additional 3,700 hours, for a total of over 20,000 hours.
- In year 2003, a 250 kW CHP system, the largest atmospheric pressure SOFC system ever built, began operation in Toronto, Canada, at the test facilities of Kinectrics Inc. The system demonstration was sponsored by Ontario Power Generation, the US Department of Energy and Natural Resources Canada. Kinectrics, Inc. was responsible for system integration at the Kippling test facility in Toronto. The system was designed by Siemens Power Generation, fabricated by both Siemens Power Generation and Kinectrics, and assembled in Kinectrics' facility in Toronto. Siemens Power Generation supplied the SOFC module and other equipment, and Kinectrics supplied the rest of the balance of plant systems to Siemens Power Generation specifications. As of 2004 the system has operated for more than 1,100 hours.

- In June 2000, Siemens Power Generation delivered the world's first SOFC/gas turbine hybrid system to Southern California Edison for operation at the University of California, Irvine's National Fuel Cell Research Center. The hybrid system included a pressurized SOFC module integrated with a microturbine/generator supplied by Ingersoll-Rand Energy Systems. The system had a design output of 220 kW, with 200 kW from the SOFC and 20 from the microturbine generator. It operated for nearly 3400 hours, and achieved an electrical efficiency of approximately 53%.
- By year 2003, Siemens-Westinghouse has demonstrated in Pittsburgh, USA, a nominal 300 kW SOFC/Gas Turbine hybrid system for more than 3,000 hours and achieved an electrical efficiency of 53%.
- In 2004, a 250 kW atmospheric CO_2 separating SOFC demonstration unit was developed. The feasibility study indicated that this pressurized hybrid system would allow efficiencies to exceed 60% and possibly reach 70% on larger units. This demonstration project is funded mainly by A/S Norske Shell with some additional grant assistance from both the Norwegain Government and the US DOE.

Planar Solid Oxide Fuel Cell

- A fully integrated, thermally sustaining multi-kW system demonstration by SOFCo, through its partners Ceramatec and McDermott Technology is underway. The system integrates in one thermal enclosure the planar SOFC stacks with an advanced heat exchanger, a steam generator, a sulphur remover, a fuel processor, and a start-up burner. The initial system will deliver a 2 kW output operating on pipeline natural gas.

Further development of larger systems will be based upon scale-up of this unit in the 10-50 kW range (Khandkar et al. 1999)

In Section 4 of this thesis, five SOFC based power generation cycles are introduced and simulated in AspenPlus^{TM} based on the developed SOFC model. Simulations results are discussed in detail.

2.4 CO_2 Abatement from SOFC

2.4.1 Reduction of CO_2 emission

Carbon dioxide (CO_2) is by far the greatest contributor to climate change, accounting for about 64% of estimated current global warming due to the enhanced greenhouse effect. The primary sources of carbon dioxide emissions to the atmosphere are the production, transportation, processing, and consumption of fossil fuels (86%), tropical deforestation and other biomass burning (12%), and miscellaneous sources (2%), such as cement manufacturing and oxidation of carbon monoxide (Gurney,1998). Power plants are the biggest individual emitters of carbon dioxide.

Current CO_2 emission levels are expected to continue increasing for some years and, based on World Energy Council growth projections, emissions from all sources are estimated to grow by 36% in 2010 (to 18.24 Gt/y) and by 76% in 2020 to 23.31 Gt/y (compared to the 2000 base level).

According to Environment Canada, in year 1990, approximately 93% of total CO_2 emissions in Canada resulted from the combustion of fossil fuels. Between 1990 and 2003, the net increase in Canada's annual CO_2 emissions totalled about 126 Mt. Over the same period, emissions from the energy industries increased by 118 Mt, accounting for most of the overall increase. Therefore, the reduction of CO_2 emission from power plants and factories is one of the most important subjects in fighting global warming.

There are a number of options for reducing CO_2 emissions from power plants such as:

- Improving power generation efficiency;
- Switching to low or no-carbon fuel; and,
- Capturing CO_2 for sequestration

In most cases, improving efficiency and switching to low carbon fuel are cost-effective and will deliver useful reductions, but on their own, are unlikely to be enough. Greater reductions could be attained by switching to no-carbon fuels or energy sources based on renewable sources or nuclear power. However, the world is presently heavily dependent on the exploitation and use of fossil fuels, and there still exist large reserves of coal. For this reason, it is important that there should also be technology options that will allow for the continued use of fossil fuels without substantial emissions of CO_2. In this respect, one route forward would be the development and deployment of technologies for the capture and storage of CO_2 produced by the combustion of fossil fuels (IEA, 2001).

2.4.2 Benefits of SOFC technology for CO_2 Reduction

SOFC technology attracts more and more attentions as it offers a combination of benefits in the reduction of CO_2 emissions:

- High efficiency;
- Low or no carbon fuel ready; and
- Low cost CO_2 capture.

2.4.2.1 High efficiency

As Figure 2-4 indicates, the electric efficiency of fuel cells are higher than combustion-based power plants. The fuel-to-electricity efficiencies of solid oxide fuel cells are expected to be around 50 percent. If the hot exhaust of the cells is used in a hybrid combination with gas turbines, the electrical generating efficiency might exceed 70 percent. In applications designed to capture and utilize the system waste heat, overall fuel use efficiencies could top 80-85 percent. Moreover, SOFCs retain their efficiency at part load.

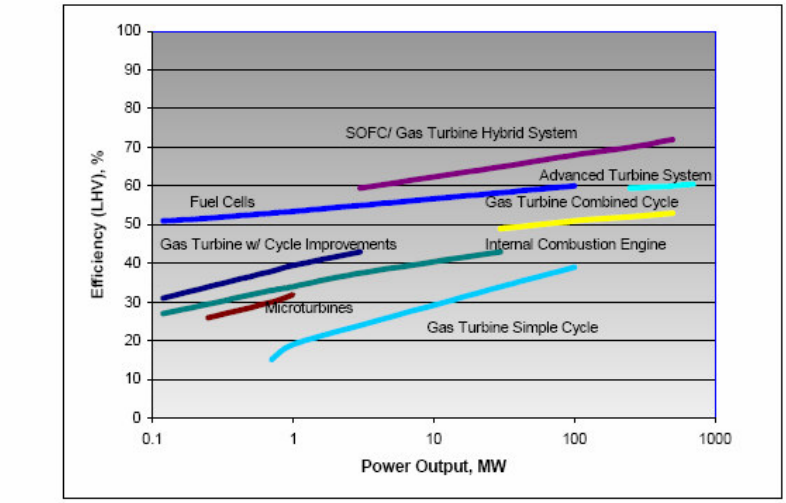

Figure 2-4: Estimated Efficiency of Different Power Generation Systems (EG&G, 2002)

The high efficiency of SOFC results in less fuel being consumed to produce a given amount of electricity, and thus lower emissions of carbon dioxide. Moreover, emissions

from SOFC systems will be very low with near-zero levels of NOx, SOx and particulates. Generally speaking, SOFCs provide the lowest emissions of any non-renewable power generation method such as traditional thermal power plants, as shown in Table 2-2 (Stambouli and Traversa, 2002).

Air emissions[a]	SO_X	NO_X	CO	Particles	Organic compounds	CO_2
Fossil fuelled plant	12,740	18,850	12,797	228	213	1,840,020
SOFC system	0	0	32	0	0	846,300

[a] kgs of emissions per 1650 MWh from one year full operation

Table 2-2: Typical SOFC plant air emissions from one year of operation

2.4.2.2 Low or no carbon fuel ready

Although high temperature fuel cells as SOFC have great flexibility in fuel options, H_2 driven SOFC can achieve higher electrical efficiencies and have no net emissions of CO_2. The electrical efficiency of a SOFC driven by hydrogen can reach 60% and a reduction of carbon dioxide emissions by more than 2 million kg per year can be obtained (Stambouli and Traversa, 2002).

2.4.2.3 Low cost in CO_2 capture

While the most important solutions to climate change will remain energy efficiency and cleaner energy sources, capturing and storing carbon dioxide can also play an important role in dealing with global warming.

Capture of CO_2 during power generation can be achieved by three main classes of process: pre-combustion, oxy-combustion and post combustion. Pre-combustion uses fuel

reforming to make hydrogen and CO_2 with recovery of CO_2 prior to combustion. Oxy-combustion uses pure oxygen to combust the fuel so that a steam/CO_2 exhaust, undiluted with nitrogen, is produced from which the CO_2 is easily recovered. Post combustion covers all those technologies which extract CO_2 from fuel gases, such as an amine absorption. These processes all suffer from high cost and reduction of generating efficiency because of their parasitic heat and electrical power needs. The post combustion processes are the most developed and have the lowest cost and smallest efficiency reduction. It still requires massive fuel gas scrubbers and consumes significant amounts of energy of regeneration of the absorption solvent (Haines et al., 2002). According to Dijkstra and Jansen (2004), typically, CO_2 capture with an amine absorption/desorption unit at a gas fired combined cycle results in an efficiency drop of 9%-points (16% relative), an investment increase of 59%, and in costs of 50–60 Euro/ton CO_2 captured. They also point out that the energy consumption of the amine absorption/desorption unit is mainly caused by the steam demand of the desorption step. The recovery of CO_2 is largely hindered by the dilution of the CO_2 with nitrogen from the combustion air.

A main factor spoiling the economics of CO_2 capture from the fossil fueled power plants is the low CO_2 content of the flue gas, which in the case of a gas turbine power plant is typically in the range of 3% (Langeland and Wilhemesen, 1993). Recovering CO_2 at this low concentration is expensive and requires significant amounts of energy, which reduces the power plant's net output by as much as 20% (Herzog, Drake and Adams, 1997). The reason for the low concentration is that the combustion processes uses air instead of pure

oxygen so the exhaust stream will contain huge amounts of nitrogen. To avoid dilution, pure oxygen instead of air has to be used but the cost for delivering oxygen is high.

SOFCs inherently feature a distinctive characteristic which offers a relevant advantage in CO_2 capture. The electrolytes transport oxygen ions from cathode to anode for oxidation of the fuel without mixing them with the air. The driving force for this oxy-combustion type process is oxidization process and hence no additional oxygen separation energy required compared with other oxy-combustion processes. Moreover, the absence of nitrogen increases CO_2 concentration in the fuel exhaust discharged from the SOFC, therefore reducing the energy cost related to its capture if compared to the case of conventional power plants.

Studies of SOFC with CO_2-capture have been performed earlier by several researchers. An excellent overview of the different concepts is given by Dijkstra and Jansen, 2004. This thesis pays special attention to post-fuel cell oxidation concept. It can achieve >90% of CO_2 recovery from the SOFC system by removing the H_2O, H_2 and CO contained in the nitrogen-free SOFC anode off-gas stream. Different oxidation methods under this concept are studied in details in section 5.0.

3.0 Simulation of SOFC Using AspenPlus™ Unit Operation Model

The goal of this thesis is to perform system analysis of SOFC based power generation processes that can generate electricity efficiently and produce economically a concentrated CO_2 stream for sequestration. A commercial process simulator, AspenPlus™ is chosen to conduct the studies. It contains rigorous thermodynamic and physical property database and provides comprehensive built-in process models, thus offering a convenient and time saving means for chemical process studies, including system modeling, integration and optimization. When using AspenPlus™ for a power generation cycle including a SOFC, one challenge is that SOFCs have not been included in its built-in models. Moreover, AspenPlus™ does not accommodate electrochemical reactions easily, and the stream mixing and transfer functions do not accommodate the transfer of ions. The current commercial process simulation software packages do not contain these features. In the literature, the most common SOFC system modeling approach using process simulators is to develop a complete SOFC stack model in a programming language, such as Fortran, Visual Basic or C++, first and then link it to AspenPlus™ or any other commercial simulator as a user defined model or subroutines (Riensche et al., 1998; Fuller and Chaney, 2000; Mozaffairan, 1994; Palsson et al., 2000). In this case, the user defined models or subroutines have to incorporate SOFC phenomena such as chemical/electro-chemical reactions, heat transfer and mass transfer in order to calculate the desired outputs for whole system analysis.

The approach introduced in this thesis is to develop a SOFC model by using existing AspenPlus™ functions and unit operation models without the requirement for linking

with other software. This approach fully utilizes the existing capabilities of the process simulator and provides a convenient way to perform detailed thermodynamic and parametric analysis of SOFC based power generation cycles. It can easily be extended to study the entire process, consisting of the SOFC and balance of plant. This model is based on the tubular internal reforming SOFC technology developed by Siemens-Westinghouse.

3.1 Siemens-Westinghouse Tubular SOFC technology

The Siemens Westinghouse tubular SOFC technology is a SOFC technology closest to commercialization.

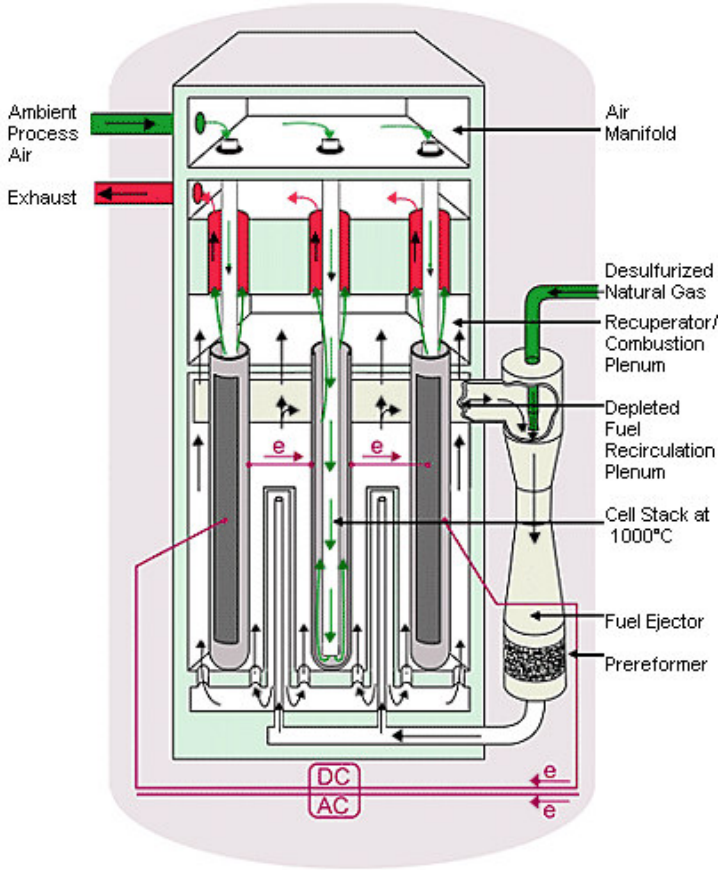

Figure 3-1: Sketch of a Tubular SOFC module

(http://www.powergeneration.siemens.com/en/fuelcells/technology/operation/index.cfm)

As Figure 3-1 shows, the key component of a natural gas feed tubular SOFC is a tubular solid oxide cell closed at one end with an effective length of 1500 mm, a diameter of 22 mm, a wall thickness of about 2 mm and an active area of about 834 cm^2 (Veyo and Fobes, 1998; Singhal, 1997). When operating at atmospheric pressure, 1000°C, 85% fuel utilization, and 25% air utilization, the electrochemical process can achieve up to 210W dc power output per cell. At an elevated pressure of 10 atm., maximum power output per cell can be increased by 10 per cent (www.powergeneration.siemens.com).

Air, the oxidant gas, is introduced into the cells via a central injector tube, and natural gas, the fuel gas is supplied at the exterior of the closed end tubular cells. The injection tube extends to the proximity of the closed end of the tube, and the oxidant flows back past the cathode surface to the open end. The fuel gas flows past the anode on the exterior of the cell and in a parallel direction to the oxidant gas to conduct electrochemical reactions (EG&G, 2002). At open circuit, a potential of about 1 volt will be generated. When an external circuit is connected, a current will flow in the external circuit that is in direct proportion to the flow of oxygen ions through the electrolyte. The fuel is oxidized electrochemically in complete isolation from atmospheric nitrogen with no potential for NOx production (www.powergeneration.siemens.com).

The cells are interconnected electrically to form bundles to generate commercially meaningful quantities of electricity. In-stack reformer sections are placed between rows of bundles to reform the hydrocarbon fuel coming from the pre-reformers located in the anode gas recycle loop, which converts the higher hydrocarbons and a small amount of

methane adiabatically to hydrogen and carbon monoxide (Veyo and Forbes, 1998; Riensche et al., 2000). The anode gas recycle loop, sustained by fresh fuel driven ejectors, provides the steam for the reforming reactions in the pre-reformer. The depleted gases are exhausted into a combustion plenum (so called afterburner) where the remaining active gases react, and the generated heat serves to preheat the incoming air stream. Part of the electrochemical reaction excess heat will directly support the endothermal reforming reactions instead of being transported via the cooling air (Riensche et al., 2000).

A standard Siemems-Westinghouse SOFC stack of 1152 cells can produce up to 200 kW dc with a nominal rating of 100 kw ac (Forbes et al., 2000).

3.2 Simulation of a Tubular SOFC Stack in AspenPlus™

The characteristics of the natural gas feed tubular SOFC stack described above are implemented in AspenPlus™ using standard, built-in unit operation modules and functions. The AspenPlus™ simulation flow sheet is shown in Figure 3-2. It includes all the components and functions contained in the SOFC stack, such as ejector, pre-reformer, fuel cell (anode and cathode) and afterburner. The simulation approach of each of the components is described below. In the following sections, terms in italics represent actual AspenPlus™ terminology.

3.2.1 Recirculation and Mixing of Fuel In the Ejector

Fresh desulfurized natural gas fed to the SOFC stack mixes with recycled anode gas containing the electrochemical reaction products (mostly H_2O and CO_2 but also some

amount of unreacted H_2 and CO). This mixed stream is then fed to the pre-reformers through the ejectors. The ratio of recycling is determined by a specified steam/carbon (S/C) ratio required for the pre-reformers (see Table 3-1). An AspenPlus™ *Mixer* and *Fsplitter* are used to simulate this process.

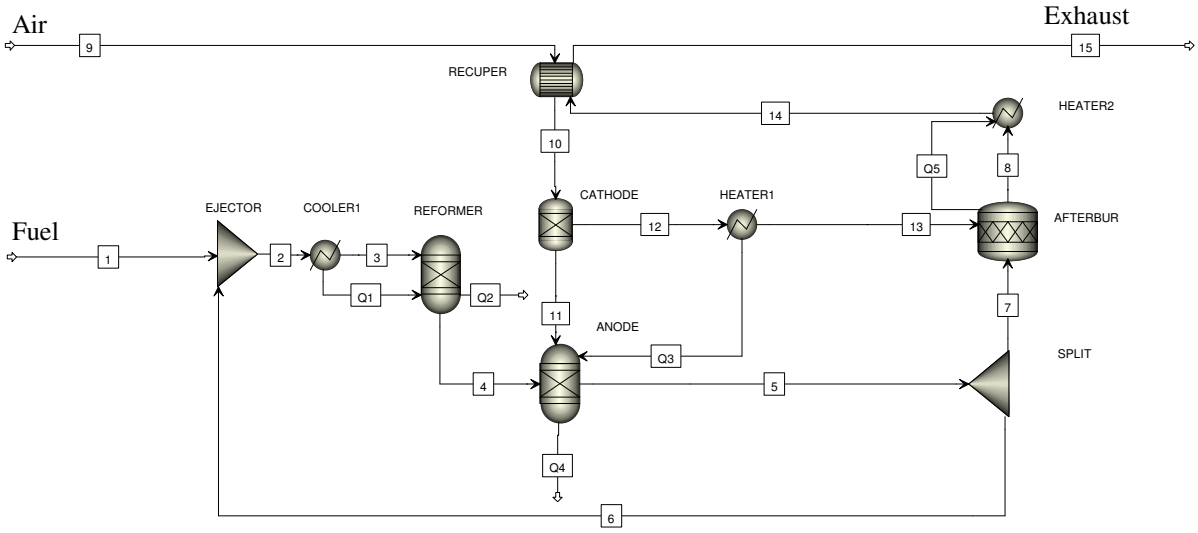

Figure 3-2: AspenPlus™ SOFC Stack Model Flowsheet
(solid lines represent material streams and dotted lines represent energy streams)

The feed stream (stream 1) to the *Mixer* block (named ‘‘EJECTOR’’) represents the fresh natural gas fuel feed into the SOFC. The recycling gas (stream 6) is split from the anode off-gas (steam 5) using the *Fsplitter* block (named ‘‘SPLIT’’). The fraction of the split is calculated to meet the desired S/C ratio value using AspenPlus™ *Design-spec* function (AspenPlus™ 12.1 User Guide). Another *Design-spec* is used to calculate the required inlet fresh fuel pressure P_{fresh} to drive recycling of the anode gas. In the current model, the calculation is based on an assumed ejector fresh fuel pressure ratio P_{fresh}/P_{cell} (see Table 3-1).

Table 3-1: Assumptions for the SOFC Stack Simulation

Fuel Inlet Composition (Campanari, 2001)	CH_4 81.3%, C_2H_6 2.9%, C_3H_8 0.4%, C_4H_{10} 0.2%, N_2 14.3%, CO 0.9%
Cell Operating Temperature	1000 ºC
Cell Operating Pressure (Veyo and Lundberg, 1999)	1.08 atm
Power Output (DC)	120 kW
Active Area (Veyo and Forbes, 1998)	96.1 m^2 (1152 Cells)
Cell Exhausts Temperature (streams 13 and 5)	910 ºC
Inlet Air Temperature (stream 9)	630 ºC
Inlet Fuel Temperature (stream 1)	380 ºC
After-burner Efficiency	100%
DC to AC Inverter Efficiency	91%
Overall Fuel Utilization Factor	85%
S/C ratio	2.5
Ejector Fresh Fuel Pressure Ratio	3
ΔT Between the Outlet of Cold and Hot Stream in the "RECUPER" Block	10 ºC
Pressure Drops inside the SOFC	0
SOFC Thermal Losses	5%

3.2.2 Pre-reforming of Mixed Fuel

Not only can complete internal reforming lead to carbon formation at the anode, but also, it can cause large temperature gradients due to the endothermic nature of the reforming reaction (Peters et al., 1999). To prevent this, a pre-reformer has to be included in the SOFC design. The higher hydrocarbons and a small amount of methane in the natural gas are converted in the adiabatic performer by steam reforming reactions, which result in a temperature decrease of the fuel gas. An AspenPlus™ equilibrium reactor module *Rgibbs* (named ''REFORMER'') is selected to simulate the reforming reactions occurring inside

the pre-reformer. An AspenPlus™ *Heater* module (named ‘‘COOLER1’’) is used to simulate the temperature decrease due to the overall endothermic reactions and predict the fuel gas temperature at the outlet of the pre-reformer. The chemical reactions specified in the pre-reformer block are:

Steam reforming reactions: $C_nH_{2n+2} + n\,H_2O \Leftrightarrow (2n+1)H_2 + nCO$ (R3-1)

Water-gas shift reaction: $CO + H_2O \Leftrightarrow CO_2 + H_2$ (R3-2)

As Figure 3-2 shows, the fuel gas entering ‘‘COOLER1’’ (stream 2) represents the fuel gas entering the pre-reformer. The temperature of the stream leaving ‘‘COOLER1’’ (stream 3) represents the fuel gas temperature at the exit of the pre-reformer. The ‘‘REFORMER’’ is specified to operate at this temperature. All reactions in the block are also specified to reach thermodynamic equilibrium at this temperature. By introducing a heat stream (Q1) from ‘‘COOLER1’’ into the ‘‘REFORMER’’, this temperature can be calculated by using an AspenPlus™ *Design-spec* to specify that the ‘‘REFORMER’’ net heat duty (Q2) equals zero. In other words, this temperature is selected to make sure that it is an adiabatic pre-reformer. Thus, the heat absorbed by the reactions is used to cool the fuel gas. The fuel gas leaving ‘‘REFORMER’’ (stream 4) represents the fuel gas leaving the adiabatic pre-reformers. Its temperature is equal to the ‘‘REFORMER’’ operating temperature, which is generally above 500°C to avoid large temperature gradients in the stack.

3.2.3 Internal Reforming and Electrochemical Reaction At the Anode

At 1000°C, direct oxidation of the CO and CH_4 contained in the pre-reformed fuel (stream 4) is feasible in the SOFC without a catalyst, but it is less favoured than the water gas shift of CO to H_2 and reforming of CH_4 to H_2 (EG&G, 2002). It is common system analysis practice to assume that H_2, the more readily oxidized fuel, is the only fuel electrochemically reacting. It is fortunate that shifting CO to H_2 and reforming CH_4 to H_2 and, then, reacting within the cell simplifies the analysis while accurately predicting the electrochemical behaviour of the fuel cell (EG&G, 2002). To simulate the reactions inside the cell, an equilibrium reactor module *Rgibbs* (named ''ANODE'') is used. The stoichiometry of the electrochemical reaction is based on the reaction of hydrogen with oxygen. The reactions considered in the block are:

Electrochemical Reaction $H_2 + \frac{1}{2}O_2 \rightarrow H_2O$ (R2-5)

Water-gas shift reaction $CO + H_2O \Leftrightarrow CO_2 + H_2$ (R3-2)

Methane steam reforming $CH_4 + H_2O \Leftrightarrow CO + 3H_2$ (R3-3)

The three reactions above are specified to reach thermodynamic equilibrium at a given temperature to simplify the simulation. Although the electrochemical reaction is not represented as a reversible reaction, the simulation results will closely simulate the electrochemical conversion because of the very high temperature conditions, which result in an extremely large equilibrium constant, K, for reaction (R2-5). Within the model, the equilibrium and exhaust temperature are set at 910°C (Campanari, 2001). The steam reforming reaction is found to be nearly complete at this temperature. The hydrogen

participating in the electrochemical reaction (R2-5) is comprised of the hydrogen produced from reactions (R3-2) and (R3-3) along with any hydrogen in stream 4.

3.2.4 Air Stream Preheating and Oxygen Supply

The SOFC stack inlet air (stream 9) is preheated by the hot exhaust from the afterburner (stream 14), and then enters the cell cathode to provide oxygen for the electrochemical reaction. Inside the cells, the air stream is further heated by the heat from the electrochemical reactions. This process is implemented in AspenPlus^{TM} using the rigorous heat exchanger module *Heatx* (named ''RECUPER''), the separator module *Sep* (named ''CATHODE'') and the temperature changer module *Heater* (named ''HEATER1''). The inlet air stream will exchange heat with the exhaust in the ''RECUPER'' block and then enter the ''CATHODE'' block. A certain amount of oxygen (stream 11) is separated in the ''CATHODE'' block and enters the ''ANODE'' block to oxidize the fuel. This step simulates the oxygen splitting into ions, and then the oxygen ions crossing over to the anode side. An AspenPlus^{TM} *Calculator* is used to calculate the molar flow rate of stream 11 ($n_{O2,required}$) based on the anode fuel equivalent hydrogen molar flow rate ($n_{H2,equivalent}$) and expected fuel utilization factor (U_f) as:

$$n_{O2,required} = 0.5\ (U_f)\ (n_{H2,equivalent}) \qquad \text{(E3-1)}$$

The $n_{H2,equivalent}$ is the equivalent hydrogen contained in the fresh fuel. It can be calculated as:

$$n_{H2,equivalent} = n_{H2,in} + 1 \times n_{CO,in} + 4 \times n_{CH4,in} + 7 \times n_{C2H6,in} + \ldots \qquad \text{(E3-2)}$$

where $n_{H2,in}$ represents the molar flow rate of H_2 contained in the fresh fuel; $1 \times n_{CO,in}$ represents the molar flow rate of H_2 that could be produced from CO contained in the fresh fuel by shift reaction (R3-2); $4 \times n_{CH4,in}$ represents the molar flow rate of H_2 that could be produced from CH_4 contained in the fresh fuel (each CH_4 mole generates 4 moles of H_2 - 3 from the steam reforming (reaction R3-3) and 1 from the shift reaction for the CO resulting from the steam reforming (reaction R3-2); for higher hydrocarbons, similar to the case of CH_4. The utilization factor, U_f is defined as: $U_f = n_{H2,consumed} / n_{H2,equivalent}$, where $n_{H2,consumed}$ is the molar flow rate of H_2 consumed in the electrochemical reaction (R2-5). The heat provided to the air stream by the electrochemical reaction is considered by taking a heat stream (Q_3) from the "HEATER1" block to the "ANODE" block. The heat (Q_3) is calculated by specifying the temperature of the depleted air stream (stream 13) to be equal to the temperature of the anode outlet.

3.2.5 Afterburner

After undergoing the electrochemical and chemical reactions, part of the depleted fuel gases recycles to mix with the fresh fuel and provide steam for the pre-reforming reactions. The rest of the depleted fuel gases enter the combustion plenum. The remaining H_2 and CO in the fuel (stream 7) will react with the oxygen in the depleted air (stream 13) in the combustion plenum. The reactions release heat, which will be transferred to the exhaust gases and incoming air stream. An AspenPlus™ reactor module *Rstoic* (named ''AFTERBUR'') is selected to simulate the combustion. This module is suitable when the reaction stoichiometry and conversion is known (AspenPlus™ 12.1 User Guide). The

reactions specified in the ‘‘AFTERBUR’’ block are considered as reaching completion (100% conversion) and include:

Hydrogen oxidation $$H_2 + \frac{1}{2}O_2 \rightarrow H_2O \quad \text{(R3-4)}$$

Carbon monoxide oxidation $$CO + \frac{1}{2}O_2 \rightarrow CO_2 \quad \text{(R3-5)}$$

The “RECUPER” block and an AspenPlus™ *Heater* module (named “HEATER2”) are used to simulate the heat exchange process in the combustion plenum. The heat generated by the oxidation reactions of H_2 and CO is calculated by the block “AFTERBUR” and put into stream Q_5. The heat is then put into the exhaust in the “HEATER 2” block. By exchanging the heat between the heated exhaust (stream 14) and incoming air (stream 9) in the “RECUPER” block, both the temperature of the exhaust leaving the stack (stream 15) and the temperature of the air leaving the afterburner to the cathode (stream 10) can be determined.

3.2.6 Calculation of Cell Voltage, Required Fresh Fuel and Cell Efficiency

The cell voltage calculation is the core of any fuel cell modeling. The method adopted in the proposed model is based on a number of sources (EG&G, 2002; Campanari, 2001). It utilizes a performance curve obtained by interpolation of experimental data at standard operating conditions for reference and then predicts the cell voltage by using semi-empirical correlations, accounting for the performance adjustments due to the specified operating conditions. This method avoids a detailed analysis of the cell physical structure and the consequent introduction of a number of cell microscopic and geometrical parameters, thereby making the model easily calibrated. At this stage of continuous and

rapid technological development in the field of SOFC materials and design, empirical correlations such as this are most useful in systems models as they are easily updated to accommodate new technology (Campanari, 2001) Moreover, this method provides a way to predict cell performance, which is simple enough to be implemented in AspenPlus™ using a *Design-Spec* Fortran block function without complex linkage with other codes. The current model adopts an experimental curve published in the Fuel Cell Handbook as the reference curve to define the reference voltage V_{ref} at the referenced operating condition (inlet fuel composition: 67% H_2, 22% CO, 11% H_2O; 85% U_f; 25% U_a; T = 1000 °C and P = 1 bar). It also incorporates four more semi-empirical equations (Campanari, 2001; EG&G, 2002) to account for the effects of operating pressure, temperature, current density and fuel/air composition on the actual voltage. They are:

- Operating Pressure

$$\Delta V_p(mv) = 76 \times \ell og \frac{P}{P_{ref}} \qquad \text{(E2-2)}$$

Where P is the operating pressure (1-10 bar) and P_{ref} is the reference operating pressure (here Pref = 1 bar)

- Operating Temperature and Current Density

$$\Delta V_T(mV) = 0.008 \times (T - T_{ref})(^oC) \times I_c(mA/cm^2) \qquad \text{(E2-3)}$$

Where T is the operating temperature (950-1050°C), I_c is the current density in mA/cm^2 and T_{ref} is the reference operating temperature (here T_{ref} = 1000°C)

- Fuel Composition

$$\Delta V_{anode}(mV) = 172 \times \ell og \frac{P_{H_2} \Big/ P_{H_2O}}{(P_{H_2} \Big/ P_{H_2O})_{ref}} \qquad \text{(E2-4)}$$

Where P_{H_2} / P_{H_2O} is the ratio of H_2 and steam partial pressure in the system and $(P_{H_2} / P_{H_2O})_{\text{ref}}$ is ratio of H_2 and steam partial pressure in the system under reference condition. (here $(P_{H_2} / P_{H_2O})_{\text{ref}} = 0.15$)

- Oxidant Composition

$$\Delta V_{Cxathod}(mv) = 92 \times \ell og \frac{(P_{O_2})}{(P_{O_2})_{ref}} \quad \text{(E2-5)}$$

Where P_{O_2} and $(P_{O_2})_{ref}$ are the average oxygen partial pressure at the cathode for the actual case and the reference case, respectively. (here $(P_{O_2})_{ref} = 0.164$)

Please be noted that for co-flow configurations like tubular SOFCs, the flow compositions in the ΔV_{anode} and $\Delta V_{\text{cathode}}$ are calculated at the fuel cell outlet (Campanari, 2001). Thus the $(P_{H_2} / P_{H_2O})_{\text{ref}}$ and $(P_{O_2})_{ref}$ represents stream conditions at the cell outlet at the reference operating conditions.

By summing up the four correlations, the actual cell voltage V can be calculated as

$$V_C(mv) = V_{ref} + \Delta V_p + \Delta V_T + \Delta V_{Cathod} + \Delta V_{anode} \quad \text{(E2-6)}$$

The fuel cell power output is the product of the cell voltage and current. The developed model takes the desired power output as an input to calculate the corresponding voltage and current required to generate the power. Another option of this model is to calculate the corresponding voltage and power output based on a given current (current density and

size). The equivalent hydrogen flow rate, $n_{H2,equivalent}$, can be calculated based on the current to be generated:

$$n_{H\,2,equivalent}(mol/hr) = \frac{n_{H\,2,consumed}(mol/hr)}{U_f} = \left(\frac{current(A)}{2U_f F(C/mol)}\right)\left(\frac{3600s}{hr}\right)$$

$$= \frac{0.018655 \times current(A)}{U_f} \qquad \text{(E3-3)}$$

The amount of fresh fuel required can then be determined based on the value of $n_{H2,equivalent}$ and the known composition of inlet fuel (C_i) from equation (E3-2) as:

$$n_{fresh\ fuel}(mol/hr) = \frac{n_{H\,2,equivalent}(mol/hr)}{C_{H_2} + C_{co} + 4 \times C_{CH_4} + 7 \times C_{C_2H_6} + \ldots} \qquad \text{(E3-4)}$$

The cell electrical efficiency is calculated according to:

$$\eta = \frac{Power}{n_{fresh\ fuel}(mol/hr) \times LHV_{fuel}(J/mol)} = \frac{current(A) \times V(V)}{n_{fresh\ fuel}(mol/hr) \times LHV_{fuel}(J/mol)} \qquad \text{(E3-5)}$$

The calculations described in this section are performed in an AspenPlus™ *Design-spec* Fortran block. This block calculates the voltage, current and amount of fresh fuel for producing the desired power output. The calculated current can further be used to determine the current density and the active reaction area. The hierarchy of the calculations is shown in Figure 3-3.

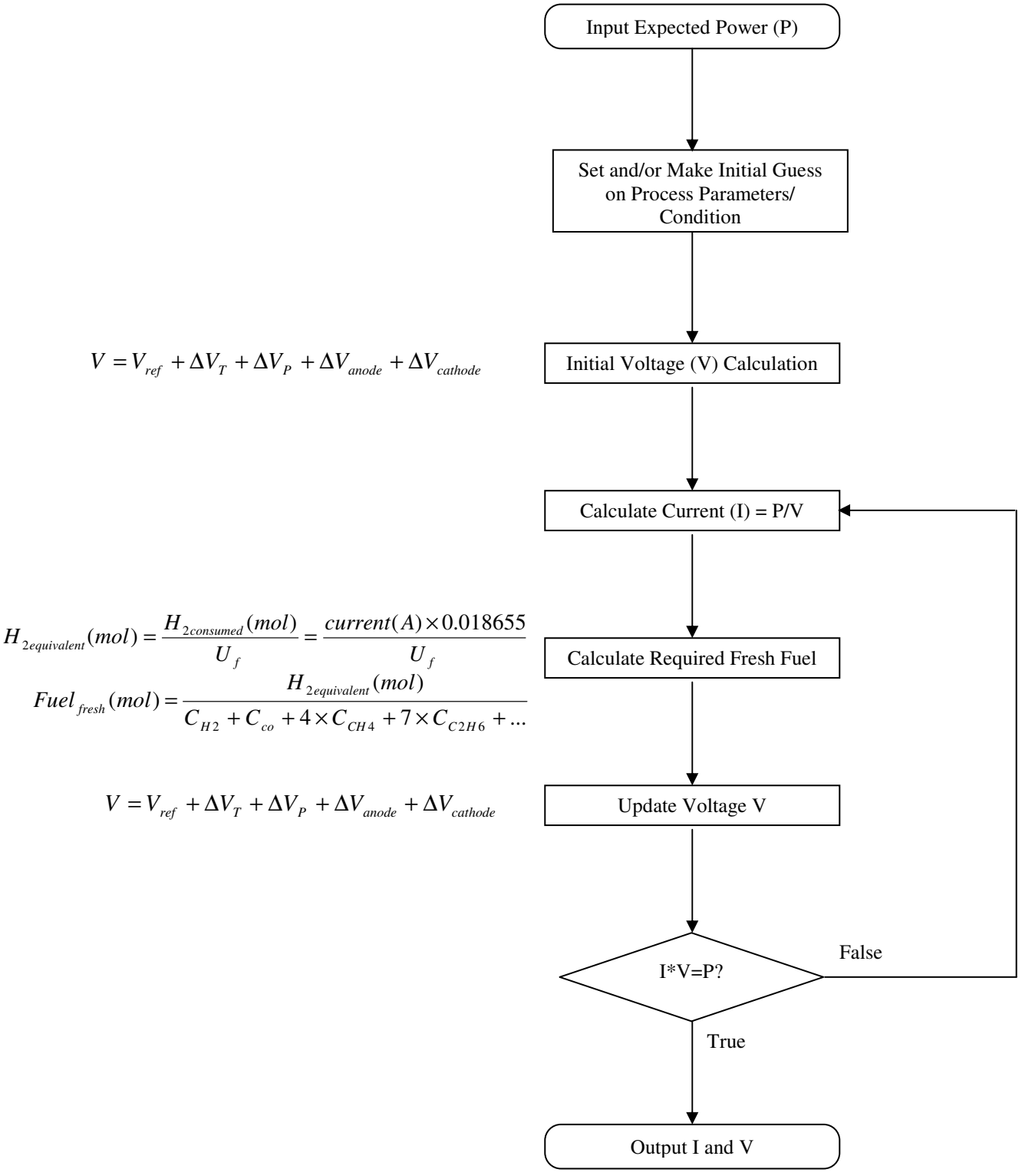

Figure 3-3: Simulation Hierarchy of Cell Voltage Calculation

3.2.7 Calculation of Heat Generation and Requested Air Flow

The SOFC only converts part of the chemical energy of the fuel into power and the rest will become heat as a result of loss in the system. Some of the heat is used in the inlet fuel and air stream but a significant part of the heat is used by the endothermic reforming reaction. To maintain the cell operating temperature at a stable point, additional airflow is used to cool the stack. Since AspenPlus™ performs block net heat duty calculation (AspenPlus™ 12.1, User Guide), for the "ANODE" block model, the net heat duty (Q_3) is calculated in AspenPlus™ as

$$Q_4 = Q_e + Q_s + Q_r - Q_g \qquad \text{(E3-6)}$$

where Q_e, Q_s and Q_r are the reaction heat for the reactions R2-5, R3-2 and R3-3 specified in the "ANODE" block, and Q_g represents the heat given into the fuel and air stream, which includes the heat streams feed into the block (Q_3). Therefore, by assuming a certain amount of heat losses (Q_l) (see Table 3-1), the requested airflow can be determined by using an AspenPlus™ *Design-spec* satisfying the following equation:

$$Q_4 - Q_l - W_{elec} = 0 \qquad \text{(E3-7)}$$

3.3 Validation of Simulation Results

The proposed model has been used to carry out a complete simulation based on a 100 kW class atmosphere SOFC stack (1152 cells) as detailed in the literature (Veyo, 1996; Veyo and Forbes, 1998; Veyo and Lundberg 1999; Singhal, 1997). Major calculation results and some comparisons between the simulation results and literature data are listed in Table 3-2, shows that the SOFC model consisting of AspenPlus™ built-in unit operation modules

can predict the fuel cell stack performance. Reasonable assumptions are made for this simulation to match the reference paper. The inlet fuel composition (mole basis) is set to CH_4 81.3%, C_2H_6 2.9%, C_3H_8 0.4%, C_4H_{10} 0.2%, N_2 14.3%, and CO 0.9%. The inlet air temperature is set to 630ºC, and the inlet fuel temperature is set to 380ºC. The total active reaction area is set to 96.1 m^2, which is the active reaction area of 1152 cells (Veyo, 1996). The reference curve used for estimating the stack performance is based on experimental data obtained under the inlet fuel condition of 67% H_2, 22% CO and 11% of H_2O, 85% U_f and 25% U_a. According to the simulation, the SOFC will deliver 120 kW DC power at an efficiency of 52% (LHV). A summary of simulation assumptions and simulated stream properties can be found in Table 3-2 and 3-3.

Table 3-2: SOFC Model Simulation Results (120 kW dc output)

	Literature Data	Model Simulation Data
Voltage (volt)	-	0.70
Current Density (mA/cm^2)	180	178
Air Utilization Factor	25%	23%
Pre-reformer Outlet Temperature (°C)	550	544
Heavy Hydrocarbons Pre-reforming Fraction	100%	100%
Methane Pre-reforming Fraction	10-15%	29.6%
Anode Outlet Composition (stream 5)	48% H_2O, 28% CO_2, 14% H_2, 5% CO, 5% N_2	50.9% H_2O, 24.9% CO_2, 11.6% H_2, 7.4% CO, 5.1% N_2
Stack Exhaust Composition (stream 15)	77% N_2, 16% O_2, 5% H_2O, 2% CO_2	76.9% N_2, 14.8% O_2, 5.5% H_2O, 2.8% CO_2
Stack Exhaust Temperature (°C)	847	846
Gross AC Efficiency (LHV)	50%	51%

-: Data unavailable

3.4 Sensitivity Study of the SOFC Model Using AspenPlus™

One of the benefits to use the developed AspenPlus™ SOFC stack model is that sensitivity analyses can be performed in an easy and timesaving manner, which helps to understand the effects of the variation of operating parameters on the SOFC's performance. The following section illustrates the results of several sensitivity analyses performed using AspenPlus™ based on the developed SOFC model.

Table 3-3: Stream properties for the AspenPlus™ SOFC Model
(data in italic represents the input to the model –either streams or the blocks, data in regular represents output of the model)

Strm No.	Temp. (K)	Press. (atm)	Mole Flow (kmol/hr)	Gas Composition (mole %)						
				H_2	CH_4	H_2O	CO	CO_2	O_2	N_2
1[a]	*653*	3.24	1.08	-	*81.3*	-	*0.9*	-	-	*14.3*
2[b]	1051	*1.08*	5.79	9.4	15.1	41.5	6.0	20.4	-	6.8
3[b]	817	1.08	5.79	9.4	15.1	41.5	6.0	20.4	-	6.8
4	817	1.08	6.47	28.1	9.5	27.3	6.2	22.8	-	6.1
5	*1183*	1.08	7.70	11.6	-	50.9	7.4	24.9	-	5.1
6	1183	1.08	4.70	11.6	-	50.9	7.4	24.9	-	5.1
7	1183	1.08	3.00	11.6	-	50.9	7.4	24.9	-	5.1
8	*1183*	1.08	34.0	-	-	5.5	-	2.8	14.8	76.9
9	*903*	*1.08*	32.9	-	-	-	-	-	21.0	79.0
10	1109	1.08	32.9	-	-	-	-	-	21.0	79.0
11	1109	1.08	1.61	-	-	-	-	-	100.0	-
12	1109	1.08	31.3	-	-	-	-	-	16.9	83.1
13	*1183*	1.08	31.3	-	-	-	-	-	16.9	83.1
14	1309	1.08	34.0	-	-	5.5	-	2.8	14.8	76.9
15	1119	1.08	34.0	-	-	5.5	-	2.8	14.8	76.9

a. For the gas composition of stream 1, add C_2H_6 2.9% / C_3H_8 0.4% / C_4H_{10} 0.2%.

b. For the gas composition of stream 2, add C_2H_6 0.5%/ C_3H_8 0.07% / C_4H_{10} 0.04%.

3.4.1 Effect of Overall Utilization Factor (U_f)

The utilization factor is one of the most important operating parameters for fuel cells and has significant effects on the cell voltage and efficiency. It also affects the unburned fuel concentration in the exhaust of the fuel channel, which is of critical importance when considering CO_2 capture processes. Figure 3-4 shows the effect of fuel utilization on the cell voltage, cell efficiency, current density and required fuel input for a SOFC at a constant power output of 120 kW (DC). If U_f is increased from 0.6 to 0.95, the cell voltage will decrease because the fuel is more depleted and the polarization losses at the anode are increased. The current density will increase, which can be realized by increasing air flow (Campanari, 2001), resulting in more H_2 being consumed. Since $n_{fresh\ fuel} \propto n_{H2,equivlant} \propto current/U_f \propto Power/(V_c \times U_f)$ (see equations E3-3 and E3-4), at lower values of U_f, the required fuel input decreases when U_f increases because the cell voltage (V_c) change is not significant. But for higher U_f, when the decrease in voltage, due to the concentration losses, becomes more important than the increase in fuel utilization, and as a consequence, more fresh fuel is needed. Thus, a minimum value of the required fuel input is found for a value of U_f close to 0.85 as shown in Figure 3-4.

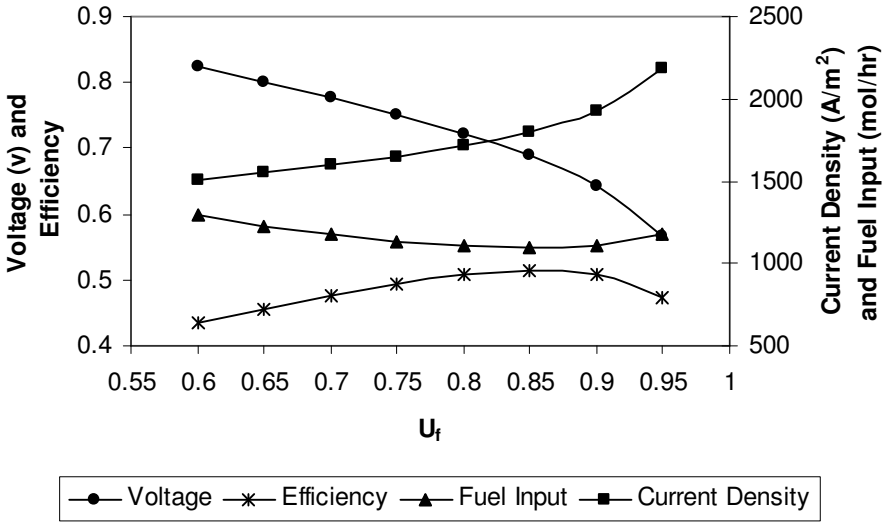

Figure 3-4: Effects of U_f on the cell voltage, current density, required fuel input and cell efficiency. (constant DC power output of 120 kW)

It is also observed that the cell electrical efficiency (η) reaches a maximum value of 52% at the maximum value of U_f. In fact, since the cell efficiency is proportional to $V_c \times U_f$:

$$\eta = \frac{Power}{Fuel_{fresh} \times LHV_{fuel}} \propto \frac{I \times V_c}{H_{2,consumed} / U_f} \propto \frac{I \times V_c \times U_f}{I} \propto V_c \times U_f \qquad \text{(E3-8)}$$

the efficiency should reach the maximum around U_f = 0.85 independent of the power output.

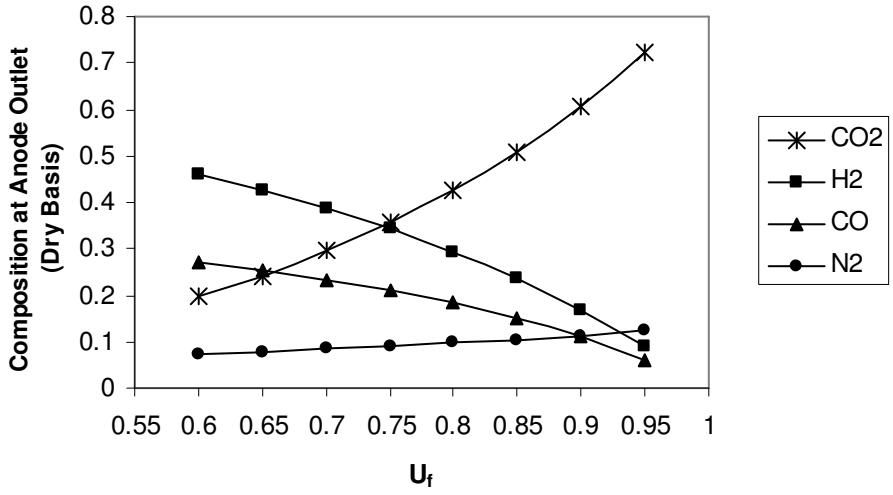

Figure 3-5: Effects of U_f on the exhaust anode stream (fuel channel) composition (dry basis)

U_f has also a significant impact on the composition of the anode exhaust stream. This model is intended to be used in the future for simulation of overall SOFC-based power generation with CO_2 capture. As such the CO_2 concentration in the exhaust is of significant interest. As shown in Figure 3-5, the CO_2 concentration at the anode outlet increases when U_f is increased because the fuel is more depleted (less CO and H_2). When U_f reaches the value of 0.95, the concentration of CO_2 is 72.2% (dry basis) compared to 50.8% (dry basis) when U_f is 0.85. This concentration calculation is based on the input fuel composition CH_4 81.3%, C_2H_6 2.9%, C_3H_8 0.4%, C_4H_{10} 0.2%, N_2 14.3%, and CO 0.9%. If the input fuel has already been depleted and contains high level of CO_2, the outlet CO_2 concentration will easily achieve the desired level for sequestration although the power output will be much lower. Thus, if CO_2 capture is part of the specification, the use of two fuel cell stacks in series might be an option. This idea was first proposed to

capture CO_2 in the Norsky-Shell demonstration project (Haines et al., 2002): the first fuel cell is fed with the fresh fuel running at 0.85 U_f to generate power and the second one is fed with the depleted fuel exhausted from the first fuel cell to achieve an overall 98% fuel conversion without high expectation for power output.

3.4.2 Effect of Current Density (Ic)

Figure 3-6 shows the effect of the variation of current density over voltage, cell efficiency, inlet airflow and inlet fuel flow when U_f is constant (0.85). The voltage decreases as the current density increases due to increased losses. Since the efficiency is proportional to $V_c \times U_f$, it also decreases with current density. The total power output increases when I_c increases from 160 to 250 mA/cm^2. The required inlet fuel flow also increases as the fuel consumption increases with the increase of I_c. The increased current density requires the increase of airflow to provide more oxygen ion. Moreover, the decreased efficiency results in more unconverted chemical energy, which is transformed into heat, and thus to maintain the cell operating temperature, the cooling duty of inlet air increases. Therefore, the inlet airflow increases as the I_c increases. The operation at low current density yields higher efficiency but produces less power. It requires higher capital cost (more cells) to produce same level of power compared to high current density operation.

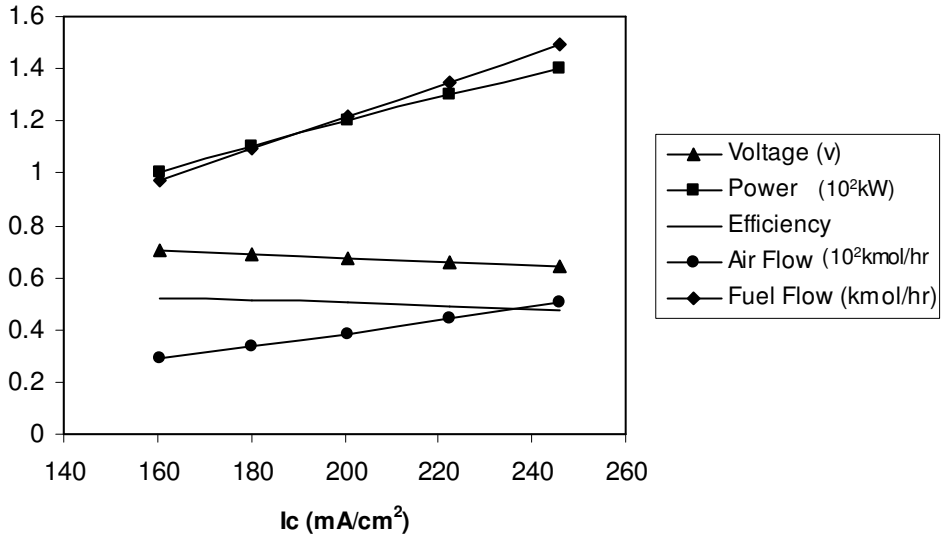

Figure 3-6: Effects of variation of current density over voltage, DC power output, cell thermal efficiency, inlet airflow and inlet fuel flow. (constant utilization factor of 0.85)

3.4.3 Effect of Power Output

Power output increase can be realized by an increase in current and/or an increase in voltage. As Figure 3-7 shows, when U_f is kept constant, an increase in current density from 160 to 340 mA/cm^2 can increase the power output despite of the decreased cell voltage and efficiency. The increase of current density in this case can be realized by increasing inlet airflow and the inlet fuel flow. If constant current is desired, an increase in voltage can also increase the power output. This can be realized by decreasing the fuel utilization, U_f. This method has limited capacity in adjusting the power output because that the voltage increase is limited. As shown in Figure 3-6, if constant cell voltage and efficiency are desired, an increase in power output may be realized by increasing current density and decreasing U_f. As a result, inlet airflow and fuel flow needs be increased to

produce more power. Therefore, variation of inlet airflow, inlet fuel flow and fuel utilization factor is the major method to adjust the power output.

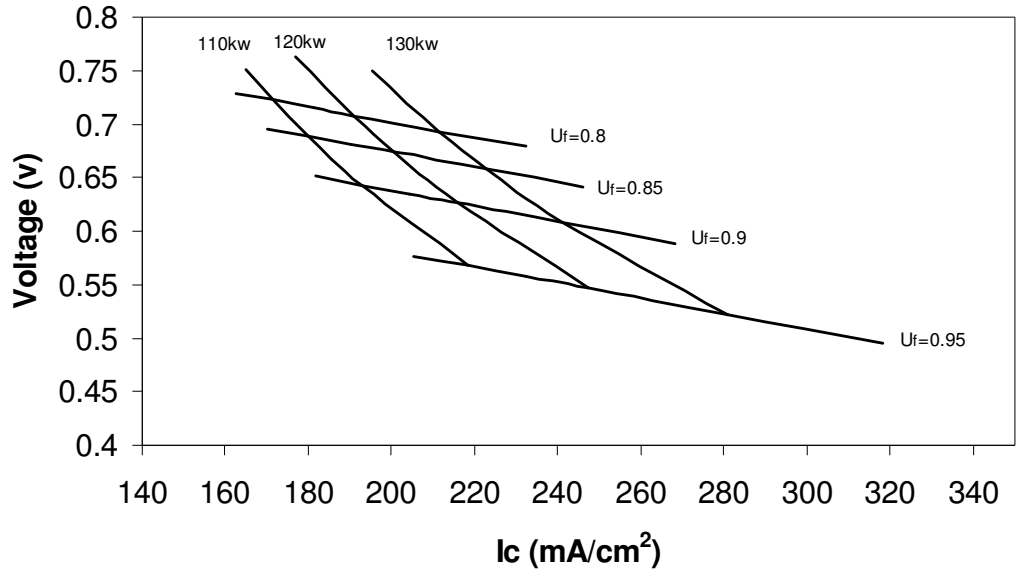

Figure 3-7: Effects of power output (DC) over voltage, current density and utilization factor

3.4.4 Effect of Steam/Carbon Ratio

A minimum steam-carbon (S/C) ratio at the pre-reformer inlet is required to prevent carbon formation. It is defined as the ratio between the number of the H_2O molecules and the number the C-atoms in the combustible components (EG&G, 2002). This ratio is controlled by the re-circulated fraction of the depleted fuel. The variation of S/C ratio has an impact on the inlet temperature of pre-reformer and influences the methane pre-reforming fraction. It also impacts the single passage fuel utilization factor of the fuel cell. As shown in Figure 3-8, an increase of S/C ratio results in an increase in fuel inlet

temperature to pre-reformer, as it requires recycling of more high temperature depleted fuel. The increased S/C ratio also promotes the methane steam reforming reaction in the pre-reformer therefore increases the methane pre-reforming fraction. The temperature of fuel exit the adiabatic pre-reformer to anode is found increased as the S/C ratio increased from 1.5 to 6.5, which is desirable because it reduces the SOFC thermal gradient. However, an increase in S/C ratio also decreases the single passage fuel utilization factor (the global fuel utilization remains 85%) because it increases the flow rate of fuel inlet the pre-reformer. This change is undesirable because it will require a larger pre-reformer and larger fuel cell stack, which would increases the capital cost. Therefore, the S/C ratio should remain low as long as it can meet the carbon formation and thermal gradient limits of the SOFC.

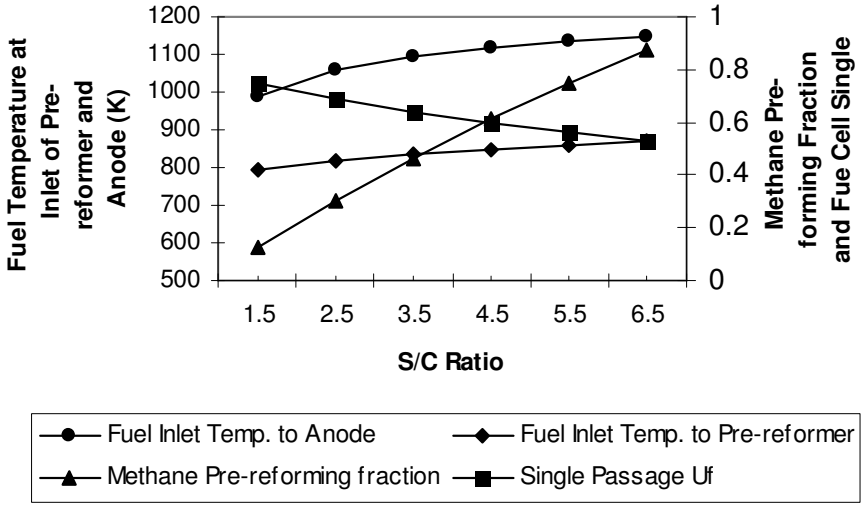

Figure 3-8: Effects of S/C ratio on the fuel temperature at inlet of per-reformer and anode, methane pre-reforming fraction and single passage U_f

4.0 Simulation of SOFC Based Power Generation Cycles

The design of a fuel cell system involves both the fuel cell stack and the balance of plant with respect to efficiency and economics. In the previous section, an AspenPlus^{TM} SOFC stack model was introduced based on literature descriptions of a tubular internal reforming SOFC technology from Siemens-Westinghouse (Veyo, 1996; Veyo and Forbes, 1998; Veyo and Lundberg 1999; Singhal, 1997). In this section, this model is extended to study the entire power generation process consisting of the SOFC stack and balance of plant.

There are many potential SOFC based power generation cycles proposed in the literature. They can be categorized into two main processes depending on the SOFC working pressure: atmospheric and pressurized. Although most of the proposed cycles are still in a conceptual stage, Siemens Power Generation has successfully implemented a couple of natural gas feed tubular SOFC based power generation systems for demonstration (refer to section 2). The processes of theses prototype systems are simulated in this study extended from the developed AspenPlus^{TM} SOFC model and the results are compared to the reported performance data in the literature (Veyo, 1999; Veyo and Lundberg, 2002). For the simulation performed in this study, assumptions used in Chapter 3 still hold. Additional assumptions for the system simulations are documented in Table 4-1.

Table 4-1: Assumptions for Simulation of SOFC Based Power Generation Cycles

Pressure drops, heat exchanger gas side, atm	0.02
Pressure drops, heat exchanger water side, atm	0.08
Pressure drops, fuel cell stack, atm	0.02
Pressure drops, fuel cell desulfurizer, atm	0.02
Fuel/Air/Water Feed Temperature, ºC	15
Fuel/Air Blower/Compressor Efficiency	65%
Feed Water Pump Efficiency	50%
Air Preheat Temperature, ºC	600
Natual Gas Preheat Temperature, ºC	400
ΔT across Desulfurizer, ºC	20
Cold Water Return Temperature, ºC	50
Hot Water Supply Temperature, ºC	120
Exhaust Temperature, ºC	70
Process Fuel Pressure, atm	1
Process Air Pressure, atm	1
Process Water Pressure, atm	3
Power for instrumentation and controls, etc., kW	2
Expander Isentropic Efficiency	74%
SOFC Stack Heat Loss (pressurized)	2%
SOFC Stack Heat Loss (atmospheric)	5%

4.1 Atmospheric SOFC-Based Power Generation System

4.1.1 System Descriptions

A 100 kW SOFC cogeneration system is currently installed in Essen, Germany. It operates at atmospheric pressure with an electrical efficiency of 47% and has achieved over 20,000 working hours so far. The SOFC stack in this system contains 1,152 cells (2.2 cm diameter, 150 cm active length), which are arranged in twelve rows (Singhal 1997). The

performance of this SOFC stack has been studied in details in the previous section. The process schematic for this 100 kW atmospheric pressure tubular SOFC power generation system is shown in Figure 4-1.

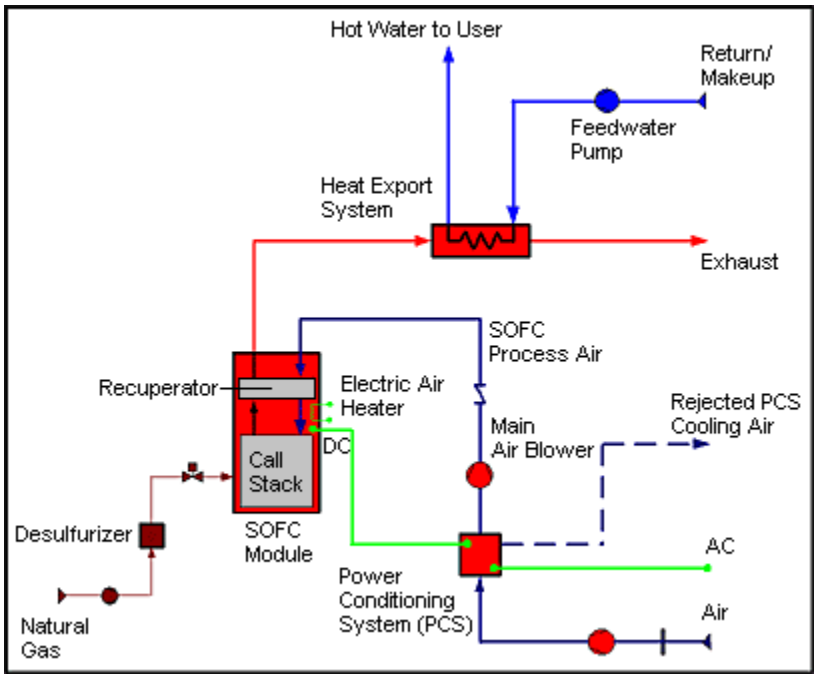

Figure 4-1: Simplified atmospheric pressure tubular SOFC power generation system cycle (http://www.powergeneration.siemens.com)

In this atmospheric design, ambient air is drawn through an air filter and compressed to the appropriate process pressure by a compressor or blower. The process air is then routed through a recuperator heated by the exhaust gas to increase the air temperature to approximately 600°C before introduction to the SOFC generator module. Pipeline natural gas at a pressure between 1 and 3 atmospheres above process pressure is desulphurized before being introduced to the SOFC generator module. Within the SOFC generator module, the fuel is electrochemically oxidized producing dc electricity. Nominally 85% of the fuel is electrochemically oxidized with the balance burned in the stack's combustion

zone. The SOFC exhaust exits the generator module at a temperature of between 800°C and 850°C and in atmospheric pressure systems is passed through the exhaust gas heat recovery train. This heat can be adapted to generate process heat or hot water for a combined heat and power application (CHP) (Forbes et al., 2002).

4.1.2 System Simulation

This atmospheric SOFC system is implemented in AspenPlus™ and the simulation flow sheet is shown in Figure 4-2. It includes all the components and functions described above such as the air and fuel blower. Refer to Section 3 for the simulation of the SOFC stack. The simulation approach of the balance of plant is described below. In the following sections, terms in italics represent actual AspenPlus™ terminology.

- **Air Compression and Preheat**

Process air is introduced to the SOFC stack by a conventional motor-driven blower and preheated by heat recovered from the SOFC generator exhaust (stream 24). The air compression is simulated by an AspenPlus™ module *Compr* (named "AIRBLOW") and specified using the AspenPlus™ *Polytrophic Using ASME Method* with a polytrophic efficiency of 65% and a discharge pressure high enough to overcome the system pressure drops (1.12 atm.). The air preheat process is simulated using the AspenPlus™ *MHeatX* module (named "PREH") and specified to meet the air preheat temperature of 600°C. Stream 9 represents the preheated air stream ready to enter the SOFC stack.

- **Natural Gas Compression, Preheat and Desulfurization**

The natural gas fuel is compressed to the required pressure to overcome the system pressure drops as well as to drive recycling of the SOFC stack anode gas (refer to section 3 for details). It is preheated to about 400°C against the SOFC stack exhaust gas (stream 15) to obtain the best efficiency for the desulfurization process (Campanari, 1998). The AspenPlus™ module *Compr* (named "FUELBLOW") and *MHeatX* (named "PREH") are used to simulate the compression and preheating processes. The fuel compressor is specified using the AspenPlus™ *Polytrophic Using ASME Method* with a polytrophic efficiency of 65%. The desulfurization process is presented by an AspenPlus™ *Heater* module with 20°C temperature drop specified. The "PREH" block is specified to meet the desired fuel and air preheating temperature. Stream 1 represents the preheated fuel stream ready to enter the SOFC stack.

- **Hot Water Production**

The exhaust gas (stream 15) exits the SOFC stack at around 846°C. This hot stream is used to preheat the fuel and air and then leaves the systems at around 291°C (stream 27). The heat contained in this stream is recovered by producing hot water. The AspenPlusTM module Pump (named "FWPUMP") and HeatX (named "CHP") are used to simulate the feed water pump and the heat recovery system. The flow of the feed water is adjusted to make sure the temperature of the final exhaust (stream EXHAUST) is around 70°C.

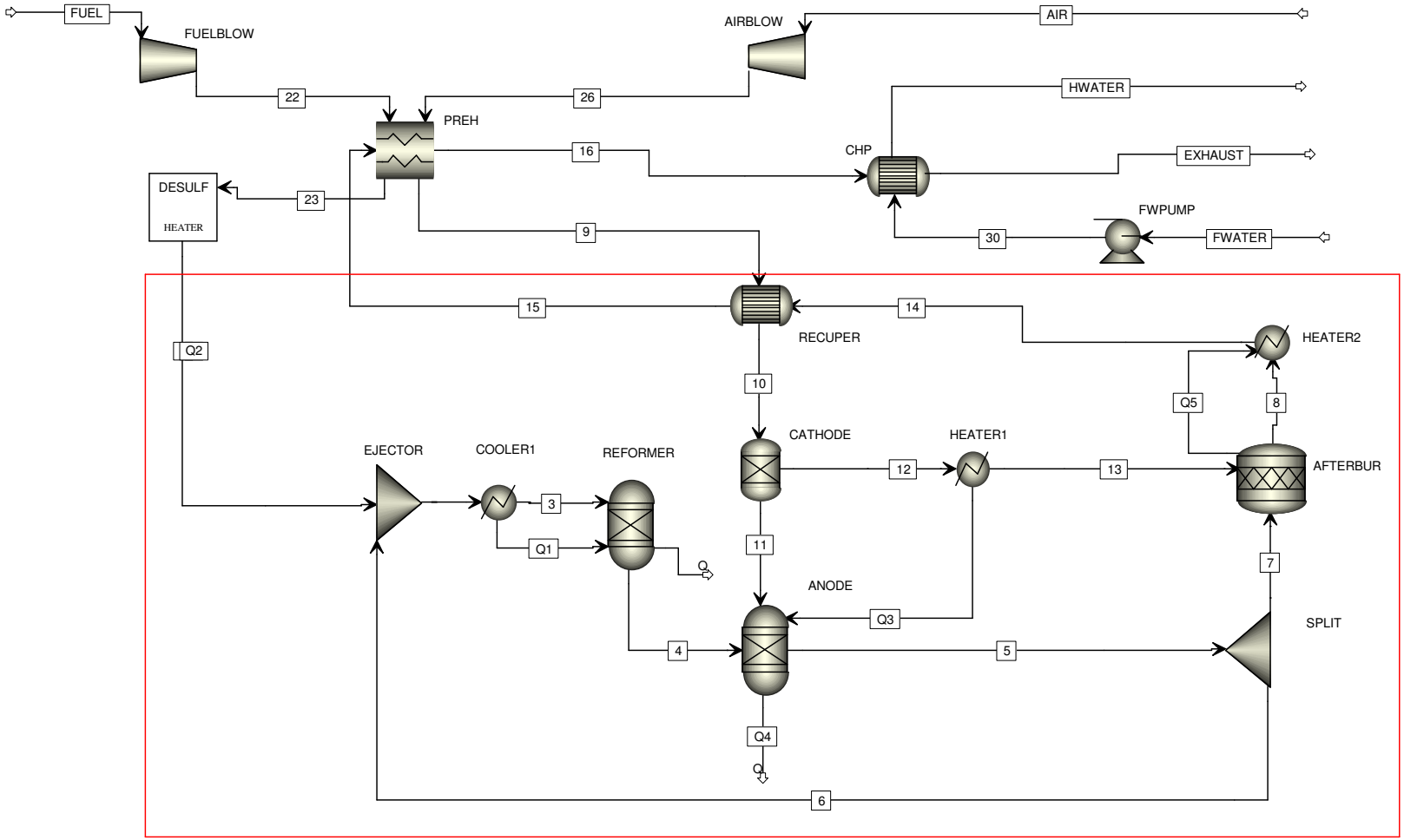

Figure 4-2: AspenPlus™ Flowsheet of Atmospheric Pressure SOFC Power Generation System

4.1.3 Simulation Results

Simulation shows that this 100 kW atmospheric pressure SOFC power generation system has a potential to achieve 47% of maximum electric generation efficiency (net AC/LHV). Including the hot water produced, the system efficiency reaches 80%. Stream properties for this cycle are presented in Table 4-2. Refer to section 4.3 for the details analysis of the system performance.

Table 4-2: Stream properties for the atmospheric SOFC system

(data in italic represents the input to the model –either streams or the blocks, data in regular represents output of the model)

Strm No.	Temp. (K)	Press. (atm)	Mole Flow (kmol/hr)	Gas Composition (mole %)						
				H_2	CH_4	H_2O	CO	CO_2	O_2	N_2
1[a]	*653*	3.24	1.08	-	81.3	-	0.9	-	-	14.3
2[b]	1051	*1.08*	5.78	9.4	15.1	41.5	6.0	20.5	-	6.8
3[b]	817	1.08	5.78	9.4	15.1	41.5	6.0	20.5	-	6.8
4	817	1.08	6.47	28.1	9.5	27.3	6.2	22.8	-	6.1
5	*1183*	1.08	7.70	11.6	-	50.9	7.4	24.9	-	5.1
6	1183	1.08	4.71	11.6	-	50.9	7.4	24.9	-	5.1
7	1183	1.08	2.99	11.6	-	50.9	7.4	24.9	-	5.1
8	*1183*	1.08	35.7	-	-	5.2	-	2.7	15.0	77.0
9	*873*	1.1	34.6	-	-	-	-	-	21.0	79.0
10	1092	1.08	34.6	-	-	-	-	-	21.0	79.0
11	1092	1.08	1.61	-	-	-	-	-	100.0	-
12	1092	1.08	33.0	-	-	-	-	-	17.1	82.9
13	*1183*	1.08	33.0	-	-	-	-	-	17.1	82.9
14	1301	1.08	35.7	-	-	5.2	-	2.7	15.0	77.0
15	1101	1.08	35.7	-	-	5.2	-	2.7	15.0	77.0
16	578	1.06	35.7	-	-	5.2	-	2.7	15.0	77.0
22[a]	431	*3.28*	1.08	-	81.3	-	0.9	-	-	14.3

Strm No.	Temp. (K)	Press. (atm)	Mole Flow (kmol/hr)	Gas Composition (mole %)						
				H_2	CH_4	H_2O	CO	CO_2	O_2	N_2
23[a]	*673*	3.26	1.08	-	81.3	-	0.9	-	-	14.3
26	303	*1.12*	34.6	-	-	-	-	-	21.0	79.0
30	323	*3.80*	44.1	-	-	100.0	-	-	-	-
AIR	*288*	*1.00*	34.6	-	-	-	-	-	*21.0*	*79.0*
EXHAUST	343	1.04	35.7	-	-	5.2	-	2.7	15.0	77.0
FUEL[a]	*288*	*1.00*	1.08	-	*81.3*	-	*0.9*	-	-	*14.3*
FWATER	*323*	*3.00*	*44.1*	-	-	*100.0*	-	-	-	-
HWATER	*393*	3.00	44.1	-	-	100.0	-	-	-	-

a. For the gas composition of streams 1, Fuel, 22 and 23, add C_2H_6 2.9% / C_3H_8 0.4% / C_4H_{10} 0.2%.

b. For the gas composition of stream 2, add C_2H_6 0.5%/ C_3H_8 0.07% / C_4H_{10} 0.04%.

4.2 Pressurized SOFC-Based Power Generation Systems

4.2.1 Introduction

As shown in Equation E2-2 from Section 2 and 3, pressurization of an SOFC yields a smaller gain in fuel cell performance. For example, the Siemens-Westinghouse tubular SOFC at 3 atmospheres increases the power output by about 10% compared to its power output at atmospheric operation (http://www.powergeneration.siemens.com). Therefore, SOFC operation at an elevated pressure will yield increased power and efficiency for a given cycle. Please, note that this improved performance alone may not justify the expense of pressurization, but may offer the ability to integrate the SOFC with a gas turbine, which needs a hot pressurized gas flow to operate. Since the SOFC stack operates at 1000°C and produces a high temperature exhaust gas, if operated at an elevated

pressure, the exhaust becomes a hot pressurized gas flow that can be used to drive a turbine. By pressurizing the SOFC stack and employing the simplest integration with the gas turbine, system efficiency of 60% or higher (net AC/LHV) at multi-hundred kW and Muti-MW capacities are expected (Veyo and Lundberg, 2002). In addition to high electric efficiency, this SOFC/GT hybrid system offers low-CO_2, low NO_x and low SO_x emissions, thanks for the characteristics of SOFC. That is the why the pressurized SOFC hybrid system concept attracts more and more attention nowadays.

In the pressurized system design the turbine work is extracted from the exhaust gas stream of the SOFC by an expander before the exhaust passes through the recuperator. Such systems can be configured in a number of ways depending on the turbine under consideration and the capacity required. Analysis has shown that for recuperated gas turbines with a turbine inlet temperature at about the SOFC exhaust temperature (850°C), there is no benefit to exceeding a maximum process pressure of 6 to 10 atmospheres. Further, analysis shows that there is no efficiency advantage to burning fuel in a gas turbine combustor to increase the turbine inlet temperature (Forbes et al., 2002).

The world's first SOFC/GT hybrid system designed by Siemens-Westinghouse was demonstrated in Southern California at the University of California, Irvine's National Fuel Cell Research Center. The hybrid system included a pressurized SOFC module integrated with a microturbine/generator supplied by Ingersoll-Rand Energy Systems (formerly Northern Research and Engineering Corp.) The system has a design output of 220 kW, with 200 kW from the SOFC and 20 from the microturbine generator. It operated for

nearly 3400 hours, and achieved an electrical efficiency of about 53% (http://www.powergeneration.siemens.com).

A 300 kW pressurized SOFC/GT system is also designed by Siemens-Westinghouse and is being demonstrated in Pittsburgh, Pennsylvania. Its performance is reported in the literature and a maximum system electrical efficiency of 55.7% was estimated (Veyo and Lundberg, 2002).

For the purpose of this study, the 220 kW pressurized SOFC/GT hybrid cycle is selected for studying in details.

4.2.2 Descriptions of the 220 kW Pressurized SOFC/GT Hybrid System

The concept of this system is presented in Figure 4-3. During normal operation of the pressurized SOFC hybrid, air enters the compressor and is compressed to around 3 atmospheres. This compressed air passes through the recuperator where it is preheated and then enters the SOFC. Pressurized fuel from the fuel pump also enters the SOFC and the electrochemical reactions takes place along the surface of the cells. The hot pressurized exhaust leaves the SOFC and goes directly to the expander section of the gas turbine, which drives both the compressor and the generator. The gases from the expander pass into the recuperator and then are exhausted. At around 200°C the exhaust is hot enough to make hot water. Electric power is thus generated by the SOFC (dc) and the generator (ac) using the same fuel/air flow.

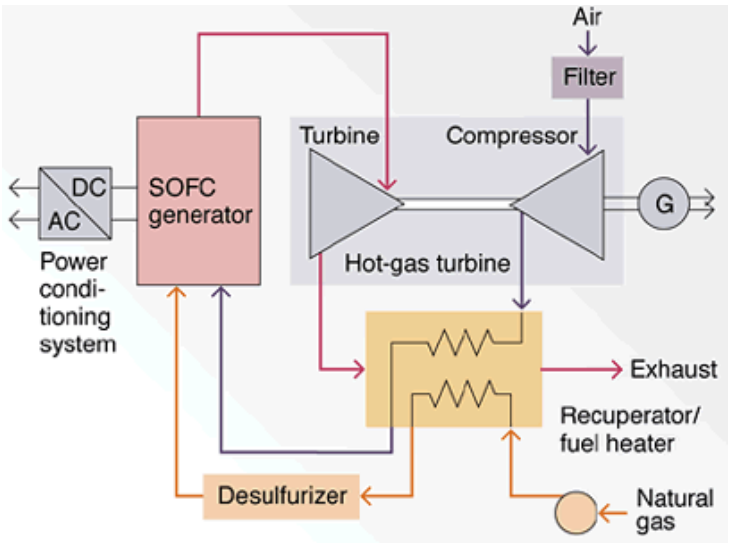

Figure 4-3: Pressurized SOFC/GT Hybrid System Diagram

(http://www.powergeneration.siemens.com/en/fuelcells/hybrid/index.cfm)

The cell design of this system is identical to that employed in the atmospheric pressure 100 kW SOFC power system described in Section 3. The micro gas turbine generator (MTG) in this system is a pre-commercial prototype 75 kW PowerWorks machine built by Ingersoll-Rand Energy Systems. This MTG has two shafts. One is to drive the compressor; another is to drive the generator.

4.2.3 System Simulation

This pressurized SOFC system is implemented in AspenPlus™ and the simulation flowsheet is shown in Figure 4-4. Refer to Section 3 for the simulation of the SOFC stack. The simulation of natural gas compression, desulphurization and preheat and the hot water production is identical to the atmospheric cycle (Section 4.1.2). The cycle specific simulation is described below. In the following sections, terms in italics represent actual AspenPlus™ terminology.

- **Air Compression and Preheat**

Process air is introduced to the SOFC stack by an air compressor driven by a turbine and preheated by heat recovered from the generator loaded turbine exhaust (stream 24). The air compression is simulated by an AspenPlus™ module *Compr* (named "AIRBLOW") and specified using the AspenPlus™ *Polytropic Using ASME Method* with a polytropic efficiency of 65% and a discharge pressure of 2.8 atm. The air preheat process is simulated using the AspenPlus™ *MHeatX* module (named "PREH") and specified to meet the air preheat temperature of 600°C and the fuel preheat temperature of 400°C. Stream 9 represents the preheated air stream ready to enter the SOFC stack.

- **Exhaust Expansion and Heat Recovery**

The exhaust from the pressurized SOFC generator enters the compressor loaded turbine and is expanded to drive the air compressor. The balance of the exhaust expansion occurs across the power turbine, which drives the turbine/generator producing around 20 kW electricity. The heat contained in the hot exhaust from this generator loaded turbine (stream 17) is recovered by heating up the incoming fuel and air. The additional heat is used for hot water production. The compressor loaded turbine is simulated in AspenPlus™ using Module *Compr* (named "EXPAND1") with the *isentropic method* selected. The same principle applies to the generator loaded turbine (named "EXPAND2"). The "EXPAND1" is specified by the brake horse power, which is equal to the brake horse power of the air compressor "AIRBLOW". The "EXPAND2" is specified by the discharge pressure of 1.06 atm. Work stream "W1" represents the work that the generator generated.

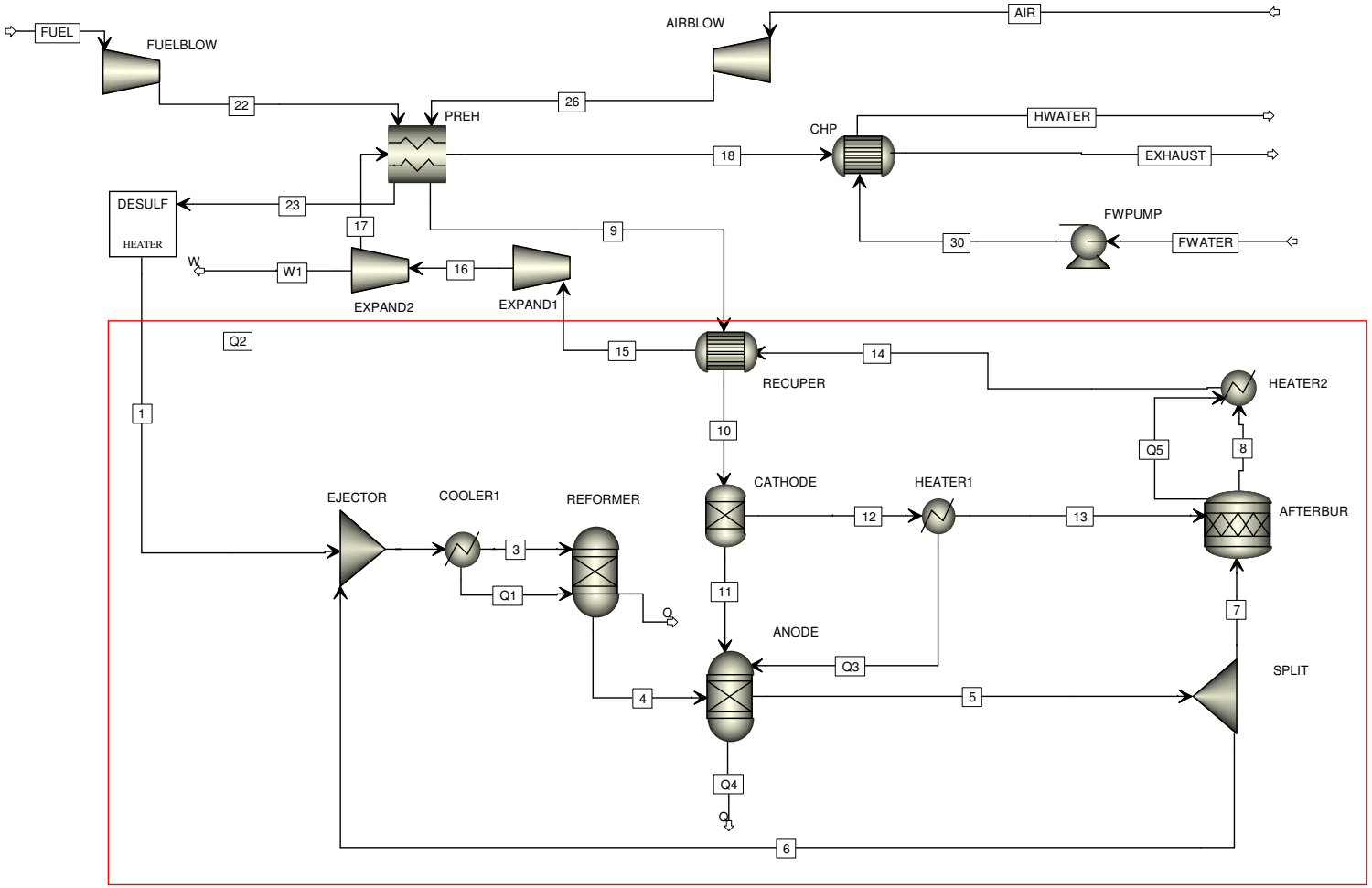

Figure 4-4: AspenPlus™ Flowsheet of Pressurized SOFC/GT Hybrid Power Generation System

4.2.3 Simulation Results

Simulation shows that this 220 kW pressurized SOFC/GT hybrid power generation system has a potential to approach 57% of maximum electric generation efficiency (net AC/LHV). Including the hot water produced, the system efficiency approaches 87%. Stream properties for this cycle are presented in Table 4-3. Refer to section 4.3 for the details analysis of the system performance.

Table 4-3: Stream Properties for the Pressurized SOFC/GT Hybrid Cycle
(data in italic represents the input to the model –either streams or the blocks, data in regular represents output of the model)

Strm No.	Temp. (K)	Press. (atm)	Mole Flow (kmol/hr)	Gas Composition (mole %)						
				H_2	CH_4	H_2O	CO	CO_2	O_2	N_2
1[a]	*653*	8.28	1.55	-	81.3	-	0.9	-	-	14.3
2[b]	1051	*2.76*	8.30	9.4	15.1	41.4	6.0	20.5	-	6.8
3[b]	854	2.76	8.30	9.4	15.1	41.4	6.0	20.5	-	6.8
4	854	2.76	9.13	25.2	10.5	29.4	6.4	22.3	-	6.2
5	*1183*	2.76	11.1	11.6	-	50.9	7.4	24.9	-	5.1
6	1183	2.76	6.76	11.6	-	50.9	7.4	24.9	-	5.1
7	1183	2.76	4.30	11.6	-	50.9	7.4	24.9	-	5.1
8	*1183*	2.76	62.3	-	-	4.3	-	2.2	16.1	77.4
9	*873*	2.78	60.7	-	-	-	-	-	21.0	79.0
10	1080	2.76	60.7	-	-	-	-	-	21.0	79.0
11	1080	2.76	2.31	-	-	-	-	-	100.0	-
12	1080	2.76	58.4	-	-	-	-	-	17.9	82.1
13	*1183*	2.76	58.4	-	-	-	-	-	18.3	81.7
14	1280	2.76	62.3	-	-	4.3	-	2.2	16.1	77.4
15	1090	2.76	62.3	-	-	4.3	-	2.2	16.1	77.4
16	953	1.30	62.3	-	-	4.3	-	2.2	16.1	77.4
17	921	1.08	62.3	-	-	4.3	-	2.2	16.1	77.4

Strm No.	Temp. (K)	Press. (atm)	Mole Flow (kmol/hr)	Gas Composition (mole %)						
				H_2	CH_4	H_2O	CO	CO_2	O_2	N_2
22[a]	557	8.32	1.55	-	81.3	-	0.9	-	-	14.3
23[a]	*673*	8.30	1.55	-	81.3	-	0.9	-	-	14.3
26	451	*2.80*	60.7	-	-	-	-	-	21.0	79.0
30	323	*3.80*	56.5	-	-	100.0	-	-	-	-
AIR	*288*	*1.00*	60.7	-	-	-	-	-	*21.0*	*79.0*
EXHAUST	343	1.04	62.3	-	-	4.3	-	2.2	16.1	77.4
FUEL[a]	*288*	*1.00*	1.55	-	*81.3*	-	*0.9*	-	-	*14.3*
FWATER	*323*	*3.00*	*56.5*	-	-	*100.0*	-	-	-	-
HWATER	*393*	3.00	56.5	-	-	100.0	-	-	-	-

a. For the gas composition of stream 1, Fuel, 22 and 23, add C_2H_6 2.9% / C_3H_8 0.4% / C_4H_{10} 0.2%.

b. For the gas composition of stream 2, add C_2H_6 0.5%/ C_3H_8 0.07% / C_4H_{10} 0.04%.

4.3 Comparisons of Simulation Results with Literature Data

In sections 4.1 and 4.2, two tubular SOFC based power generation systems are simulated in AspenPlus^{TM} extended from the SOFC stack model described in Section 3. One system is a 100 kW atmospheric SOFC based power generation system. Another one is a 220 kW pressurized SOFC/GT hybrid power generation system. Both systems have been developed by Siemens-Westinghouse for demonstration purpose and employ the same 1152-cell SOFC stack design. The estimated performance of these two systems are summarized in Table 4-4 and compared to the available literature data (Veyo and Lundberg, 1999, 2002). Assumptions used for the simulation work are summarized in Table 4-1.

Table 4-4: Performance Data Comparisons for SOFC Power Generation Cycles

Parameter	Atmospheric SOFC Cycle		Pressurized SOFC/GT Hybrid Cycle	
	Simulation	Literature	Simulation	Literature
Cell Voltage, volts	0.7	-	0.7	-
Current Density, mA/cm^2	178	180	256	-
Operating Pressure, bar	1.08	1.08	2.76	~2.8
Air Intake rate, kg/s	0.28	-	0.49	0.56
Pre-reforming Percentage, %	29.6	-	23.6	-
Compressor Pressure Ratio	-	-	2.8	2.8
Turbine Inlet Temp., °C	-	-	817	720
SOFC AC Power, kW	109	109	162	162
Turbine AC Power, kW	-	-	18.8	20.6
System Net AC Power, kW	100	102	173	180.6*
System Electrical Efficiency (LHV) %	47.2	47	56.9	52*
System Fuel Effectiveness with CHP, %	80.6	~80	86.6	-

-: Data not available or not applicable

*: Fuel compressor kW not included

The comparison results documented in Table 4-4 confirm that the system efficiency can be improved by operating the SOFC at pressure and integrating it with the turbine. Compared to the atmospheric cycle, the system electrical efficiency of the pressurized SOFC/GT hybrid cycle is 10% higher based on the simulation results. Please note that, for the 220 kW hybrid systems, the reported system efficiency (52%) is lower than targeted (55%-60%) due to oversized turbine (Veyo and Lundberg, 2002). It likely

explains the relevant difference between the simulation and literature data on the efficiency of the hybrid cycle.

The results also confirms that the simulation approach proposed in this study is reasonable and the developed AspenPlus™ model can be extended for SOFC based power generation cycles studies.

System performance studies of the 100 kW SOFC cogeneration system and 220 kW hybrid power system demonstrations indicate that SOFC based power generation system is capable of generating clean electric power at high efficiency. On natural gas fuel, simple atmospheric pressure SOFC system designed for CHP applications can achieve 47% electric generation efficiency (net AC/LHV) and 75% fuel effectiveness ((net AC+useful heat)/LHV). By operating at pressure and integrating thermally with a gas turbine, the pressurized SOFC/GT hybrid system can achieve an electrical efficiency of 57% and 87% of fuel effectiveness.

It is expected that with such SOFC/GT hybrid systems an electrical efficiency of 60% can be achieved at power plant capacities as low as 1 MW using small gas turbines and up to 70% at the 2 to 3 MW capacity level with larger, more sophisticated gas turbines (http://www.powergeneration.siemens.com/en/fuelcells/hybrid/index.cfm).

4.4 Simulation of a 100MW Atmospheric SOFC/GT Hybrid System

The SOFC technology has demonstrated its potential to produce power at high efficiencies with very low levels of emissions. Although demonstrations system are still in a range of less than 1MW, to compete with the state-of-the-art combined gas and steam turbine power plants, an eventual market for fuel cell systems should be the large (100 to 300 MW), base-loaded, stationary plants operating on coal or natural gas (EG&G, 2002).

Although atmospheric SOFC cycles offer somewhat lower efficiency horizons than pressurized cycles, it is dangerous to draw a conclusion right away that the hybrid system has greater potential. The atmospheric SOFC cycles are less complex to develop and quicker to implement. Because they would require less integration of the SOFC and gas turbine, they have the potential to also be less expensive and could accommodate a wider variety of gas turbines (http://www.powergeneration.siemens.com/). The trade-off between the process performance and the cost of providing pressurization need to be evaluated especially when plants increase in size to approximately 1 MW or larger (EG&G, 2002).

Heat is produced in a fuel cell stack and must be removed, and thus a fuel cell power system must remove the heat from the stack, and use this heat productively elsewhere in the system in order to maintain overall system efficiency. Depending upon the size of the system, the temperature of the available heat and specific site requirements, this thermal energy can be either rejected, used to produce steam or hot water, or converted to electricity via a gas turbine or a bottoming cycle or some sorts of combinations. When small quantities of heat and/or low temperatures typify the waste heat, it is more

reasonable to recover it by producing hot water or low-pressure steam. An SOFC stack operates at around 1000°C, and often has a cell exhaust temperature of more than 800°C after air and fuel preheating. Thus a steam bottoming cycle appears to be most suitable in on SOFC power system, but such a sub-system requires that large quantities of waste heat be available.

Based on the above discussion, a SOFC-based power generation cycle is conceptualized and simulated in the following section. is the simulation considers a combined Brayton-Rankine cycle, which consists of a 100 MW atmospheric SOFC hybrid system and a steam bottoming cycle.

4.4.1 System Descriptions

This conceptual SOFC system is built on the atmospheric pressure fuel cell system (section 4.2.1) by supplanting the motor-driven air blow with a turbine-expander-driven compressor. The heat input required by the turbine Brayton cycle is provided via the recuperator, which recovers the heat from the low-pressure, high temperature SOFC exhaust. The expander delivers more power than is required by the air compressor, and the surplus shaft power is harnessed by an alternator. Since more power is produced by the SOFC/GT system due to the addition of the turbine-alternator, a high system efficiency can be achieved. A Rankine bottoming cycle is then employed to maximize the system efficiency. It consists of a heat recovery steam generator operating on the exhaust stream from the fuel cell at atmospheric pressure. The steam produced from the generator drives the steam turbine and is then condensed and pumped back to the steam generator.

This system is implemented in AspenPlus™ and the simulation flow sheet is shown in Figure 4-5: The simulation assumptions are summarized in Table 4-5. If not specifically outlined in Table 4-5, other assumptions are identical to those presented in Table 4-1. The system simulation is detailed in the following section. Terms in italics represent actual AspenPlus™ terminology.

Table 4-5 Assumptions for Simulation of a 100MW SOFC Based Power Generation Cycle

Fuel Inlet Composition	CH_4 80.9%, C_2H_6 9.4%, C_3H_8 4.7%, C_4H_{10} 2.3%, N_2 2.0%
Pressure drops, Heat Recovery Steam Generator, atm	1
Fuel/Air Compressor Efficiency	85%
Feed Water Pump Efficiency	70%
Gas Turbine Inlet Pressure, atm	4
Gas Turbine Inlet Temperature, ºC	800
Steam Turbine Inlet Pressure, atm	7.5
Natual Gas Preheat Temperature, ºC	400
Gas Turbine Isentropic Efficiency	80%
Steam Turbine Isentropic Efficiency	85%
Inverter Efficiency	96%
Turbine Alternator Efficiency	98%
Motor Efficiency	97%
SOFC Stack Thermal Loss	2%
Power for Instrumentation and Controls, etc., kW	100

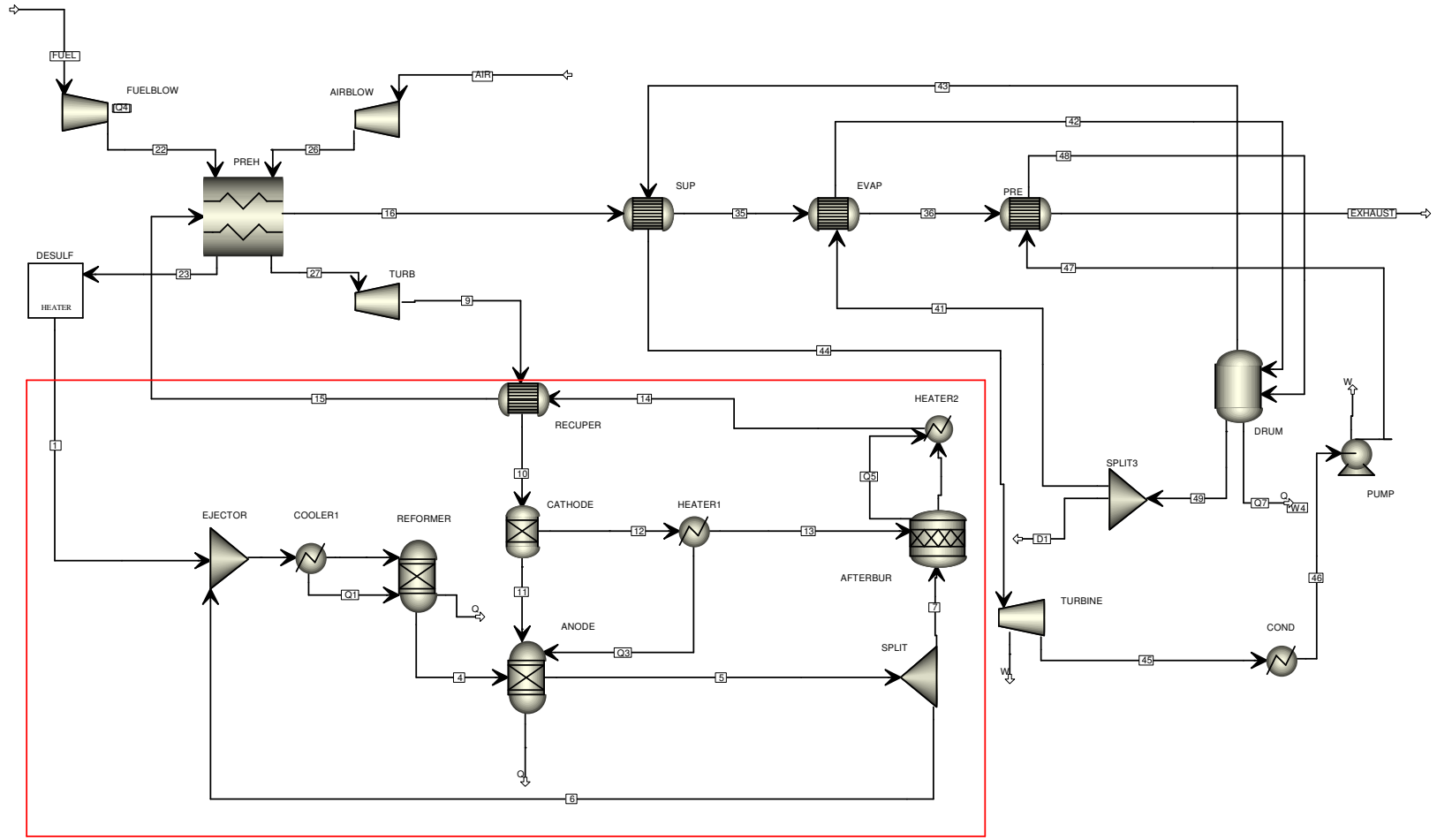

Figure 4-5: AspenPlus™ Flowsheet of a 100MW SOFC Based Power Generation System with Bottoming Cycle

4.4.2 System Simulations

The simulation approach of this 100MW SOFC system is quite similar to the atmospheric SOFC system, which are described in section 4.1.2 with the following exceptions:

- The power generation capacity of the SOFC stack is proportionally scaled up from 100 kW to 100 MW.
- The motor driven air blower is replaced with a turbine-expander-driven air compressor.
- The hot water production CHP system is replaced with a simple Rankine steam cycle with superheat, but no reheat and no multi-steam regeneration included.

The turbine-expander-driven air compressor is simulated in AspenPlus™ using module *Compr* (named "AIRBLOW") with the *Polytropic Using ASME Method* selected. The air is compressed in the "AIRBLOW" and then is heated with the exhaust from the SOFC generator (Stream 15). The recuperator (named "PREH") is specified to satisfy the fuel preheat temperature of 400°C and the desired turbine inlet temperature of 820°C. The compressor loaded turbine-expander is simulated in AspenPlus™ using module *Compr* (named "TURB") with the *Isentropic Method* selected and the discharge pressure specified. The turbine inlet temperature is the maximum temperature that can be obtained from the recuperator "PREH" assuming 10K approach in this heat exchanger with the SOFC exhaust at around 830°C. The pressure ratio of the turbine-driven compressor is selected so that the system efficiency is maximized and the temperature of the air into the SOFC stack (stream 9) is maintained around 630°C (Campanari, 1999). After exchanging

heat with the fuel and the air, the exhaust from the system (stream 16) flows to the heat recovery steam generator and then to the stack.

A heat recovery steam generator (HRSG) is used to recover energy from the hot exhaust gases from the SOFC system. The component a counterflow heat exchanger composed of a series of superheater, evaporator, and economizer sections mounted in the exhaust stack to maximize heat recovery (the economizer is a heat exchange device that heats the water up to (but not beyond) the boiling point). HRSGs are flexible in design depending upon the specific applications. They can be designed for operation with one or multi separate pressure steam-water loops to meet application requirement and maximize heat recovery. They can be unfired (only use the sensible heat of the gas as supplied) or may include supplementary fuel firing to improve system efficiency. To simplify the simulation work, a single pressure HRSG system is selected without reheat and multi-pressure steam generation.

The superheater, evaporator and economizer sections of the HRSG are simulated in AspenPlus^{TM} using module *HeatX* (named "SUP", "EVAP" and "PRE"). The approach temperatures for these sections are critical parameters for the HRSG processes.. Reasonable ranges of these temperatures are given in the literature (Babcock & Wilcox, 1992) and used in the simulation. For the "SUP", the approach temperature is specified to 22K. For the "PRE", the approach temperature is specified to 17K. For the "EVAP", the cold outlet stream vapor fraction (0.05) is specified to simulate the recirculation rate of the boiler circuit. This recirculation steam (stream 41) is adjusted to maximize the efficiency

while maintaining the pinch point of "EVAP" around 11K. A number of simulations were performed to determine the maximum system pressure that could be used. The steam pressure (8 atm) presented is within the pressure range where the system efficiency is maximized.

The Economizer "PRE" is used to preheat the feedwater (stream 47) being introduced to the system by the feed water pump to replace the steam (vapor) being removed from the system via the superheater. The feed water pump is simulated in AspenPlus™ using module *Pump* (Named "PUMP") with the discharge pressure specified.

In the Evaporizer "EVAP", the effluent (stream 41) is heated to the saturation point for the pressure it is flowing and return to the steam drum, where the saturation steam vapor is separated (stream 43) and get superheated in the Superheater "SUP". The superheated steam (stream 44) drives the steam turbine to produce power, which is simulated in AspenPlus™ using module *Compr* (Named "TURBINE") with the discharge pressure specified. The steam (stream 45) is then condensed in the condenser and pumped back to the Economizer "PRE". The condenser is simulated in AspenPlus™ using module *Heater* (Named "COND") with the outlet stream vapour fraction specified zero.

To converge the simulation of the cycle, an AspenPlus™ module *FSplit* (named "SPLIT3") is used. It allows the simulation to start with an initial difference between stream 41 and stream 49. A material balance will be automatically performed on the

"SPLIT3" to allow the converging begins by using AspenPlus™ function *Balance*. Once the process is converged, the flow rate of stream 41 is identical to stream 49.

4.4.3 Simulations Results

A 100MW atmospheric SOFC-based hybrid power generation system was simulated in AspenPlus™ including a simple steam Rankine cycle. Stream properties for this cycle are presented in Table 4-6. The estimated performance of this system is summarized in Table 4-7.

Table 4-6: Stream Properties for the 100MW Atmospheric SOFC/GT Hybrid Cycle (data in italic represents the input to the model –either streams or the blocks, data in regular represents output of the model)

Strm No.	Temp. (K)	Press. (atm)	Mole Flow (kmol/hr)	Gas Composition (mole %)						
				H_2	CH_4	H_2O	CO	CO_2	O_2	N_2
1[a]	*653*	3.30	755	-	80.9	-	-	-	-	2.0
2[b]	1062	*1.10*	5244	10.2	11.7	44.3	7.1	23.6	-	0.8
3[b]	826	1.10	5244	10.2	11.7	44.3	7.1	23.6	-	0.8
4	826	1.10	5991	29.3	9.3	27.7	7.6	25.5	-	0.7
5	*1183*	1.10	7102	11.9	-	51.7	8.3	27.5	-	0.6
6	1183	1.10	4489	11.9	-	51.7	8.3	27.5	-	0.6
7	1183	1.10	2613	11.9	-	51.7	8.3	27.5	-	0.6
8	*1183*	1.10	39774	-	-	4.2	-	2.3	16.1	77.3
9	903	*1.12*	38923	-	-	-	-	-	21.0	79.0
10	1094	1.10	38923	-	-	-	-	-	21.0	79.0
11	1094	1.10	1497	-	-	-	-	-	100.0	-
12	1094	1.10	37426	-	-	-	-	-	17.8	82.2
13	*1183*	1.10	37426	-	-	-	-	-	17.8	82.2
14	1282	1.10	39774	-	-	4.2	-	2.3	16.1	77.3

Strm No.	Temp. (K)	Press. (atm)	Mole Flow (kmol/hr)	Gas Composition (mole %)						
				H_2	CH_4	H_2O	CO	CO_2	O_2	N_2
15	1104	1.10	39774	-	-	4.2	-	2.3	16.1	77.3
16	448	1.08	39774	-	-	4.2	-	2.3	16.1	77.3
22[a]	380	3.34	755	-	80.9	-	-	-	-	2.0
23[a]	*673*	3.32	755	-	80.9	-	-	-	-	2.0
26	416	*3.00*	38923	-	-	-	-	-	21.0	79.0
27	*1093*	2.98	38923	-	-	-	-	-	21.0	79.0
35	447	1.06	39774	-	-	4.2	-	2.3	16.1	77.3
36	437	1.04	39774	-	-	4.2	-	2.3	16.1	77.3
41	*426*	*5*	*6095*	-	-	*100*	-	-	-	-
42	426	5	6095	-	-	100	-	-	-	-
43	426	5	300	-	-	100	-	-	-	-
44	436	4.5	300	-	-	100	-	-	-	-
45	387	1.5	300	-	-	100	-	-	-	-
46	375	1	300	-	-	100	-	-	-	-
47	375	*4.5*	300	-	-	100	-	-	-	-
48	419	5	300	-	-	100	-	-	-	-
49	426	5	6095	-	-	100	-	-	-	-
AIR	*288*	*1.00*	38923	-	-	-	-	-	*21.0*	*79.0*
EXHAUST	436	1.02	39774	-	-	4.2	-	2.3	16.1	77.3
FUEL[a]	*288*	*1.00*	755	-	*80.9*	-	-	-	-	*2.0*

a. For the gas composition of stream 1, Fuel, 22 and 23, add C_2H_6 9.4% / C_3H_8 4.7% / C_4H_{10} 2.3%.

b. For the gas composition of stream 2, add C_2H_6 1.4%/ C_3H_8 0.7% / C_4H_{10} 0.3%.

The simulation results indicate that the atmospheric SOFC hybrid cycle is capable of achieving very high electrical generation efficiency (68.7%). At a 100 MW capacity level, this efficiency is very attractive compared to the present efficiency leaders,

specifically state-of-the-art combined gas and steam turbine power plants, which are characterized by an efficiency of just under 60 %. Pressurized SOFC hybrid cycle should be able to reach even higher efficiency (up to 70%) with the cost of increased system complexity (Veyo and Lundberg, 2002).

The bottoming cycle employed only contributes 0.3 MW to the total system power production due to the very low exhaust temperature from the recuperator (stream 16: 447K). One way to increase the exhaust temperature is to decrease the gas turbine inlet temperature, which not only will decrease the power produced from the gas turbine but also will decrease the inlet air temperature to the SOFC at a given pressure ratio across the turbine-expander-driven compressor. This decreased air temperature will increase the air utilization factor (less air required to cool the SOFC stack), which in turn will also have negative impact over the power production from the gas turbine. In any case, this temperature should be maintained above 500°C to avoid thermal stress of the SOFC (EG&G, 2002). Simulation shows that when the gas turbine and SOFC air inlet temperatures are reduced to 750°C and 505°C, the exhaust temperature from the recuperator for steam generation raises to 531 K. The power production from the gas turbine is reduced to 16.2 MW while the steam turbine power production increases to 2.2 MW. But the overall electrical generation efficiency is reduced to 65.3%. Therefore, higher gas turbine inlet temperature appears more favourable to the overall system efficiency than high exhaust temperature to the HRSG steam generating system. Note that the Rankline cycle simulated is a simple cycle without incorporating reheat and multi-pressure steam generation. More complex setup can lead to higher system efficiency but

also increase in complexity. At <10 MW capacity, it is reasonable to assume that the steam turbine is non-reheat type (EG&G, 2002). The simulations show that the Rankine cycle is not favourable in this type of system setup because it contributes little in power production and increases the system complexity. But in applications where cogeneration and the supply of heat are desired, it provides a source of steam.

Table 4-7: Performance Data for the 100MW SOFC/GT Hybrid Power Generation System

Performance Parameters	**Value**
Cell Voltage, volts	0.71
Current Density, mA/cm^2	166
Operating Pressure, bar	1.08
Air Utilization Factor, %	18
Fuel Utilization Factor, %	85
Pre-reforming Percentage, %	9.2
S/C Ratio	2.5
Compressor Pressure Ratio	3
Steam Turbine Pressure Ratio	3
SOFC AC Power, MW	109
Gas Turbine AC Power, MW	27.3
Steam Turbine AC Power, MW	0.25
System Net AC Power, MW	135.7
System Electrical Efficiency (LHV) %	68.7

5.0 CO_2 Capture in SOFC-Based Power Generation Plants

5.1 Introduction

With the growing concerns about the impact of CO_2 emission on global warming, as the number one contributor, the power generation industry has a rapidly growing interest in the field of CO_2 emission reduction. Generally speaking, as long as fossil fuel is used for power generation, only two options are available to achieve CO_2 reduction:

- Improve the power plant electrical generation efficiency; or
- Capture the CO_2 generated from the power plants for permanent sequestration

To reduce the penalties of CO_2 capture in system efficiency and cost, novel concepts are proposed. Among them, SOFC technology is considered as one of the most promising technologies for CO_2 emission reduction in the future. One reason is that SOFC has a greater potential to achieve higher electrical efficiency than any other power generation technology. Most importantly, an SOFC power generation system has a distinctive feature that the fuel conversion takes place without the dilution of the CO_2 with nitrogen, which offers the prospect of reducing the CO_2 capture penalty in terms of efficiency and costs.

Previous studies have confirmed that SOFC-based power generation cycles can achieve very high electrical generation efficiency. However, the ultimate goal of this study is to explore the features of SOFC in CO_2 removal and investigate solid oxide fuel cell-based power generation processes that can simultaneously achieve high electricity generation efficiencies and generate a concentrated CO_2 stream for subsequent sequestration.

Studies of SOFC with CO_2 capture have been performed earlier by several researchers. An overview of the different concepts is given by Dijkstra and Jansen (2004), which presents a classification dividing the different systems in pre-combustion CO_2 capture, post-combustion CO_2 capture and post-combustion off-gas treatment. This work focused on the last option, which fully utilizes the potential of SOFC in providing a nitrogen-free off-gas.

To keep the electrochemical reaction progressing at reasonable rate, SOFCs require a certain partial pressure of unburned fuel be maintained. Therefore, not all of the fuel is burned and the fuel utilization of a SOFC is normally kept in the range of 80-90%. To achieve CO_2 separation in the exhaust stream it is necessary to burn the unused fuel without directly mixing with air which would introduce nitrogen. In the following sections, the "CO_2 separating SOFC" and two afterburning concepts (oxygen transport membrane and second modified SOFC unit) are described in details.

5.1.1 The "CO_2 Separating SOFC"

In the conventional tubular SOFC design, exhaust air and exhaust fuel are allowed to mix through controlled leakage of fuel through baffle boards which separate air and fuel in the generator. By introducing additional baffle boards and careful management of internal flows and pressure drops, it is expected that the required segregation of anode from cathode gases can be realized (Haines et al., 2002). This modification has been already proposed by Shell and Siemens-Westinghouse and the resulting stack is shown in Figure 5-1. With this modification, two outlet streams (depleted fuel and depleted air) will leave

the SOFC stack instead of one single exhaust stream. The simulation approach for this modification is introduced in Section 5.2.1.

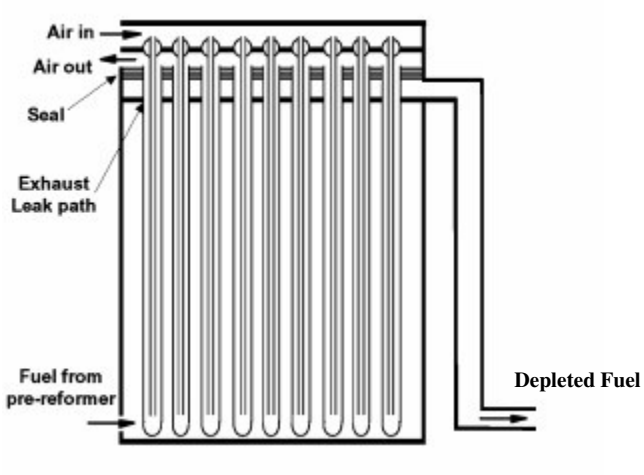

Figure 5-1: Modified SOFC Stack for CO2 Separation (Haines et al., 2002)

5.1.2 Oxygen Transport Membrane (OTM) Afterburner

The OTM afterburner is a technology being developed by Praxair Inc. that will selectively transport oxygen across the membrane to oxidize the remaining H_2 and CO in the SOFC anode off-gas.

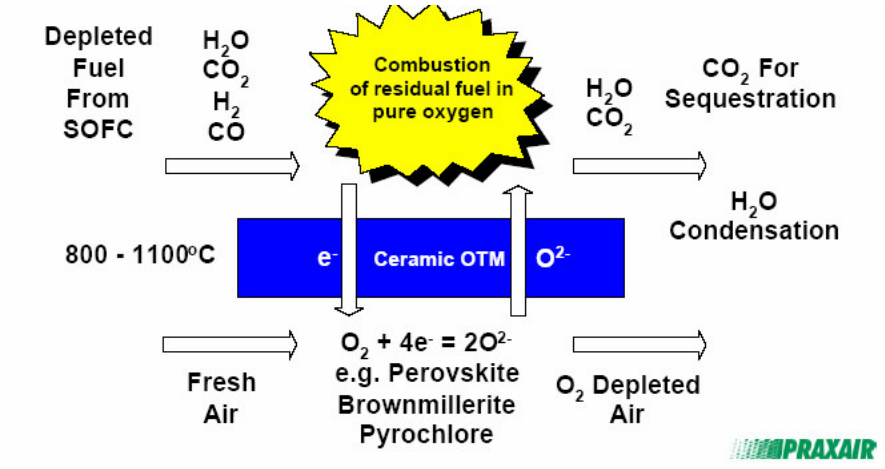

Figure 5-2: Principle of OTM Afterburner Operation

(Shockling and Christie, 2001)

As shown in Figure 5-2, the exhaust stream from SOFC is directed to one side of an OTM and air is fed to the opposite side of the dense, gas tight membrane. The chemical potential difference between the high temperature SOFC depleted fuel gas and the supplied air provides the driving force for oxygen transport. Pure oxygen is then transported as O^{2-} ions through the dense wall of ceramic and oxidizes the residual CO and H_2 remaining in the SOFC exhaust.

Similar in nature with tubular SOFC, OTM modules are also tubular high temperature (800°C-1100°C) ceramic systems. The air is introduced inside of the closed ended tube-shape membrane and flow up the reactor, co-concurrent with the fuel flowed over the membrane's external surface to oxidize the fuel. Laboratory test and demonstration projects performed by Praxair and Siemens demonstrated that the depleted fuel stream from SOFC anode could be completely oxidized using unmodified dense membranes without the need for additional membrane oxidation catalysts. The dried afterburner exhaust composition has been found to be stable at 97%-99.5% CO_2, 0-1% N_2, and 0-2% O_2 (Christie et al., 2003).

The similarity of the SOFC and OTM systems allows for a high level of integration of the balance of plant components. Although the energy from the oxidation of the depleted fuel is not available to the SOFC module anymore, that depleted fuel energy is now oxidized in the OTM afterburner. With adequate insulation and a relatively large recuperator, the OTM afterburner would require no additional energy (beyond the depleted fuel and air) to function. The resulting power generation efficiency is expected to be only marginally

lower than a standard SOFC power system with the incorporation of the OTM afterburner (Huang K, 2003).

The simulation of the integration of SOFC and OTM is introduced in section 5.2.2.

5.1.3 Modified SOFC Afterburner

The electrolyte of the SOFC acts as highly selective membrane for the transport of oxygen ions from the cathode and the anode. When fuel utilization is maximized, the SOFC can approach complete oxidization of the fuel without introducing nitrogen, thus acting as an "afterburner" and enhancing the CO_2 concentration of the anode exhaust gas. This concept has been proposed in the literature as a demonstration project funded mainly by A/S Norske Shell (Haines et al., 2002).

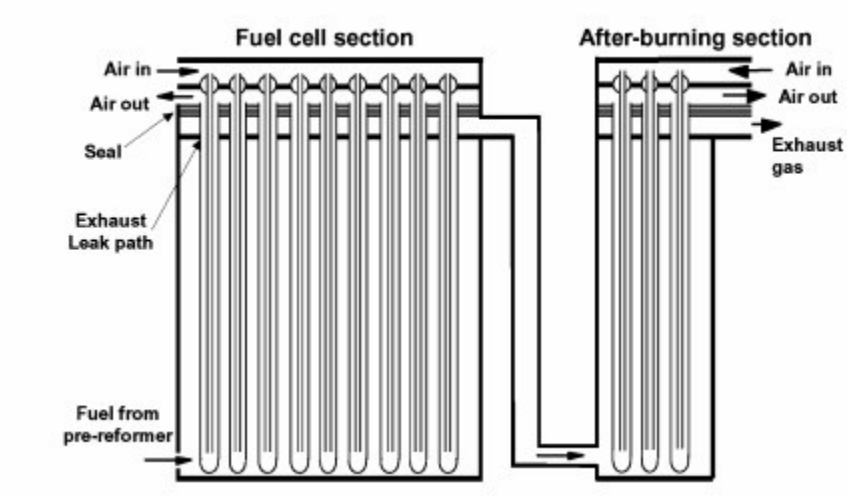

Figure 5-3: Modified SOFC Afterburner (Haines et al., 2002)

As Figure 5-3 shows, this concept is accomplished based on minor modifications to the tubular SOFC design developed by Siemens Westinghouse Power Corporation. Additional

oxygen separating tubes are added in a separate but similar stack section allowing almost all the residual fuel to be oxidized. The "afterburner" section will increase the overall fuel oxidization from the normal 85% leaving the main stack, to around 98% with minimum expectation on power generation from the "afterburner" section (Haines et al., 2002).

The simulation of the integration of SOFC and OTM is introduced in section 5.2.3. The assumptions for the simulation are identical to Table 4-5 if not mentioned in the following section.

5.2 System Simulations

5.2.1 Base Case Development

Both afterburner concepts mentioned above do not require pure oxygen to combust the fuel remaining in the exhaust, thus avoid an expensive and energy demanding air separation plant. In order to establish a comparison platform and evaluate the potential benefits of the two "afterburner" concepts, a base case that utilizes the CO_2 separating SOFC stack (section 5.1.1) and pure oxygen fed afterburner is developed. It is a modification based on the 100MW atmospheric SOFC/GT hybrid cycle described in section 4.4. The simulation of this base case is introduced below and the AspenPlus™ flowsheet of this case is presented in Figure 5-4. Terms in italics represent actual AspenPlus™ terminology.

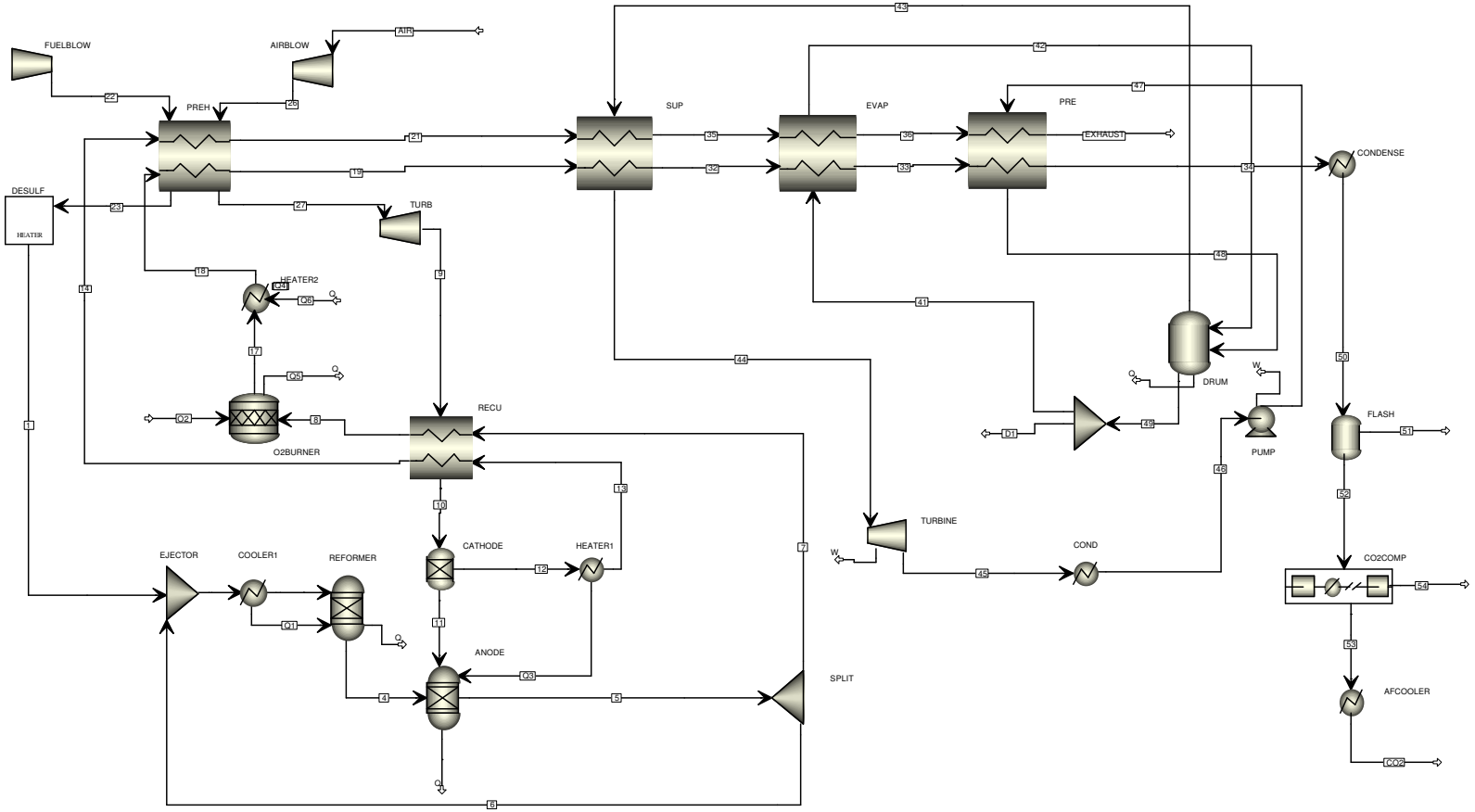

Figure 5-4: AspenPlus^{TM} Flowsheet of a 100MW SOFC Based Power Generation System with CO2 Capture (Base Case)

- Simulation of a "CO_2 separating SOFC" stack

The simulation approach of the CO_2 separating SOFC stack (section 5.1.1) should be identical to the conventional SOFC stack described in section 3 with the following exception: The "CO_2 separating tubular SOFC" design no longer includes air preheating and combustion plenum (Campanari, 2002). Therefore, blocks "AFTERBUR", and "HEATER2" and "RECUPER" representing the combustion plenum and air preheating process are removed from the initial flowsheet (Figure 4-5). Stream 13 (depleted air) and stream 7 (depleted fuel) leave the stack as two separate streams. Steam 7 then enters the oxygen feed afterburner for oxidization.

- Simulation of an oxygen feed afterburner

To burn the remaining fuel in the SOFC anode off-gas, an afterburner is simulated in AspenPlus™ using reactor module *RStoic* (named "O2BURNER"). The reactions specified in the ''AFTERBUR'' block are considered as reaching completion (100% conversion) and include:

Hydrogen oxidation $$H_2 + \frac{1}{2}O_2 \rightarrow H_2O \quad \text{(R3-4)}$$

Carbon monoxide oxidation $$CO + \frac{1}{2}O_2 \rightarrow CO_2 \quad \text{(R3-5)}$$

An AspenPlus™ *Heater* module (named "HEATER2") is used to simulate the heat exchange process in the O_2 burner. The heat generated by the oxidation reactions of H_2 and CO is calculated by the block "O2BURNER" and put into stream Q_5. The heat is then put into the exhaust in the "HEATER 2" block after taking account of assumed 2% heat loss of the burner. This is achieved by using an AspenPlus™ *Calculator* to satisfy:

$Q_6 = 0.98\ Q_5$.

The flowrate of the oxygen stream (assumed 95% O_2 and 5% Ar) is adjusted to make sure no extra O_2 contained in the burner outlet (stream 17). An AspenPlus™ *Design-spec* can be used to perform this function.

- Simulation of the heat recovery process

By exchanging the heat between the heated exhaust (stream 13 and 18) and incoming air and fuel (stream 26 and 22) in the "PREH" block, the temperature of the exhausts (stream 19 and 21) leaving the system to the HRSG can be determined. The inlet temperature of the expander is specified at 900°C assuming 10K approach in the "PREH" heat exchanger.

- Simulation of the Rankine bottoming cycle

The simulation is identical to what is described in section 4.4. The only difference is that the AspenPlus™ module *MHeatX* is used to simulate the superheater "SUP", evaporator "EVAP" and economizer "PRE" instead of *HeatX* to accommodate multi-stream exchange. The recirculation flow (Stream 41) and temperature of stream 44 are adjusted to make sure that the approach and pinch in these heat exchangers are the same as what were assumed in section 4.4 for comparison purpose.

- Simulation of the CO_2 Concentration and Sequestration

After burning all the remaining fuel from the SOFC with oxygen, the exhaust stream from this system is concentrated with CO_2. It flows through the HRSG to recover the heat and then is ready for sequestration. Before sequestration, the wet CO_2 stream needs to be dried to remove the water contained in the stream. A gas-water heat exchanger and a "knock–out" drum can perform this function. This water condensing process is simulated in AspenPlus™ using module *HeatX* (named "CONDENSE") and *Flash2* (named "FLASH"). The "CONDENSE" is specified with an outlet temperature 298K. The stream 51 represents the water removed from the exhaust and the stream 52 represents the dried CO_2 stream ready to be compressed for sequestration.

An AspenPlus™ module *MCompr* is used to simulate the multi-stage inter-cooled CO_2 compressor (named "CO2COMP"). It is specified with 7 stages and a discharge pressure of 120 atm. Also specified in the block is an intercooled temperature of 318K and polytrophic efficiency of 85%. Stream 54 represents the remaining water knocked out from the CO_2 stream during the compression process. Stream 53 represents the dried and compressed CO_2 stream leaving the compressor. This stream is then condensed and ready for storage. The condensing process is simulated using an AspenPlus™ module *HeatX* (named "AFCOOLER") with a specified outlet temperature 298K. The stream CO_2 represents the dried, compressed and liquefied CO_2 stream ready for storage.

Stream properties for this cycle are presented in Table 5-1. The estimated performance of this system is summarized in Table 5-4 with detailed analysis in section 5.3.

Table 5-1: Stream Properties for the 100MW SOFC Based Power Generation System with CO_2 Capture (Base Case)

(data in italic represents the input to the model –either streams or the blocks, data in regular represents output of the model)

Strm No.	Temp. (K)	Press. (atm)	Mole Flow (kmol/hr)	Gas Composition (mole %)						
				H_2	CH_4	H_2O	CO	CO_2	O_2	N_2
1[a]	*653*	3.30	769	-	80.9	-	-	-	-	2.0
2[b]	1062	*1.10*	5342	10.2	11.7	44.3	7.1	23.6	-	0.8
3[b]	826	1.10	5342	10.2	11.7	44.3	7.1	23.6	-	0.8
4	826	1.10	6103	29.3	9.3	27.7	7.6	25.5	-	0.7
5	*1183*	1.10	7234	11.9	-	51.7	8.3	27.5	-	0.6
6	1183	1.10	4573	11.9	-	51.7	8.3	27.5	-	0.6
7	1183	1.10	2662	11.9	-	51.7	8.3	27.5	-	0.6
9	971	*1.12*	17836	-	-	-	-	-	21.0	79.0
11	971	1.12	1525	-	-	-	-	-	100.0	-
12	971	1.12	16311	-	-	-	-	-	13.6	86.4
13	*1183*	1.12	16311	-	-	-	-	-	13.6	86.4
17[c]	*1183*	1.08	2676	-	-	63.3	-	35.6	-	0.6
18[c]	2121	1.08	2676	-	-	63.3	-	35.6	-	0.6
19[c]	704	1.06	2676	-	-	63.3	-	35.6	-	0.6
21	704	1.12	16311	-	-	-	-	-	13.6	86.4
22[a]	380	3.34	769	-	80.9	-	-	-	-	2.0
23[a]	*673*	3.32	769	-	80.9	-	-	-	-	2.0
26	416	*3.00*	17836	-	-	-	-	-	21.0	79.0
27	*1173*	2.98	17836	-	-	-	-	-	21.0	79.0
32[c]	681	1.04	2676	-	-	63.3	-	35.6	-	0.6
33[c]	548	1.02	2676	-	-	63.3	-	35.6	-	0.6
34[c]	447	1.02	2676	-	-	63.3	-	35.6	-	0.6
35	526	1.1	16311	-	-	-	-	-	13.6	86.4
36	456	1.08	16311	-	-	-	-	-	13.6	86.4
41	*537*	*50*	*52760*	-	-	*100*	-	-	-	-

Strm No.	Temp. (K)	Press. (atm)	Mole Flow (kmol/hr)	Gas Composition (mole %)						
				H_2	CH_4	H_2O	CO	CO_2	O_2	N_2
42	537	50	52760	-	-	100	-	-	-	-
43	537	50	2442	-	-	100	-	-	-	-
44	670	49.5	2442	-	-	100	-	-	-	-
45	387	1.5	2442	-	-	100	-	-	-	-
46	375	1	2442	-	-	100	-	-	-	-
47	375	*50.5*	2442	-	-	100	-	-	-	-
48	514	50	2442	-	-	100	-	-	-	-
49	537	50	52760	-	-	100	-	-	-	-
50[c]	*298*	1	2676	-	-	63.3	-	35.6	-	0.6
51	298	1	1669	-	-	100	-	-	-	-
52[d]	298	1	1007	-	-	2.6	-	94.5	-	1.5
53[d]	381	120	983	-	-	-	-	97.0	-	1.6
54	318	1	23	-	-	100	-	-	-	-
AIR	*288*	*1.00*	17836	-	-	-	-	-	*21.0*	*79.0*
CO2[d]	*298*	120	983	-	-	-	-	97.0	-	1.6
EXHAUST	486	1.08	16311	-	-	-	-	-	13.6	86.4
FUEL[a]	*288*	*1.00*	769	-	*80.9*	-	-	-	-	*2.0*
O2[c]	*288*	*1.1*	*288*	-	-	-	-	-	*99.5*	-

a. For the gas composition, add C_2H_6 9.4% / C_3H_8 4.7% / C_4H_{10} 2.3%.

b. For the gas composition, add C_2H_6 1.4%/ C_3H_8 0.7% / C_4H_{10} 0.3%.

c. For the gas composition, add Ar 0.5%.

d. For the gas composition, add Ar 1.4%.

5.2.2 Oxygen Transport Membrane (OTM) Afterburner Case

Instead of using pure oxygen, a novel concept to afterburning the remaining fuel in the SOFC anode off-gas is to integrate an OTM afterburner. The introduction of this concept is introduced in section 5.1. In this section, the simulation results of a cycle with an

integration of the CO_2 separating SOFC stack and OTM is presented. It is quite similar to the base case introduced in section 5.2.1 with the exception of the "afterburner" part. The AspenPlus™ flowsheet of this case is presented in Figure 5-5. The stream properties of this case are documented in Table 5-2. The estimated performance of this cycle is summarized in Table 5-4 with detailed analysis in section 5.3. An introduction of the OTM afterburner simulation is given below.

After leaving the SOFC stack, the anode off-gas and cathode off-gas enter the OTM as two separate streams, depleted fuel (stream 7) and depleted air (steam 13). The OTM is simulated in AspenPlus™ using module *Sep* (named "MEM") and *RStoic* (named "O2BURNER").

A certain amount of oxygen (stream O2) is separated from the cathode off-gas (steam 13) in the ''MEM'' (OTM air side) and enters the ''O2BURNER'' (OTM fuel side) to oxidize the depleted fuel from the SOFC stack (stream 7). This step simulates the oxygen ion crossing over from air side of membrane to the fuel side. An AspenPlus™ *Design-spec* is used to calculate the molar flow rate of stream O2 to satisfy the O_2 composition (1%) in the final dried CO_2 stream (stream CO2) as reported in the literature (Christie et al., 2003). The oxidizations occurring on the fuel side of the membrane are considered 100% completed at 910°C with the following reactions specified:

Hydrogen oxidation $$H_2 + \frac{1}{2}O_2 \rightarrow H_2O \quad \text{(R3-4)}$$

Carbon monoxide oxidation $$CO + \frac{1}{2}O_2 \rightarrow CO_2 \quad \text{(R3-5)}$$

It is assumed that the reaction heat of the oxidizations is sufficient to sustain the OTM separation process and heat losses. Thus, the double depleted air (stream 15) and the oxidized fuel (stream 16) leave the OTM at 910°C. These two streams then enter the "PREH" recuperator to preheat the incoming air and fuel. The air preheating temperature is specified at 900°C assuming 10K approach in the "PREH" heat exchanger.

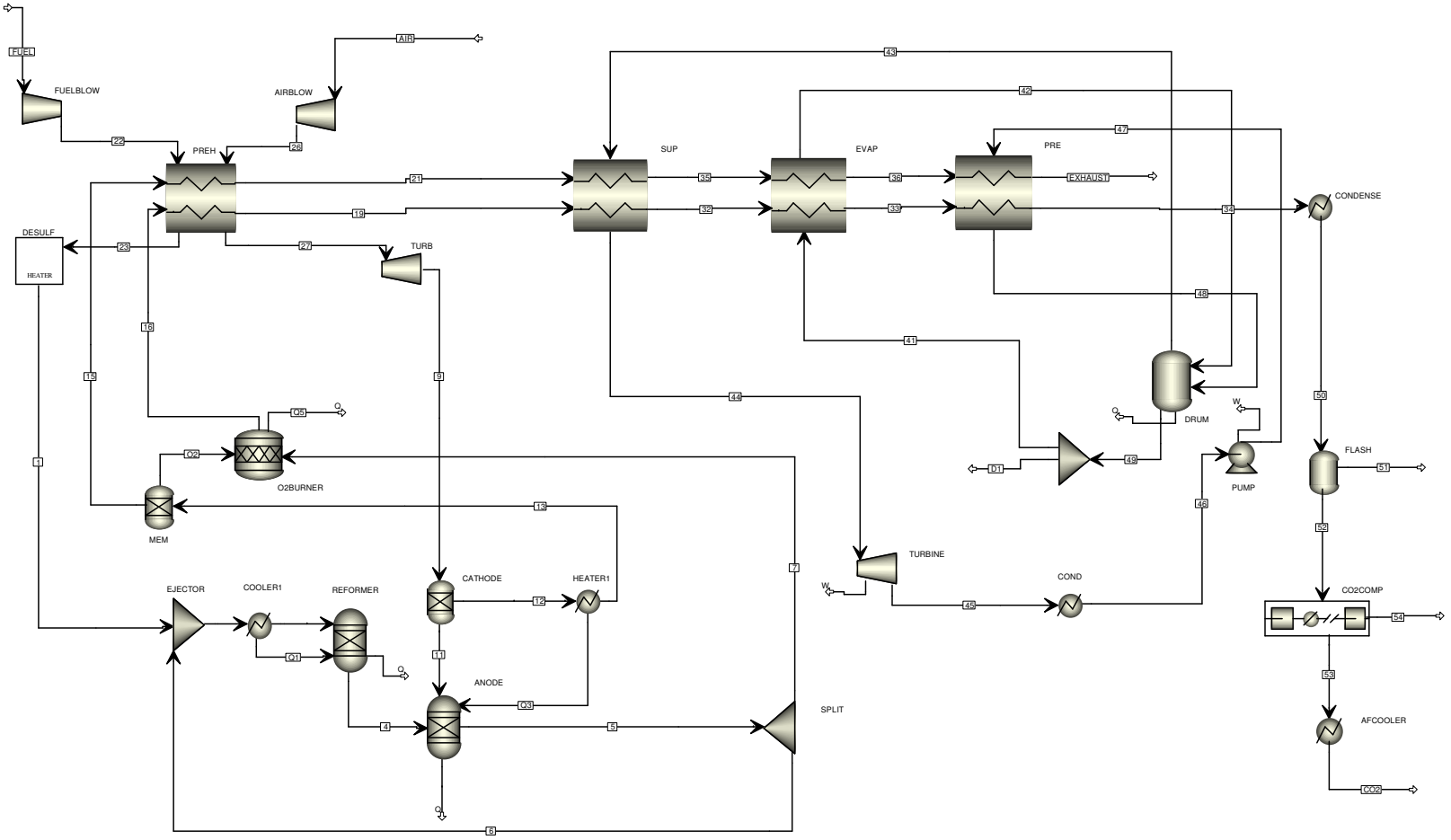

Figure 5-5: AspenPlus^{TM} Flowsheet of a 100MW SOFC Based Power Generation System with CO_2 Capture (OTM Case)

Table 5-2: Stream Properties for the 100MW SOFC Based Power Generation System with CO_2 Capture (OTM Case)

(data in italic represents the input to the model –either streams or the blocks, data in regular represents output of the model)

Strm No.	Temp. (K)	Press. (atm)	Mole Flow (kmol/hr)	Gas Composition (mole %)						
				H_2	CH_4	H_2O	CO	CO_2	O_2	N_2
1[a]	*653*	3.30	776	-	80.9	-	-	-	-	2.0
2[b]	1062	*1.10*	5391	10.2	11.6	44.3	7.1	23.6	-	0.8
3[b]	826	1.10	5391	10.2	11.6	44.3	7.1	23.6	-	0.8
4	826	1.10	6159	29.3	9.3	27.7	7.6	25.5	-	0.7
5	*1183*	1.10	7301	11.9	-	51.7	8.3	27.5	-	0.6
6	1183	1.10	4615	11.9	-	51.7	8.3	27.5	-	0.6
7	1183	1.10	2686	11.9	-	51.7	8.3	27.5	-	0.6
9	919	*1.12*	14963	-	-	-	-	-	21.0	79.0
11	919	1.12	1539	-	-	-	-	-	100.0	-
12	919	1.12	13424	-	-	-	-	-	12.0	88.0
13	*1183*	1.12	13424	-	-	-	-	-	12.0	88.0
15	*1183*	1.12	13142	-	-	-	-	-	10.0	90.0
16	1183	1.08	2696	-	-	63.4	-	35.6	0.4	0.6
19	523	1.08	2696	-	-	63.4	-	35.6	0.4	0.6
21	523	1.10	13142	-	-	-	-	-	10.0	90.0
22[a]	380	3.34	776	-	80.9	-	-	-	-	2.0
23[a]	*673*	3.32	776	-	80.9	-	-	-	-	2.0
26	457	*4.00*	14963	-	-	-	-	-	21.0	79.0
27	*1173*	3.98	14963	-	-	-	-	-	21.0	79.0
32	522	1.04	2696	-	-	63.4	-	35.6	0.4	0.6
33	496	1.02	2696	-	-	63.4	-	35.6	0.4	0.6
34	490	1.00	2696	-	-	63.4	-	35.6	0.4	0.6
35	522	1.08	13142	-	-	-	-	-	10.0	90.0
36	496	1.06	13142	-	-	-	-	-	10.0	90.0
41	*486*	*20*	*7167*	-	-	*100*	-	-	-	-

Strm No.	Temp. (K)	Press. (atm)	Mole Flow (kmol/hr)	Gas Composition (mole %)						
				H_2	CH_4	H_2O	CO	CO_2	O_2	N_2
42	486	20	7167	-	-	100	-	-	-	-
43	486	20	347	-	-	100	-	-	-	-
44	511	19.5	347	-	-	100	-	-	-	-
45	387	1.5	347	-	-	100	-	-	-	-
46	375	1	347	-	-	100	-	-	-	-
47	375	*20.5*	347	-	-	100	-	-	-	-
48	474	20	347	-	-	100	-	-	-	-
49	486	20	7167	-	-	100	-	-	-	-
50	*298*	0.98	2696	-	-	63.4	-	35.6	0.4	0.6
51	298	0.98	1684	-	-	100	-	-	-	-
52	298	0.98	1012	-	-	2.6	-	94.9	-	1.5
53	381	120	987	-	-	-	-	97.4	1	1.6
54	318	1	24							
AIR	*288*	*1.00*	14963	-	-	-	-	-	*21.0*	*79.0*
CO2	*298*	119.5	989	-	-	-	-	97.4	1	1.6
EXHAUST	490	1.04	13143	-	-	-	-	-	10.0	90.0
FUEL[a]	*288*	*1.00*	776	-	*80.9*	-	-	-	-	*2.0*
O2	1183	1.12	281	-	-	-	-	-	*100*	-

a. For the gas composition, add C_2H_6 9.4% / C_3H_8 4.7% / C_4H_{10} 2.3%.

b. For the gas composition, add C_2H_6 1.4%/ C_3H_8 0.7% / C_4H_{10} 0.3%.

5.2.3 Modified SOFC Afterburner Case

As explained in section 5.1, another option to the "afterburner" is an adoption of a second SOFC module which has the function of approaching a complete oxidization of the spent fuel flow, thus acting as an "afterburner" and enhancing the CO_2 concentration of the anode exhaust gases. Since the second SOFC "afterburner" does not require fuel

recirculation and pre-reformers (Campanari, 2002), blocks "Split", "Ejector", "Cooler1", "Reformer" and related AspenPlus™ *Calculator* and *Design-spec* of the first SOFC are not longer required in the second one. This makes the simulation approach of the second SOFC quite similar to the OTM afterburner. The AspenPlus™ flowsheet of this case is presented in Figure 5-6. The stream properties of this case are documented in Table 5-3. The estimated performance of this cycle is summarized in Table 5-4 with detailed analysis in section 5.3. An introduction of the second SOFC afterburner simulation is given below:

After leaving the first SOFC stack, the anode off-gas and cathode off-gas enter the second SOFC as two separate streams: depleted fuel (stream 7) and depleted air (steam 13).

It is assumed that the second SOFC does not produce power. Its chemical energy will then all become heat as a result of loses in the system. To maintain the cell operating temperature at a stable point, additional fresh air (stream AIR2) is required to cool the stack. It is compressed by an air blower "AIRBLOW2" (AspenPlus™ *Compr* Module) and mixed with the stream 13 before feeding the second SOFC cathode inlet. The flowrate of this fresh air stream is determined by using an AspenPlus™ *Design-spec* to satisfy the following equation:

$$Q_5 = Q_{loss} \qquad \text{(E5-1)}$$

Where Q_5 represents the net heat duty of the second SOFC, Q_{loss} is assumed heat loss of the second SOFC (1%).

Please, note that equation E-1 implies that the second SOFC generates zero power and acts as a true "afterburner". Discussions about this implication can be found in section 5.3.

Identical to the simulation approach of the power-generating SOFC, the anode of the second SOFC is simulated using AspenPlus™ reactor module *RGibbs* (named "ANODE2"). Reactions specified in this block are:

The reactions considered in the block are:

Electrochemical Reaction $H_2 + \frac{1}{2}O_2 \rightarrow H_2O$ (R2-5)

Water-gas shift reaction $CO + H_2O \Leftrightarrow CO_2 + H_2$ (R3-2)

Methane steam reforming $CH_4 + H_2O \Leftrightarrow CO + 3H_2$ (R3-3)

The three reactions above are specified to reach thermodynamic equilibrium at a given temperature (910°C) as block ANODE.

The mixed air (stream 10) enters the second SOFC cathode to provide oxygen for the electrochemical reaction. Inside the cells, the air stream is further heated by the heat from the electrochemical reactions. This process is implemented in AspenPlus™ using the separator module *Sep* (named ''CATHODE2'') and the temperature changer module *Heater* (named ''HEATER3''). A certain amount of oxygen (stream O2) is separated in the ''CATHODE2'' block from stream 10 and enters the ''ANODE2'' block to oxidize the fuel. This step simulates the oxygen ion crossing over to the anode side. An AspenPlus™ *Design-spec* is used to adjust the O_2 component *Split fraction* in the block

"CATHODE2" to satisfy the calculated molar flow rate of stream "O2" ($n_{O2,required}$) based on the fuel equivalent hydrogen molar flow rate ($n_{H2,equivalent}$), specified fuel utilization factor for the power-generating SOFC (U_f) and expected overall fuel utilization factor ($U_{f,\ overall}$) as:

$$n_{O2,required} = 0.5\ (U_{f,\ overall} - U_f)\ (n_{H2,equivalent}) \qquad \text{(E5-2)}$$

The $n_{H2,equivalent}$ is the equivalent hydrogen contained in the fresh fuel. Its calculation can be referred to equation E3-3. The expected overall fuel utilization factor ($U_{f,\ overall}$) is set to be 0.98 (Haines et al., 2002).

By specifying the HEATER3 outlet temperature to 910°C and introducing heat stream Q_6 to ANODE2, the flowrate of the cool air stream can be calculated based on equation E5-1.

The second SOFC anode off-gas (stream 17) and cathode off-gas (stream 24) leave the stack and enter the "PREH" recuperator to preheat the incoming air and fuel. The air preheating temperature is specified at 900°C assuming 10K approach in the "PREH" heat exchanger.

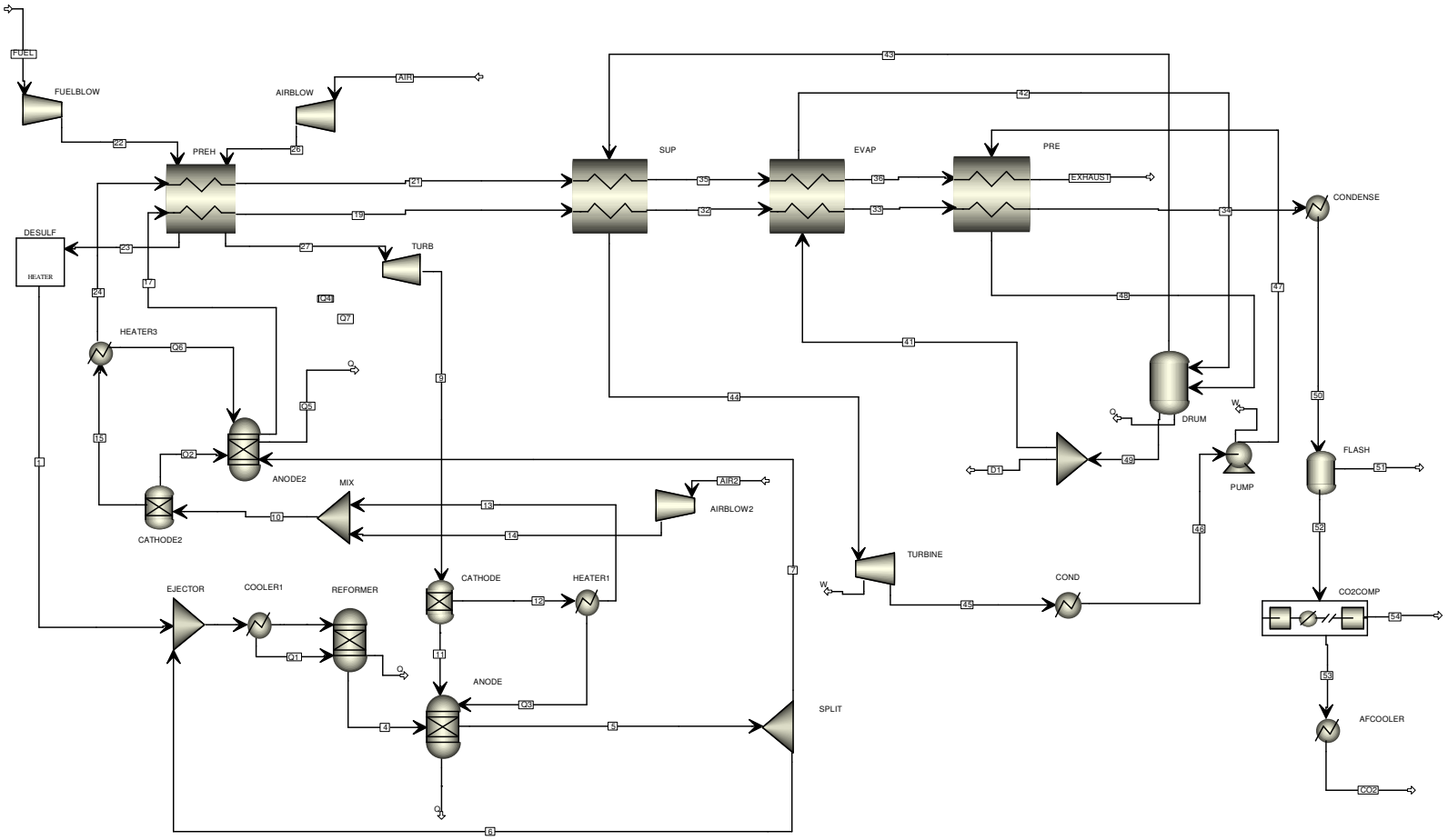

Figure 5-6: AspenPlus^{TM} Flowsheet of a 100MW SOFC Based Power Generation System with CO_2 Capture (SOFC Afterburner Case)

Table 5-3: Stream Properties for the 100MW SOFC Based Power Generation System with CO_2 Capture (SOFC Afterburner Case)

(data in italic represents the input to the model –either streams or the blocks, data in regular represents output of the model)

Strm No.	Temp. (K)	Press. (atm)	Mole Flow (kmol/hr)	Gas Composition (mole %)						
				H_2	CH_4	H_2O	CO	CO_2	O_2	N_2
1[a]	*653*	3.30	776	-	80.9	-	-	-	-	2.0
2[b]	1062	*1.10*	5391	10.2	11.7	44.3	7.1	23.6	-	0.8
3[b]	826	1.10	5391	10.2	11.7	44.3	7.1	23.6	-	0.8
4	826	1.10	6159	29.3	9.3	27.7	7.6	25.5	-	0.7
5	*1183*	1.10	7301	11.9	-	51.7	8.3	27.5	-	0.6
6	1183	1.10	4615	11.9	-	51.7	8.3	27.5	-	0.6
7	1183	1.10	2686	11.9	-	51.7	8.3	27.5	-	0.6
9	919	*1.12*	14962	-	-	-	-	-	21.0	79.0
10	978	1.12	17802	-	-	-	-	-	14.2	85.8
11	919	1.12	1539	-	-	-	-	-	100.0	-
12	919	1.12	13424	-	-	-	-	-	11.9	88.1
13	*1183*	1.12	13422	-	-	-	-	-	11.9	88.1
14	299	*1.12*	4378	-	-	-	-	-	21.0	79.0
15	978	1.12	17566	-	-	-	-	-	13.0	87.0
17	1183	1.08	2686	1.6	-	62.1	1.1	34.6	-	0.6
19	668	1.08	2686	1.6	-	62.1	1.1	34.6	-	0.6
21	668	1.10	17579	-	-	-	-	-	13.0	87.0
22[a]	380	3.34	776	-	80.9	-	-	-	-	2.0
23[a]	*673*	3.32	776	-	80.9	-	-	-	-	2.0
24	*1183*	1.12	17566	-	-	-	-	-	13.0	87.0
26	457	*4.00*	14962	-	-	-	-	-	21.0	79.0
27	*1173*	3.98	14962	-	-	-	-	-	21.0	79.0
32	654	1.04	2686	1.6	-	62.1	1.1	34.6	-	0.6
33	548	1.02	2686	1.6	-	62.1	1.1	34.6	-	0.6
34	514	1.00	2686	1.6	-	62.1	1.1	34.6	-	0.6

Strm No.	Temp. (K)	Press. (atm)	Mole Flow (kmol/hr)	Gas Composition (mole %)						
				H_2	CH_4	H_2O	CO	CO_2	O_2	N_2
35	654	1.08	17566	-	-	-	-	-	13.0	87.0
36	548	1.06	17566	-	-	-	-	-	13.0	87.0
41	*537*	*50*	*44687*	-	-	*100*	-	-	-	-
42	537	50	44687	-	-	100	-	-	-	-
43	537	50	1974	-	-	100	-	-	-	-
44	643	49.5	1974	-	-	100	-	-	-	-
45	387	1.5	1974	-	-	100	-	-	-	-
46	375	1	1974	-	-	100	-	-	-	-
47	376	*50.5*	1974	-	-	100	-	-	-	-
48	498	50	1974	-	-	100	-	-	-	-
49	537	50	44687	-	-	100	-	-	-	-
50	*298*	0.98	2686	1.6	-	62.1	1.1	34.6	-	0.6
51	298	0.98	1641	-	-	100	-	-	-	-
52	298	0.98	1045	4.0	-	2.6	2.9	90.0	-	1.5
53	382	120	1020	4.1	-	-	3.0	91.4	-	1.5
54	318	0.98	25	-	-	100	-	-	-	-
AIR	*288*	*1.00*	14962	-	-	-	-	-	*21.0*	*79.0*
AIR2	*288*	*1.00*	4378	-	-	-	-	-	*21.0*	*79.0*
CO2	*298*	119.5	1020	4.1	-	-	3.0	91.4	-	1.5
EXHAUST	514	1.04	17566	-	-	-	-	-	13.0	87.0
FUEL[a]	*288*	*1.00*	776	-	*80.9*	-	-	-	-	*2.0*
O2	978	1.12	235	-	-	-	-	-	*100*	-

a. For the gas composition, add C_2H_6 9.4% / C_3H_8 4.7% / C_4H_{10} 2.3%.

b. For the gas composition, add C_2H_6 1.4%/ C_3H_8 0.7% / C_4H_{10} 0.3%.

5.3 Comparison of Results

In sections 4 and 5, a total of four atmospheric SOFC/GT hybrid power generation systems are introduced and simulated based on a fixed SOFC power output (109 MW):

Cycle 1 - An atmospheric SOFC/GT hybrid power generation system with conventional tubular SOFC stack design (section 4.4)

Cycle 2 - An atmospheric SOFC/GT hybrid power generation system with modified SOFC stack design for CO_2 separation and pure oxygen feed afterburner (section 5.2.1)

Cycle 3 – An atmospheric SOFC/GT hybrid power generation system with modified SOFC stack design for CO_2 separation and OTM afterburner (section 5.2.2)

Cycle 4 – An atmospheric SOFC/GT hybrid power generation system with modified SOFC stack design for CO_2 separation and a second SOFC afterburner (section 5.2.3)

The detail performance of these four cycles is summarized in Table 5-4. Compared to the case without CO_2 capture (cycle 1), in the cases with CO_2 capture (cycles 2, 3 and 4), the following effects are observed:

- The electrical efficiency of the SOFC generator is reduced. (cycle 2 – 0.8%, cycle 3 and cycle 4 – 1.6%) as a result of the difference in air utilization, which is due to the difference in the air temperature into the SOFC stack (stream 9). The higher the air utilization, the less the air flows through the SOFC stack. The less air flows through the stack, the lower O_2 concentration is available in the cathode, which in turn reduces the voltage generated from the SOFC and therefore reduces electricity generation

efficiency. As the SOFC stack design is altered to accommodate CO_2 separation, the heat from afterburning the remaining fuel inside the stack can not be directly utilized to preheat the air into the stack. In cycle 2, although the combustion heat of the remaining fuel in the O_2 burner is recovered by the PREH recuperator, its configuration suffers larger heat exchanging loss, which results in 123K difference in stream 9 temperature. For cycles 3 and 4, the heat of oxidization of the remaining fuel is not recovered, which results in even lower air temperature available to the SOFC stack, therefore suffering even higher efficiency loss .

- Additional power for CO_2 compression is required. The efficiency decrease due to CO_2 compression amounts to 2.1%.
- More power is recovered from the steam bottoming cycle due to higher exhaust temperature available. The relative system efficiency gain from the steam bottoming cycle is around 3.7% for cycle 2, 0.25% for cycle 3 and 2.7% for cycle 4. The difference in the efficiency gain for different cycles is due to the degree of heat recovery from the oxidization of the remaining fuel. In cycle 2, the heat is almost fully recovered other than the heat exchanger losses at a cost of more expensive recuperator (higher working temperature) and the need to produce O_2 from an air separation plant, which has 1.2% negative impact on the system efficiency. In cycle 3, it is assumed that all of the oxidization heat is utilized for the O_2 separation process and therefore, none is available to be recovered. The observed slight gain in the bottoming cycle for cycle 3 is due to the lower pressure ratio across the expander selected to avoid air temperature too low to the SOFC stack. In cycle 4, it is assumed that zero voltage is produced from the SOFC “afterburner”, therefore the heat of

oxidization is recovered through the extra cooling air flow (AIR2) added into the SOFC "afterburner". Please, note that the assumptions mentioned above regarding the heat recovery for cycles 3 and cycle 4 have a major impact on the final calculated system efficiency. If the O_2 separating process in the OTM does not consume all the oxidization thermal energy (cycle 2) or if the second SOFC afterburner produce power more than zero (cycle 3), the overall system efficiency for both of the two cycles will be higher.

Summarized from above, the total system efficiency decrease in the CO_2 separating SOFC based power generation cycles amounts to 7.1% -10.1%. The main causes for this lower efficiency are losses in output power due to:

- Lower SOFC efficiency as a result of the increased fuel utilization
- Power required for compression of CO_2
- A lower air mass flow for the gas expander
- Cost of separating O_2 from N_2

Regardless of the 7-10% CO_2 capture penalty, the electrical efficiency of the atmospheric SOFC based power generation systems studied in this work achieved 59%-62% with a 100% CO_2 recovery, which demonstrates great advantages over the conventional power generation cycles.

It is worth mentioning that the cycle 2 has slightly higher calculated system efficiency than the other two afterburner cycles (cycle 3 and 4), but it requires more complex and expensive system – air separation plant. With simpler arrangement and competitive

system efficiency, the concept of employing a membrane (such as OTM, SOFC, etc...) afterburner appears promising.

Table 5-4: Comparison of Performance Data for Different SOFC/GT Hybrid Power Generation Systems

Performance Parameters	**Cycle 1**	**Cycle 2**	**Cycle 3**	**Cycle 4**
Cell Voltage, volts	0.71	0.7	0.69	0.69
Cell Current Density, mA/cm^2	166	169	170	170
Gas Temperature to the HRSG, K	447	704	523	668
Air Utilization Factor, %	18	41	49	49
Total Fuel Input (MW, LHV)	197	200	203	203
SOFC AC Power, MW	109	109	109	109
Gas Expander Net AC Power, MW	27.3	14.8	14.4	14.4
Steam Turbine AC Power, MW	0.25	7.7	0.76	5.7
Fuel Blower AC Power, MW	-0.85	-0.85	-0.87	-0.87
Additional Air Blower AC Power, MW	-	-	-	-0.41
CO_2 Compressor AC Power, MW	-	-4.25	-4.3	-4.5
Power Consumption for Producing O_2, MW	-	-2.4[(a)]	-	-
System Net AC Power, MW	135.7	124.0	119.0	123.3
SOFC Electrical Efficiency (LHV) %	55.3	54.5	53.7	53.7
System Electrical Efficiency (LHV) %	68.7	61.6	58.6	60.7
CO_2 Mass Flow Removed. (kg/s)	-	11.9	12.0	11.8
CO_2 Concentration in Stream CO2 (%)	-	97	97.4	91.4

Notes:

a. The electricity consumption for producing O_2 is calculated based on 1000 kJ/kg O_2 by a typical air separation plant.

6.0 Economic Evaluation

Studies in previous sections indicate that SOFC-based power generation cycles offer great advantages in terms of power generation efficiency. As for any other new technology, another critical factor that need to be investigated beside performance is the economics. Unfortunately, many important elements in the studied cycles such as SOFC and OTM are still in the research stage, thus there is a paucity of cost data in the open literature and the data available are premature.

Regardless of the limitation on the available cost data, a preliminary economic investigation is carried out just to evaluate and compare the economic performance of the studied cycles based on different capital and fuel cost scenarios. Cycle 1 and Cycle 4 proposed in section 5 are chosen for the purpose of this economic study. Cycle 1 represents a conventional tubular SOFC/GT hybrid power generation system without CO_2 capture function and Cycle 5 represents a SOFC/GT hybrid power generation system with a modified SOFC stack for CO_2 separation, a second SOFC afterburner and complete CO_2 drying and compression trains for CO_2 concentration. As parameters of evaluation, the cost of electricity (COE) as well as the cost in \$/ton CO_2 avoided are used. The overall assumptions used in carrying out the economic evaluation are:

- All values in 2003 US Dollars
- For the investment on the capital equipment:
    - 7% interest rate
    - 20 year project life
    - \$0 salvage value

- Operating and Maintenance (O&M) is 2% of the capital investment
- The plant operates for 8000 hours/year which allows for about a month of maintenance time per year
- The cost of natural gas is $4.00/MMBtu

6.1 Total Capital Cost

SOFC technology is currently at the stage of development, thus its cost information is not well established and very little data are available from the open literature. According to the Solid State Energy Conversion Alliance (SECA), current capital cost of a SOFC system is around $4000/kW, which is much higher than conventional power generation cycles. Like most new technologies, as more units are installed and new players join the market, prices are likely to fall. Price projections vary among fuel cell developers, but most are targeting costs below $1,500/kW based on volume production. It is highly unlikely that this price target will be achieved before 2007. The long term goal of the SECA is to reduce the capital cost of the SOFC system to $400/kW by 2010, while keeping the power densities, reliability, and operating characteristics compatible with commercial service in both stationary and transportation power applications. In this section, it is assumed that the equipment cost of a SOFC stack is $1000/kW which is assumed as 25% of the current capital cost of a SOFC system (Horne, 2005). This equipment cost is applied to both the conventional tubular design SOFC stack in Cycle 1 and the CO_2-seperating SOFC stack proposed in cycle 5 for preliminary economic analysis purpose.

The equipment cost of the modified SOFC afterburner (refer to section 5.2.3) is assumed to be 62.5% of the power-generating SOFC stack due to the elimination of the stack reformer and pre-reformer and anode gas recycling (Lokurlu et al., 2005).

The capital cost of the gas turbine in the cycles proposed in section 5 is assumed to be $400/kW at 30MW capacity level and $500/kW at 15 MW capacity level (http://www.nyethermodynamics.com/trader/kwprice.htm).

The capital cost of other equipment in the cycles proposed in section 5 is estimated using conventional ratio methods as follows (Chiesa et al., 2003):

$$Cost(M\$) = C_0 \times [S/S_0]^f \qquad \text{(E6-1)}$$

where the C_0 is the capital cost of the reference case, the S_0 is the size of the equipment in the reference case and the f is the scale factor.

Table 6-1: Scaling Methodology for Various Equipment

Equipment	Scaling Parameter	Base Cost C_0 (M$)	Base Size S_0	Scale Factor f
HRSG and Steam Turbine	Steam turbine gross power (MW)	94.7	200	0.67
CO_2 drying and compression	CO_2 compression power (MW)	14.8	13.2	0.67

The capital cost of the auxiliary equipment such as the fuel compressor, desulfurizer and heat exchangers are assumed to be $100/kW.

Based on the above discussion, the total capital cost of the Cycle1 and Cycle 4 proposed in section 5 are calculated and summarized in Table 6-2 using the method introduced by Peters and Timmerhaus (2003). The total capital cost in $/kW is also presented.

6.2 Total Annual Cost

The annual costs are divided into three categories:

1. The amortized capital cost (which is calculated over 20 years, with 7% interest rate and $0 salvage value).
2. Operation and Maintenance costs (which is calculated as 2% of the capital cost)
3. Natural gas cost , which is assumed to be $4.00/MMBTU

Table 6-3 summarizes the total annual costs for Cycle1 and Cycle 4. The total capital is amortized to represent an annual payment of $89,885,267 for Cycle 1 and $130, 237,957 for Cycle 4.

6.3 Cost of Electricity (COE)

The COE is estimated from the total annual cost and the power output of Cycle 1 and Cycle 4 as followed and summarized in Table 6-3.

$$COE = \frac{TotalAnnualCost(cents/yr)}{PowerOutput(kW)\times 8000(hrs/yr)} \quad \text{(E6-2)}$$

Also included in Table 6-2 is the CO_2 capture cost for Cycle 4 represented both in cents/kWh and $/ton CO_2.

Table 6-2: Total Capital Cost Calculations

	Cycle 1-w/o CO_2 capture	Cycle 4 – w/ CO_2 capture
Power Generating SOFC Stack	$109,000,000	$109,000,000
Gas Turbine	$10,920,000	$7,400,000
HRSG and Steam Turbine	$1,075,000	$8,731,644
SOFC Afterburner	-	$68,125,000

	Cycle 1-w/o CO_2 capture	Cycle 4 – w/ CO_2 capture
CO_2 Drying and Compression	-	$7,196,636
Auxiliary Equipment	$13,570,000	$12,330,000
Total Equipment Cost, E	**$134,565,000**	**$212,783,281**
Purchased Equipment installation, 47% E	$63,245,550	$100,008,142
Instrumentation(installed), 36% E	$48,443,400	$76,601,981
Piping (installed), 68% E	$91,504,200	$144,692,631
Electrical System (installed), 11% E	$14,802,150	$23,406,161
Buildings (including services), 18% E	$24,221,700	$38,300,991
Service Facility Cost, 10% E	$13,456,500	$21,278,328
Site Development Cost, 10% E	$13,456,500	$21,278,328
Total Direct Cost, D	**$403,695,000**	**$638,349,842**
Engineering and Supervision, 33% E	$44,406,450	$70,218,483
Construction Expenses, 41% E	$55,171,650	$87,241,145
Legal Expenses, 4% E	$5,382,600	$8,511,331
Contractor's Fee, 22% E	$29,604,300	$46,812,322
Contingency, 44% E	$59,208,600	$93,624,644
Total Indirect Cost, I	**$193,773,600**	**$306,407,924**
Total Capital Cost, D+I	**$597,468,600**	**$944,757,767**
Total Capital Cost, $/kW	**4403**	**7662**

Table 6-3: Cost of Electricity (COE) and Cost of CO_2 Capture

	Cycle 1-w/o CO2 capture	Cycle 4 – w/ CO2 capture
Total Capital Cost	$597,468,600	$944,757,767
Amortized Capital Cost ($/year), A	**$89,855,429**	**$130,237,957**
O&M (2% of Capital Cost), O	**$11,949,372**	**$18,895,155**
Total Fuel Input (MW, LHV)	197	203
Total Fuel Input (MMBtu/year)	5,377,312	5,541,088
Annual Fuel Cost ($4.00/MMBtu), F	**$21,509,248**	**$22,164,352**
Total Annual Cost, A+O+F	**$89,855,429**	**$130,237,957**
Cost of Electricity (COE) – cents/kWh	**8.3**	**13.2**
CO_2 Captured (ton/year)	**-**	339,840
Capture Cost, (cents/kWh)	**-**	**¢4.9**
Capture Cost, ($/ton CO_2)	**-**	**119**

6.4 Results Analysis

The SOFC based power generation cycles offer great advantages in terms of efficiency over the conventional power generation cycles. However, results in Table 6-2 and Table 6-3 indicate that there is still a long way for SOFC technology to be attractive in terms of cost. Based on the current cost of SOFC stack ($1000/kW), the Cycle 1 requires a capital investment cost of $4403/kW. This cost is much higher than the conventional power plants (gas turbine, steam turbine or combined cycle) which capital cost varies from $500kW-$2000kW(http://www.cogeneration.net/Combined_Cycle_Power_Plant.htm).

The COE of the cycle 1 is around 8 cent/kWh which is also higher than the electricity costs nowadays (about 4-6 cent/kWh).

In terms of the cost of capturing CO_2 in $/ton, the selected SOFC cycle (cycle 4) has a price of $119/ton, which is almost double the price of other competing alternative technologies reported in the literatures (Christie et al., 2003; Singh, 1997). Its electricity cost for capturing CO_2 (4.9 cents/kWh) is also on the high side comparing to the existing CO_2 capture and storage technology (Doyle A, 2005).

The study shows that regardless of the high electricity generation efficiency, the SOFC based power generation cycles have to work on lowering the cost in order to compete with other power generation technologies.

6.5 Sensitivity Studies

There are two key parameters that affect the results reported in Table 6-1 and Table 6-2. The first variable is the capital cost of the equipment. Since the capital cost of the SOFC stack is around 80% of the total equipment cost and there is much more uncertainty in its cost estimation, the equipment cost of the SOFC stack is chosen as the first parameter to investigate. The second variable is the natural gas price, which during the past years, has been quite volatile, reaching up to $14.00/MMBtu and dropping as low as $3.00/MMBtu.

6.5.1 Equipment Cost of SOFC Stack

Figure 6-1 shows the sensitivity curve for the cycle 1. The X-axis represents the equipment cost of the SOFC stack. The total capital cost ($/kW) and the COE are demonstrated.

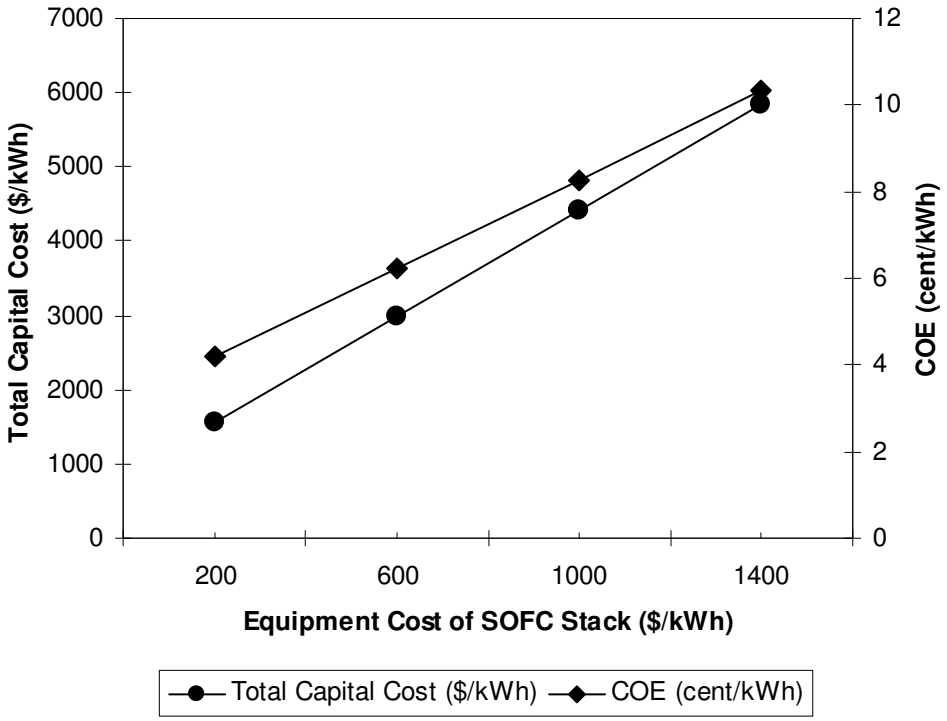

Figure 6-1: Sensitivity to Equipment Cost of SOFC Stack – Total Capital Cost and COE ($4.00/MMBtu Fuel Cost)

Figures 6-1 shows that the cost of the SOFC stack has a major impact to the total capital cost and the COE of the plant. It is important to note that the cost of the SOFC stack has to be most likely around $400/kW to be able to compete with conventional power generation cycles in terms of capital cost (<2000 $/kW) and COE (<6 cent/kW) based on this curve. Most SOFC developers are targeting installed system cost between $800-$1000/kWe for commercialization (Horne, 2005). The cost of the SOFC stack then has to be reduced to $100/kW, which is one order of magnitude lower than current cost of $1000/kW.

Figure 6-2 shows the sensitivity curve for the cycle 4. The X-axis represents the equipment cost of the SOFC stack. The CO_2 Capture Cost both in cent/kWh and $/ton are demonstrated.

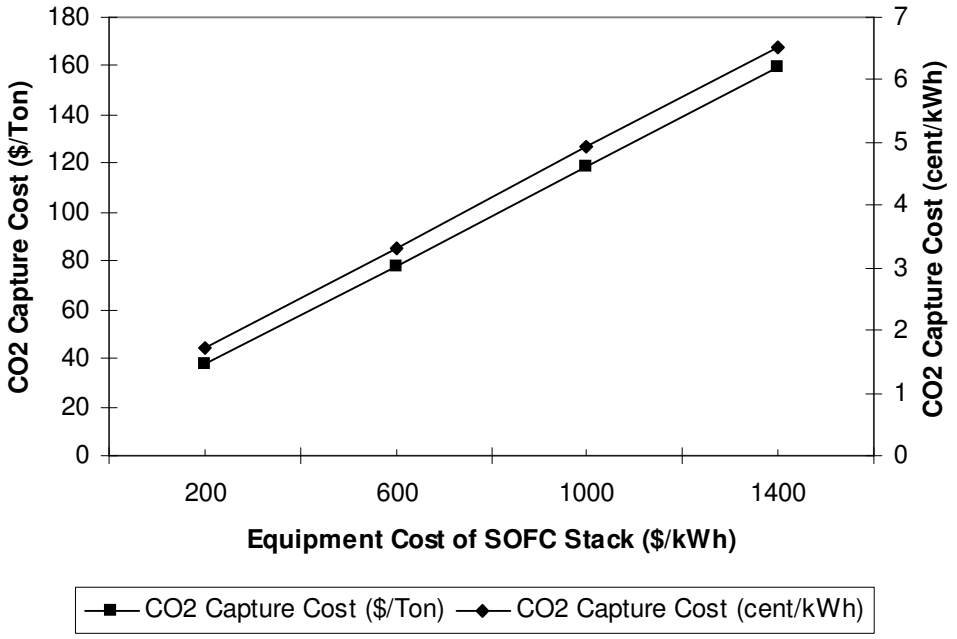

Figure 6-2: Sensitivity to Equipment Cost of SOFC Stack – CO_2 Capture Cost ($4.00/MMBtu Fuel Cost)

Figure 6-2 indicates that the equipment cost of the SOFC stack is also a dominant factor in determining the CO_2 capture cost. This is due to the factor that Cycle 4 uses a modified SOFC afterburner as the means of concentrating CO_2 and its cost is calculated as 62.5% of the normal SOFC stack cost in the cost model. According to the literature (Christie, 2003), a mean cost of $60/ton is deemed the competitive incremental cost to add CO_2 capture capability to the SOFC generator, which determines that the equipment cost of the SOFC stack need be around $400/kW from the curve. At $400/kW, the electricity cost to capture

CO_2 will be lower than 3 cent/kWh for Cycle 4, which is a very competitive value comparing to other alternative technologies (2-5 cent/kWh).

Sensitivity studies show that the equipment cost of the SOFC stack most likely need be around $400/kW so the proposed SOFC based power generation cycles can be competitive in terms of total capital cost, electricity generation cost and also CO_2 capture cost.

6.5.2 Natural Gas Price

The natural gas price affects the cost of the electricity generation and also the cost to capture CO_2. Figure 6-3 shows relationship of COE (cycle 1) and CO_2 capture cost (cycle 4) versus the natural gas price at a $400/kW of equipment cost of the SOFC stack.

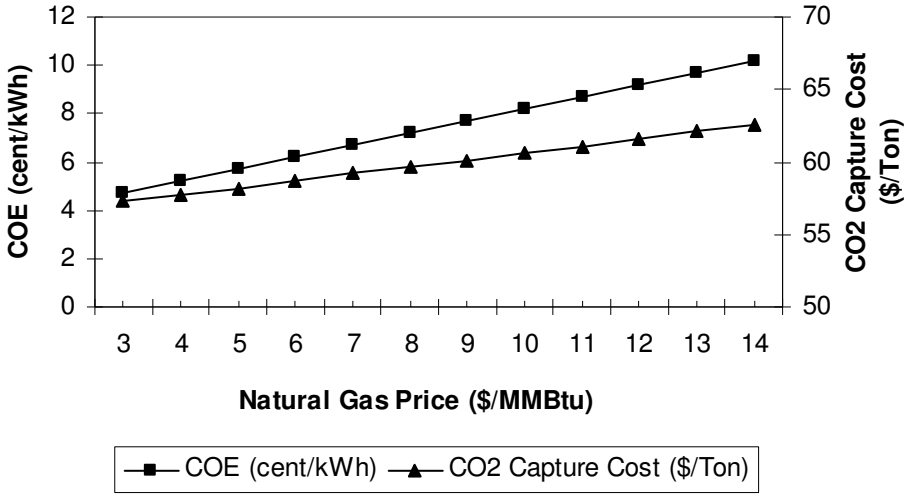

Figure 6-3: Sensitivity to Natural Gas Price ($400/kW Equipment Cost of SOFC Stack)

Figure 6-3 indicates that as the price of natural gas increases from $3.00/MMBtu to $14.00/MMBtu, the cost of electricity generation (COE) increases dramatically from 4

cent/kWh to 10 cent/kWh. As the cost of the fuel increases, the cost structure of the COE changes. At $3.00/MMBtu, the fuel cost contributes to around 31% of the cost of electricity generation. Its contribution increases to 68% when the fuel price increases to $14.00/MMBtu. Figure 6-3 shows that it is also more expensive to capture CO_2 when the fuel cost increases. As the price of the natural gas goes up to $14/MMBtu from $3.00/MMBtu, the CO_2 capture cost increases from $57/ton to $63/ton as a result of more expensive energy penalty associated to CO_2 capture.

From this preliminary economic study, it can be concluded that there is still a long way to go before SOFC technology can realize mass commercialization. The cost of the current SOFC stack needs be reduced by more than half so the SOFC based power generation cycles can provide competitive price in generation of electricity and capturing CO_2.

7.0 Conclusions

- A natural gas fed tubular SOFC stack model is developed using existing AspenPlus™ functions and unit operation models with minimum requirements for linking of a subroutine. This model fully utilizes the existing capabilities of this process simulator and provides a convenient way to perform detailed process study of SOFC based power generation cycles. The proposed model is calibrated with the performance data of a Siemens-Westinghouse 100 kW class atmospheric SOFC stack (1152 cells). Results shows that the SOFC model consisting of AspenPlus™ built-in unit operation modules can predict the fuel cell stack performance.
- Two tubular SOFC based power generation systems are simulated in AspenPlus™ extended from the proposed AspenPlus™ SOFC stack model. One system is a 100 kW atmospheric SOFC based power generation system. Another one is a 220 kW pressurized SOFC/GT hybrid power generation system. Both systems have been developed by Siemens-Westinghouse for demonstration purpose and employ the same 1152-cell SOFC stack design. System performance studies indicate that the 100 kW SOFC cogeneration system can achieve 47% electric generation efficiency (net AC/LHV) and 75% fuel effectiveness ((net AC+useful heat)/LHV) and the 220 kW hybrid power system can achieve an electrical efficiency of 57% and 87% of fuel effectiveness. The reasonable match found between the reported system performance data in the literature and the simulation results also confirms that the simulation approach proposed in this study is acceptable and the developed AspenPlus™ model can be extended for SOFC based power generation cycles study.

- A 100 MW atmospheric SOFC hybrid system with a combined Brayton-Rankine cycle is conceptualized and simulated in AspenPlus™. The simulation results indicate that this cycle is capable of achieving high electrical generation efficiency (68.7%), which is very attractive compared to the present efficiency champions—state-of-the-art combined gas and steam turbine power plants, which are characterized by an efficiency of just under 60 %. This conceptualized cycle is used as a basis to further explore the potentials of SOFC combined with CO_2 separation. Three more cycles are developed based on this 100 MW atmospheric SOFC hybrid system with a SOFC stack design modified for CO_2 separation. Each cycle employs a different type of afterburner technology for concentrating CO_2. Simulation results indicate that the system efficiency penalty due to CO_2 separation in these SOFC based power generation cycles amounts to 7% -10%. Regardless of the penalty, the electrical efficiency of the studied cycles achieved 59%-62% with a 100% CO_2 recovery, which demonstrates great advantages over the conventional power generation cycles.
- A preliminary economic study is carried out to evaluate the economic performance of the studied cycles. The study shows the high cost of the SOFC stack is the key resistance in commercialization of the SOFC technology. Very likely, the equipment cost of the SOFC stack has to be around $400/kW so that the SOFC based power generation cycles can provide competitive price in generation of electricity and capturing CO_2.
- The method and correlations adopted to calculate cell voltage are the major limiting factors to the flexibility and accuracy of the developed SOFC stack model. Further

improvement in the correlations is recommended through development of a model based on fundamental phenomena rather than based on semi-empirical relationships.

- The extent of the economic analysis performed in this work is limited by the availability of the data in the open literature. Further detailed analysis is recommended as more information is available.

References

Achenbach E. (1994) “Three-dimensional and time-dependent simulation of a planar solid oxide fuel cell stack” Journal of Power Source, 49, 333-348

Ahmed S., McPheeters C., Kumar R. (1991) “Thermal hydraulic model of a monolithic solid oxide fuel cell”, Electrochemical Society, V. 138, 2712-2718

Agnew B., Anderson A., Potts I., Frost T. H., Alabdoadaim M. A. (2003) “Simulation of combined Brayton and inverse Brayton cycles”, Applied Thermal Engineering, 23, 953-963

AspenPlus™ 12.1 Users Guide, 2004. Aspen Tech Ltd, Cambridge MA, USA.

Babcock & Wilcox Company, “Steam/its generation and use”, 40th edition, 1992

Badwal S., Forger K. (1996) “Solid oxide electrolyte fuel cell review” ,Ceram. Int., 22 [3] 257 -65

Bauen A., Hawkes A. (2004) “Decentralised Generation – Technologies and Market Perspectives”, Imperial College London Centre for Energy Policy and Technology

Boersma R., Sammes N., Fee C. (2000) “integrated fuel cell system with tubular solid oxide fuel cells”, Journal of Power Source, 86, 369-375

Brouwer J. (2002) “Solid Oxide Fuel Cell Materials Aming at Dramatic Cost Reduction”, Fuel Cell Catalyst, Vol. 2, No. 3, Spring 2002.

Campanari S. (2001) “Thermodynamic model and parametric analysis of a tubular SOFC module”, Journal of Power Source, 92, 26-34

Campanari S. (2002) “Carbon dioxide separation from high temperature fuel cell power plants” Journal of Power Source, 112, pp. 273-289

Campanari S., Chiesa P. (2000) "Potential of solid oxide fuel cells (SOFC) based cycles in low-CO2 emission power generation" Fifth International Conference on Greenhouse Gas Control Technologies, Fuel cells – 729

Campanari S., Macchi E. (1998) "Thermodynamic analysis of advanced power cycles based upon solid oxide fuel cells gas turbines and rankine bottoming cycles" ASME Journal, 98-GT-585

Carrette L., Friedrich K.A., Stimming U. (2001) "Fuel cells – fundamentals and applications", Fuel Cells 2001, 1, No. 1, 2001

Chiesa P., Consonni S., Kreutz T.G., Williams R.H. (2003) "Co-production of Hydrogen, Electricity and CO2 from Coal using Commercially-Ready Technology", Second Annual Conference on Carbon Sequestration Washington, May 5-8, 2003.

Christie G.M., Raybold T.M., Luebben E., Huang K., (2003) "Zero Emission Power Plants Using Solid Oxide Oxygen Transport Membranes – final report", June 10, 2003, DOE award number DE-FC26-00NT 40795.

Cirkel H. "SOFC fuel cells and gas turbine: a marriage of efficiency" Siemens AG, Power Generation

Colson-Inam S. (2003) "Solid Oxide Fuel Cells – Ready to Market?", www.eyeforfuelcells.com, 11/24/2003

Damen K., Troost M., Faaij A., Turkenburg W. "An Integral Comparison of Hydrogen and Electricity Production Systems with CO2 Capture and Storage by Means of a Chain Analysis" Copernicus Institute, Dept. STS, Utrecht University, 3584 CS Utrecht, The Netherlands

De Guire E.J. (2003), "Solid Oxide Fuel Cells", www.csa.com/discoveryguides/fuecell/overview.php, spring 2003

Dijkstra J.W. and Jansen D. (2004), "Novel Concepts for CO_2 Capture", Energy 29 (2004) 1249-1257

Doyle A. (2005), "Burying CO2 may curb global warming, but cost high", http://today.reuters.com/News/CrisesArticle.aspx?storyId=L26592220

EG&G Technical Services, Inc., Science Applications International Corporation, Fuel Cell Handbook (Sixth Edition), DOE/NETL-2002/1179, U.S. Department of Energy, November 2002.

Forbes C.A., George R.A., Veyo S.E., Casanova A.C. (2002), "Demonstrations: The Bridge to Commercialization for the SOFC", Electricity Today, June/July 2002, http://www.electricity-today.com/et/et_online.html

Fowler, M., "Fuel Cell Literature Review", 2001

Fuller T., Chaney L. (2000) "A novel fuel cell / microturbine combined-cycle system" McDermott Technology Inc. MTI 00-26

Gurney K. (1998) "Global Warming and the Greenhouse Effect", IEER SDA V6N2/E&S #5, http://www.ieer.org/ensec/no-5/globwarm.html

Ghosh D., Pastula M., Boersma R., Prediger D., Perry M., Horvath A., Devitt J. (2000) "Development of low temperature SOFC system for remote power and home cogeneration applications" 10th Canadian Hydrogen Conference, May, 2000.

Haines M., Heidug W., Froning D., Lokurlu A., Riensche E. (1999) "Natural gas fueled SOFC with zero CO_2 emissions system design and applications" Electrochemical society, V. 99-19

Haines M., Heidug W., Li K., Moore J. (2002) “Progress with the development of a CO2 capturing solid oxide fuel cell” Journal of Power Source, 106, pp. 377-380

Haynes C. (2001) “Clarifying reversible efficiency misconceptions of high temperature fuel cells in relation to reversible heat engines” Journal of Power Source, 92, 199-203

Herzog, H., Drake, E., Adams, E. (1997) “CO2 Capture, re-use and storage technologies for mitigating global climate change”, White Paper Final Report, publ. Energy Laboratory, Massachusetts Institute of Technology, US Department of Energy Order No: DE-AF22-96PC01257.

Horne C. (2005) “Solid Oxide Fuel Cells” MIT-Stanford-Berkeley Nanotech forum, Kainos Energy Corporation

Huang K., Christie G.M., (2003) “Zero-Emmision Power Plants Using Solid Oxide Fuel Cells and Oxygen Transport Membranes”, 2003 Fuel Cell Annual Report

IEA Greenhouse Gas R&D Programme, “Putting carbon back to the ground”, February 2001, http://www.ieagreen.org.uk/

Inui Y., Yanagisawa S., Ishida T. (2003) “Proposal of high performance SOFC combined power generation system with carbon dioxide recovery” Energy Conversion Mgmt, V 44, 597-609

Jülich F. (2002) “Methods for CO2 Separation” Exploring Technology Perspectives and Visions with Industry and RTD Communities Workshop

Khandkar A., Elangovan S., Hartvigsen J., Rowley D., Privette R., Tharp M. (1999) “Status of SOFCo's Planar SOFC Development”, Sixth International Symposium on Solid Oxide Fuel Cells

Khandkar A., Hartvigsen J., Elangovan S. (1999) "A Techno-Economic Model for SOFC Power Systems", 12th International Conference on Solid State Ionics

Kuchonthara P., Bhattacharya S., Tsutsumi A. (2003) "Energy recuperation in solid oxide fuel cell (SOFC) and gas turbine (GT) combined system" Journal of Power Source, 117, 7-13

Langeland, K., Wilhelmsen, K. (1993) "A study of the costs and energy requirement for carbon dioxide disposal", Energy Conversion and Management 34 (9-11): 807-814

Lee J., Lark T. (1998) "Modeling fuel cell stack systems" Journal of Power Source, 73, 229-241

Li K., Shell N., Haines M., Heidug W. (2000) "CO2 recovery for sequestration from a solid oxide fuel cell power plant" SPE 61027

Liese E., Gemmen R., Jabbari F., Brouwer J. (1999) "Technical development issues and dynamic modeling of gas turbine and fuel cell hybrid system" Joint Fuel Cell Technology Review Conference, Aug. 3-5, 1999

Lobachyov K., Richter H. (1997) "High efficiency coal-fired power plant of the future" Energy Conversion Mgmt, V 38, No. 15-17, pp. 1693-1699

Lokurlu A., Bakke K., Blum L., Heidug W., Li K. & Riensche E., "CO2 Sequestration from Solid Oxide Fuel Cells: Technical Options and Costs" Institute for Materials and Processes in Energy Systems (IWV-3), Research Centre Jülich, D-52425 Jülich, Germany

Lundberg W., Veyo S., Moeckel M. (2003) "A high-efficiency solid oxide fuel cell hybrid power system using the mercury 50 advanced turbine systems gas turbine" Journal of engineering for gas turbines and power, V. 125, 51-58

Magistri L., Costamagna P., Massardo A., Rodgers C., McDonald C. (2002) " A hybrid system based on a personal turbine (5kW) and a solid oxide fuel cell stack: a flexible and high efficiency energy concept for the distributed power market" Journal of engineering for gas turbines and power, V. 124, 850-857

Massardo A., Lubelli F. (2000) "Internal reforming solid oxide fuel cell-gas turbine combined cycles (IRSOFC-GT): part A-cell model and cycle thermodynamic analysis" Journal of engineering for gas turbines and power, V. 122, 27-35

Maurstad O., Bredesen R., Bolland O., Kvamsdal H., Schell M. "SOFC and gas turbine power systems – evaluation of configurations for CO2 capture" SINTEF energy research, N-7456 Trondheim, Norway

Moller B., Arriagada J., Assadi M., Potts I. (2004) "Optimization of an SOFC/GT system with CO2 capture" Journal of Power Source, 131, 320-326

Monanteras N., Frangopoulos C. (1999) "Towards synthesis optimization of a fuel-cell based plant" Energy Conversion Mgmt, 40, 1733-1742

Mozaffarian M. (1994) "Solid oxide fuel cell for combined heat and power applications" Netherlands energy research foundation ECN Petten

Northwest Power Planning Council (2002) "Natural Gas Combined-cycle Gas Turbine Power Plants" New Resource Characterization for the Fifth Power Plan

ONSITE SYCOM Energy Corporation (1999) "Review of Combined Heat and Power Technologies" The California Energy Commission under grant number 98R020974 with the U.S. Department of Energy

Pålsson J., Hansen J., Christiansen N., Nielsen J., Kristensen S. (2003) "Solid Oxide Fuel Cells, Assessment of the technology from an industrial perspective" Risø International Energy Conference

Pålsson J., Selimovic A., Sjunnesson L. (2000) "Combined solid oxide fuel cell and gas turbine systems for efficient power and heat generation" Journal of Power Source, 86, pp. 442-448

Parsons Power Group, Inc. (1998) "Market-Based Advanced Coal Power System, Appendix C-Natural Gas Combined Cycle Units".

Peters M.S., Timmerhaus K.D., "Plant Design and Economics for Chemical Engineers," McGraw-Hill, NY (1991) pp 361-367, 496-498

Peters R., Riensche E., Cremer P. (1999) "Pre-reforming of natural gas in solid oxide fuel-cell systems" Journal of Power Source, 86, 432-441

Pyke S., Burnett A., Leah R. (2002) "Systems Development for Planar SOFC Based Power Plant" ALSTOM Research and Technology Centre

Rao A., Samuelsen G. (2003) "A thermodynamic analysis of tubular solid oxide fuel cell based hybrid systems" Journal of engineering for gas turbines and power, V. 125, 59-66

Rao A., Samuelsen G., Yi Y. (2005) "Gas Turbine Based High Efficiency 'Vision 21'Natural Gas and Coal Central Plants" Journal of Power and Energy, Vol. 219, No. 2, pp. 127-136

Riensche E., Achenbach E., Froning D., Haines M., Heidug W., Lokurlu A. (2000) "Clean Combined-cycle SOFC power plant – cell modeling and process analysis" Journal of Power Source, 86, 404-410

Riensche E., Meusinger J., Stimming U., Unverzagt G. (1998) “Optimization of a 200 kW SOFC cogeneration power plant Part II: Variation of the flowsheet” Journal of Power Source, 71, pp. 306-314

Riensche E., Stimming U., Unverzagt G. (1998) “Optimization of a 200 kW SOFC cogeneration power plant Part I: Variation of process parameters” Journal of Power Source, 73, pp. 251-256

Selimovic A., Palsson J., Sjunnesson L. (1998) “Integration of a solid oxide fuel cell into a gas turbine process” Lund Institute of Technology

Shockling L., Huang K., Gilboy T., Christie G., Raybold T. (2001) “Zero Emission Power Plants Using Solid Oxide Fuel Cells and Oxygen Transport Membranes” Vision 21 Program Review Meeting, Session1 - Technology Development

Singhal S. (1997) “Recent progress in tubular solid oxide fuel cell technology” Electrochemical Proceedings V. 97-18

Skjæveland H. (2002) “Market Scenarios for the Fuel Cell towards 2010 and beyond” Shell Technology Norway, Exploring Technology Perspectives and Visions with Industry and RTD Communities Workshop

Stambouli A.B., Traversa E. (2002) “Solid oxide fuel cells (SOFCs): a review of an environmentally clean and efficient source of energy”, Renewable and Sustainable Energy Reviews, 6 (2002) 433–455

Subramanyan K., Diwekar U. (2005) “Characterization and quantification of uncertainty in solid oxide fuel cell hybrid power plants” Journal of Power Source, 142, 103-116

Tanaka K., Wen C., Yamada K. (2000) “Design and evaluation of combined cycle system with solid oxide fuel cell and gas turbine” Fuel, 79, pp. 1493-1507

Veyo S.E. (1996) “The Westinghouse solid oxide fuel cell program – a status report” Westinghouse Science & Technology Center

Veyo S.E., Forbes C. (1998) “Demonstrations based on Westinghouse’s prototype Commercial AES design” Westinghouse Science & Technology Center

Veyo S.E., Lundberg W. (1999) “Solid oxide fuel cell power system cycles” ASME Journal, 99-GT-356

Veyo S.E., Lundberg W. (2002) “Status of pressurized SOFC/gas turbine power system development at Siemens Westinghouse” ASME GT-2002-30670

Williams M. (2001) “status and promise of fuel cell technology” Fuel Cells 2001, 1, No. 2, 87-91

Yi Y., Rao A., Brouwer J., Samuelsen G. (2004) “Analysis and optimization of a solid oxide fuel cell and intercooled gas turbine (SOFC-ICGT) hybrid cycle” Journal of Power Source, 132, 77-85